

**UCSF**

**UC San Francisco Electronic Theses and Dissertations**

**Title**

The location of substrate binding

**Permalink**

<https://escholarship.org/uc/item/7kf1f8tq>

**Author**

Harris, Robert Z

**Publication Date**

1993

Peer reviewed|Thesis/dissertation

**The Location of Substrate Binding: A Major Determinant of Hemoprotein Reactivity**

by

**Robert Z. Harris**

**DISSERTATION**

**Submitted in partial satisfaction of the requirements for the degree of**

**DOCTOR OF PHILOSOPHY**

in

**Pharmaceutical Chemistry**

in the

**GRADUATE DIVISION**

of the

**UNIVERSITY OF CALIFORNIA**

**San Francisco**

*Robert Z. Harris*



**In loving memory of my mother, Beatrice**

## **Acknowledgments**

I would like to thank Dr. Paul Ortiz de Montellano for always being available to discuss any scientific question or problem and for treating me with an abundance of respect. I wish to also thank Dr. Roger Ketcham and Dr. George Kenyon for thoroughly and promptly reading this thesis.

I wish to acknowledge all the members of the POM group for not only being good colleagues and coworkers, but for also being terrific friends. I especially would like to thank William Chan for all of his help in the lab and, more importantly, for introducing me to weight lifting.

I wish to acknowledge my parents for all of the love and encouragement they have given me over the years. I would like to express my gratitude to my stepfather Jack, and my best friend, Steve, for their support over some difficult times. Finally, I wish to thank my fiancée, Parnian, for making my final 2 years at UCSF the happiest of my life.



# **The Location of Substrate Binding: A Major Determinant of Hemoprotein Reactivity**

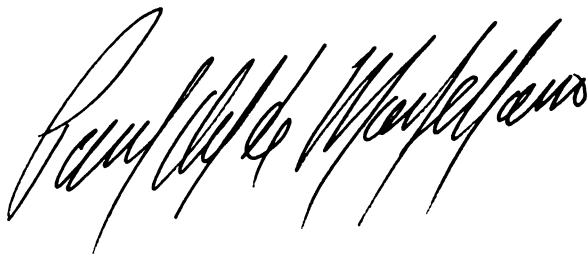
**Robert Z. Harris**

## **Abstract**

Manganese peroxidase (MnP), which normally oxidizes Mn(II) to Mn(III), is rapidly inactivated by sodium azide. The inactivation is paralleled by formation of azidyl radicals and conversion of the heme into a *meso*-azido adduct. MnP is also inactivated by methylhydrazine ( $K_I = 402$  mM and  $k_{\text{inact}} = 0.22 \text{ min}^{-1}$ ) and phenylhydrazine. Phenylhydrazine inactivation does not yield an iron-phenyl complex. Apo-MnP reconstituted with  $\delta$ -*meso*-ethylheme is capable of forming a Compound II-like species yet has diminished catalytic activity. Co(II) inhibits the enzyme competitively with respect to Mn(II) but does not inhibit its inactivation by azide or alkylhydrazines. The results argue that substrates interact with the heme edge in the vicinity of the  $\delta$ -*meso* carbon. They also suggest that Mn(II) and Co(II) bind to a common site close to the  $\delta$ -*meso* carbon without blocking the approach of small molecules to the heme edge.

Horseradish peroxidase (HRP) enantioselectively oxidizes thioanisole to the (S)-(-) sulfoxide in 70% enantiomeric excess. The sulfide oxygen is derived primarily from hydrogen peroxide. Manganese peroxidase and hemoglobin oxidize thioanisole to sulfoxides having 88% and 4% enantiomeric excess, respectively. HRP reconstituted with  $\delta$ -*meso*-ethylheme or preincubated with phenylhydrazine cannot oxidize guaiacol, yet is fully able to oxidize thioanisole. Thioanisole noncompetitively inhibits guaiacol oxidation by HRP. These results suggest that the thioanisole binding site is distinct from the guaiacol binding site, and that the site of binding may dictate whether a hemoprotein exhibits oxygenase or peroxidase activity.

HRP reconstituted with 8-formylheme and 8-hydroxymethylheme has the potential to model the mammalian enzymes myeloperoxidase and lactoperoxidase. However, unlike the mammalian enzymes, the reconstituted HRP does not have the ability to oxidize chloride and bromide ions. HRP reconstituted with heme to which a phenol or a TEMPO group was linked has low catalytic activity. However, this methodology of reconstituting hemoproteins with modified hemes could eventually yield novel catalysts.

A handwritten signature in black ink, reading "Randall G. Wenzel". The signature is written in a cursive style with a large initial 'R'.

## Table of Contents

<b>1.0</b>	<b>Introduction</b>	
1.1	Hemoproteins	1
1.2	Peroxidases	2
1.3	Peroxidase Catalytic Cycle	3
1.4	Compound I Formation	4
1.5	Structure and Reactivity of Compound I	6
1.6	Structure and Reactivity of Compound II	9
1.7	Structure of Compound III	10
1.8	Homologies Among Peroxidases	10
1.9	Cytochrome P-450	12
1.10	An Intriguing Question	13
1.11	Oxygenase vs Peroxidase Activity: The Effect of Proximal and Distal Residues	13
1.12	Oxygenase vs Peroxidase Activity: Miscellaneous Factors	15
1.13	Oxygenase vs Peroxidase Activity: The Role of the $\delta$ -Meso Heme Edge	16
1.14	A Hemoprotein Theory	21
1.15	Thesis Overview	22
<b>2.0</b>	<b>Inactivation of Manganese Peroxidase by Azide and Hydrazines</b>	
2.1	Introduction	24
2.2	Experimental	28
2.3	Results	36
2.4	Discussion	50

<b>3.0</b>	<b>HRP Catalyzed Thioanisole Sulfoxidation</b>	
3.1	Introduction	58
3.2	Experimental	67
3.3	Results	74
3.4	Discussion	78
		87
<b>4.0</b>	<b>Reconstitution of HRP with 8-Hydroxymethylheme and 8-Formylheme</b>	
4.1	Introduction	96
4.2	Experimental	105
4.3	Results	112
4.4	Discussion	126
<b>5.0</b>	<b>Enzyme Engineering Through the Reconstitution of HRP with Chemically Modified Hemes</b>	
5.1	Introduction	131
5.2	Experimental	137
5.3	Results	145
5.4	Discussion	169
<b>6.0</b>	<b>References</b>	<b>212</b>

## **List of Figures**

1.1.1	Structure of heme.	1
1.3.1	The classical peroxidase cycle.	4
1.4.1	Formation of HRP Compound I.	6
1.5.1	The heme structure of HRP Compounds I, II, and III.	8
1.5.2	Spectra of native HRP, Compound I and Compound II.	9
1.9.1	Catalytic cycle of P-450.	12
1.8.1	Electronic absorption spectra of HRP: ferric, compound I, and compound II.	23
1.13.1	Formation of the phenyl radical via the oxidation of phenylhydrazine or phenyldiazene.	16
1.13.2	Addition of the phenyl radical to the heme iron of P-450 and to the heme edge of HRP.	17
1.13.3	Mechanism of HRP inactivation by alkylhydrazines.	19
1.13.4	Mechanism of 8-hydroxymethylheme formation in HRP-phenyldiazene incubations.	20
1.10.5	Models of oxygenase and peroxidase active sites.	22
2.1.1	The catalytic cycle of MnP.	25
2.1.2	Degradation of a lignin model compound by Mn(III).	27
2.3.1.	Partition ratio of azide mediated MnP inactivation.	36
2.3.2	EPR spectrum of the PBN trapped azidyl radical produced in an MnP-azide incubation.	37
2.3.3	Spectra of a MnP-azide incubation.	38

2.3.4	HPLC chromatogram of $\delta$ - <i>meso</i> -azidoheme extracted from azide-inactivated MnP.	39
2.3.5	Electronic absorbance spectrum of obtained in an MnP-azide incubation.	39
2.3.6	Time-dependence of MnP inactivation by methylhydrazine.	40
2.3.7	Time-dependence of Soret absorbance loss and activity loss in an MnP-methylhydrazine incubation.	41
2.3.8	HPLC chromatogram of $\gamma$ - <i>meso</i> -ethylheme standard, $\delta$ - <i>meso</i> -ethylheme standard, and $\delta$ - <i>meso</i> -ethylheme produced in an MnP-ethylhydrazine incubation.	42
2.3.9	Partition ratios for the inactivation of MnP by phenylhydrazine and phenyldiazene.	43
2.3.10	Electronic absorption spectra of MnP reconstituted with hemin and $\delta$ - <i>meso</i> -ethylheme.	45
2.3.11	Electronic absorption spectrum of the ferric and the reduced CO complex of $\delta$ - <i>meso</i> -ethylheme-reconstituted MnP.	46
2.3.12	HPLC chromatogram of the heme extracted from a $\delta$ - <i>meso</i> -ethylheme-reconstituted MnP incubation with azide.	48
2.3.13	Competitive inhibition of manganese oxidation by cobalt.	49
2.3.14	Inactivation of MnP by cobalt in the presence or absence of H <sub>2</sub> O <sub>2</sub> .	49
2.3.15	Rate of ethylhydrazine inactivation of MnP in the presence and absence of cobalt.	50
2.4.1	A model of the MnP active site.	57
3.1.1	Mechanism of HRP oxidation of a 9-methoxyellipticine.	61
3.1.2	The peroxidase and oxygenase activities of HRP.	66

3.3.1	A typical HPLC chromatogram from an HRP incubation that contained thioanisole.	75
3.3.2	Oxidation of thioanisole and guaiacol by various enzyme species.	78
3.3.3	Spectrum of HRP reconstituted with $\delta$ -meso-ethylheme.	79
3.3.4	Mixed-type noncompetitive inhibition of guaiacol oxidation by thioanisole.	80
3.3.5	Classical mixed noncompetitive inhibition.	81
3.3.6	A plot of apparent $K_M$ /apparent $k_{cat}$ for guaiacol oxidation by HRP vs thioanisole concentration and a plot of $1/\text{apparent } k_{cat}$ for guaiacol oxidation vs thioanisole concentration.	81
3.3.7	GC chromatogram of the extract from an HRP incubation with molecule <b>2</b> .	83
3.3.8	Possible pathways of oxidation of <b>2</b> by HRP.	84
3.3.9	Difference spectra obtained for binding of guaiacol and thioanisole to HRP and $\delta$ -meso-ethylheme-reconstituted HRP.	86
3.3.10	Determination of the binding constants for guaiacol binding to HRP and $\delta$ -meso-ethylheme-reconstituted HRP.	87
3.4.1	A model of the HRP active site.	93
4.1.1	Hemes modified at the 2 and 4 positions.	97
4.1.2	Hemes modified at the 7 and 8 positions.	98
4.1.3	The structures of $\delta$ -meso modified hemes.	99
4.1.4	A chlorin in which the D ring is reduced.	101
4.1.5	Structure of heme <i>a</i> .	102
4.1.6	A possible structure of the MPO prosthetic group.	103

4.1.7	Structures of 8-hydroxymethylheme and 8-formylheme.	104
4.3.1	HPLC chromatogram of the heme products extracted from an HRP incubation with phenylhydrazine.	113
4.3.2	HPLC chromatogram of the products of a tetrapropylammonium peruthenate oxidation of 8-hydroxymethylheme.	114
4.3.3	Electronic absorption spectrum of 8-formylheme.	115
4.3.4	Electronic absorption spectrum of 8HM-HRP and 8F-HRP.	116
4.3.5	Stopped flow chromatograms of the formation and decay of 8HM-HRP Compound I.	117
4.3.6	Spectrum of 8F-HRP, its Compound I, and its Compound II species.	119
4.3.7	EPR spectrum of 8F-HRP upon addition of hydrogen peroxide.	119
4.3.8	Eadie Hofstee plot of guaiacol oxidation by HRP and by 8F-HRP.	120
4.3.9	HPLC chromatogram of the products from a guaiacol incubation with 8F-HRP.	121
4.3.10	Rates of inactivation of HRP, 8HM-HRP and 8F-HRP by ethylhydrazine.	122
4.3.11	Generation of azide and ethyl radicals by 8HM-HRP.	123
4.3.12	Inactivation of HRP and 8HM-HRP by sodium azide.	124
4.3.13	HPLC chromatogram of the hemes produced in the reaction of 8HM-HRP with sodium azide.	125
4.3.14	Mass spectrum of 8-hydroxymethyl- $\delta$ -meso-azidoheme.	125
5.1.1	A model of the HRP active site.	133



5.1.2	Hydrogen atom abstraction and manganese oxidation mediated by the phenolic radical.	134
5.1.3	A potential cycle for the catalysis of hydrogen atom abstraction by HRP reconstituted with a phenol linked heme.	135
5.1.4	TEMPO Chemistry.	136
5.1.5	The potential catalytic cycle of HRP reconstituted with a TEMPO linked heme.	137
5.3.1	EPR signal of TEMPO in the presence of HRP before, and after, the addition of hydrogen peroxide.	146
5.3.2	Magnitude of the EPR signal in incubations that contained TEMPO, HRP, and various amounts of hydrogen peroxide.	147
5.3.3	HPLC chromatogram of the products from an incubation that contained HRP, benzyl alcohol, TEMPO, and hydrogen peroxide.	148
5.3.2.4	A possible mechanism for the catalytic activity of HRP in the presence of TEMPO.	149
5.3.5	The time-dependence of benzaldehyde production.	152
5.3.6	The pH-dependence of benzaldehyde production.	153
5.3.7	The dependence of benzaldehyde production of HRP concentration.	154
5.3.8	The dependence of benzaldehyde production of TEMPO concentration.	155
5.3.9	The dependence of benzaldehyde production on ethyl hydroperoxide concentration.	155
5.3.10	Modified hemes.	157
5.3.12	EPR spectrum of heme 1.	158
5.3.13	HPLC chromatogram of heme 2 produced synthetically from 8-formylheme.	159
5.3.14	Electronic absorption spectrum of heme 2.	159

<b>5.3.15</b>	<b>Mass spectrum of heme 2.</b>	<b>160</b>
<b>5.3.16</b>	<b>Electronic absorption spectrum of HRP-1.</b>	<b>161</b>
<b>5.3.17</b>	<b>EPR spectrum of HRP-1.</b>	<b>161</b>
<b>5.3.18</b>	<b>Electronic absorption spectrum of HRP-4.</b>	<b>163</b>
<b>5.3.19</b>	<b>Spectra of native enzyme and cyanide complex of HRP and HRP-4.</b>	<b>165</b>
<b>5.3.20</b>	<b>Spectra of native, reduced, and the reduced CO complex of HRP and HRP-4.</b>	<b>166</b>
<b>5.3.21</b>	<b>Electronic absorption spectrum of HRP-2 and its compound II species.</b>	<b>167</b>
<b>5.3.22</b>	<b>Enzymatic activities of HRP-3 and HRP-4.</b>	<b>168</b>

## **List of Tables**

<b>2.3.1</b>	<b>Catalytic activity of native, hemin reconstituted and <math>\delta</math>-meso-ethylheme-reconstituted MnP.</b>	<b>47</b>
<b>3.3.1</b>	<b>Enantiomeric excess of sulfoxides produced in HRP-sulfide incubations.</b>	<b>76</b>
<b>3.3.2</b>	<b>Oxidation of thioanisole and guaiacol by various enzyme species.</b>	<b>78</b>
<b>5.3.1</b>	<b>Oxygen evolution in HRP incubations.</b>	<b>150</b>
<b>5.3.2.</b>	<b>The effect of the substitution of ethyl hydroperoxide for hydrogen peroxide on benzyl alcohol oxidation by HRP in the presence of TEMPO.</b>	<b>151</b>
<b>5.3.3</b>	<b>Benzaldehyde production in various reaction media.</b>	<b>156</b>
<b>5.3.4</b>	<b>Guaiacol activity of HRP and HRP-4 at various pH values.</b>	<b>164</b>

## List of Abbreviations

ABTS	2,2 azinobis-(3-ethylbenzthiazoline sulfonic acid)
CcP	Cytochrome c peroxidase
CPO	Chloroperoxidase
DETAPAC	Diethylenetriaminepentaacetic acid
DMPO	5,5-Dimethyl-1-pyrroline- <i>N</i> -oxide
EDTA	Ethylenediaminetetraacetic acid
ee	Enantiomeric excess
EPR	Electron paramagnetic resonance
EXAFS	Extended X-ray absorption fine structure
8F-HRP	HRP reconstituted with 8-formylheme
GC	Gas-liquid chromatography
Hb	Hemoglobin
Heme	Iron protoporphyrin IX, regardless of oxidation and ligation state.
Heme 1	O-(3-oxomethyl-PROXYL)-8-hydroxymethylheme
Heme 2	N-(2-hydroxyphenylethyl)-8-aminomethylheme
Heme 3	N-(phenylethyl)-8-aminomethylheme
Heme 4	N-(2-hydroxyphenyl)-8-aminomethylheme
8HM-HRP	HRP reconstituted with 8-hydroxymethylheme

HPLC	High performance liquid chromatography
HRP	Horseradish peroxidase
HRP-1, HRP-2, HRP-3, HRP-4	HRP reconstituted with hemes 1-4
LSIMS	Liquid secondary ion mass spectrometry
Mb	Myoglobin
MCPBA	<i>meta</i> Chloroperbenzoic acid
MMI	1-Methyl-2-mercaptoimidazole
MnP	Manganese peroxidase
Molecule 1	$p\text{-NO}_2\text{C}_6\text{H}_4\text{CH}_2\text{SC}_6\text{H}_5$
Molecule 2	$\text{C}_6\text{H}_5\text{SCH}_2\text{COCH}_3$
MPO	Myeloperoxidase
MS	Mass spectrometry
NOE	Nuclear Overhauser effect
NMR	Nuclear magnetic resonance
P-450	Cytochrome P-450
PROXYL	2,2,5,5-tetramethyl-1-pyrrolidinyloxy
PBN	<i>N-tert</i> -Butyl- $\alpha$ -phenylnitrone
PPIX	Protoporphyrin IX
R.Z.	Reinheitszahl: $\text{Abs}_{(\text{Soret})} / \text{Abs}_{(280\text{nm})}$
SOD	Superoxide dismutase
TFA	Trifluoroacetic acid
TEMPO	2,2,6,6-tetramethyl-1-piperidinyloxy

## 1.0 Introduction

### 1.1 Hemoproteins

Hemoproteins are a class of proteins that contain a heme (iron protoporphyrin IX) prosthetic group (Figure 1.1.1). The protein moiety of a hemoprotein is able to utilize the heme group to perform a variety of biologically significant functions such as oxygen transport (e.g., hemoglobin and myoglobin), electron transfer (e.g., cytochromes a<sub>3</sub>, b<sub>5</sub>, c), and substrate oxidation. There are two major types of hemoproteins that catalyze substrate oxidation: oxygenases and peroxidases. Oxygenases typically catalyze oxygen atom insertion whereas peroxidases typically catalyze electron abstraction. The studies described in this thesis provide insight into the factors that control whether a hemoprotein acts as an oxygenase or as a peroxidase.

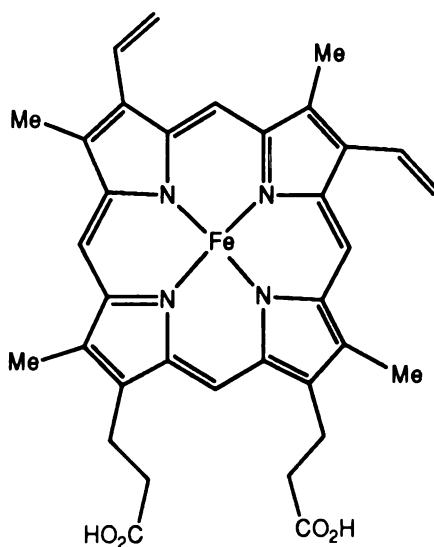


Figure 1.1.1. The structure of heme.

## **1.2 Peroxidases**

Peroxidases are found throughout nature (Ortiz de Montellano, 1992). There are plant, animal, fungal, and bacterial peroxidases. A brief overview of the variety of peroxidases that have been studied is given below. A structural comparison of various peroxidases will be made in section 1.8.

The plant peroxidases include horseradish peroxidase (HRP) (Dunford, 1991), turnip peroxidase (Mazza et al., 1968), and peanut peroxidase (van Huystee, 1991). HRP isozyme C is the prototypical peroxidase. It has been the subject of extensive studies from which much of our understanding of peroxidase electronic configuration and mechanism has been derived. There is no high resolution crystal structure of HRP isozyme C, however, because it is a highly glycosylated enzyme that does not form homogenous crystals (Brathwaite, 1976). Recently, however, a low resolution (3.1 Å) crystal structure of HRP isozyme E5, a minor isozyme that is less glycosolated, was solved (Morita et al., 1991). The exact functions of HRP and other plant peroxidases are not known, but it is speculated that these enzymes are involved in biosynthesis of plant auxins and cell wall polymers (Dunford, 1991). They may also function to protect plant cells from hydrogen peroxide mediated damage (Dunford, 1991).

The animal peroxidases include ovoperoxidase which functions to polymerize proteins that make up the envelope of the fertilized sea urchin

egg (Deits et al., 1984), and mammalian peroxidases such as thyroid peroxidase (Magnussen, 1991), myeloperoxidase (Hurst, 1991), lactoperoxidase (Thomas et al., 1991), and eosinophil peroxidase (Henderson, 1991). The first of these mammalian enzymes functions to synthesize the hormone thyroxin, whereas the latter three enzymes are thought to function as antimicrobial agents through generation of oxidized halide and pseudo-halide species.

Fungal peroxidases include *Coprinus macrorhizus* peroxidase (DePillis and Ortiz De Montellano, 1989; Lukat et al., 1988) and cytochrome c peroxidase (CCP) (Bosshard et al., 1984). CCP is the only peroxidase for which there is a high resolution crystal structure (Poulos et al., 1980; Poulos et al., 1978). Therefore, much of our knowledge of peroxidase protein structure is based on CCP. The physiological role of CCP is believed to be oxidation of cytochrome c (Bosshard et al., 1991).

Finally, bacterial peroxidases have also been discovered (Loprasert et al., 1989; Nadler et al., 1986). These peroxidases show a high degree of sequence homology to both plant and fungal peroxidases (Welinder, 1991), suggesting divergent evolution.

### **1.3 Peroxidase Catalytic Cycle**

The classic peroxidase catalytic cycle is shown in Figure 1.3.1. The peroxidase reacts with hydrogen peroxide or an alkylhydroperoxide to form a species called Compound I. Compound I is a two electron deficient enzyme that retains one of the oxygen atoms of the peroxide.



Compound I can abstract one electron from a substrate molecule giving a species called Compound II and a substrate radical. Compound II is a one electron deficient enzyme. Compound II can abstract an electron from a second substrate molecule to give a substrate radical and native peroxidase. The substrate radicals produced react in solution: they may dimerize, polymerize, disproportionate, or add oxygen. Classical peroxidase substrates include electron rich aromatic molecules such as phenols and anilines. It should be noted that HRP Compound I is able to perform a nominally direct 2 electron oxidation of certain substrates. This atypical peroxidase oxidation will be described in detail in chapter 3.

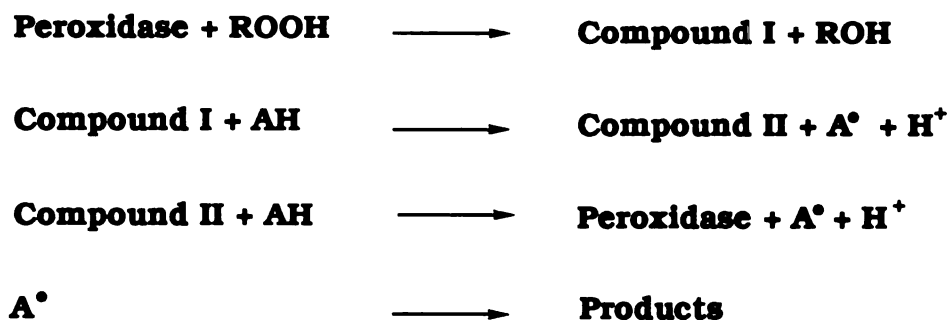


Figure 1.3.1. The classical peroxidase cycle.

#### 1.4. Compound I Formation

Compound I is an enzyme species that is two oxidation equivalents above the native ferric enzyme (Adediran and Dunford, 1983; Chance, 1952). It is formally equivalent to ferric enzyme ligated to an electron deficient oxygen atom, and thus forms through heterolytic cleavage of the peroxide oxygen-oxygen bond. A mechanism for Compound I formation,

based on the crystal structure of CCP, has been proposed (Poulos and Kraut, 1980)(Figure 1.4.1). Oxygen-oxygen bond cleavage is facilitated at the distal side of the heme by a histidine that acts as a general acid - base catalyst by first removing a proton from the oxygen atom that ligates to the heme iron and then transferring the proton to the oxygen atom that is released as water. Additionally, the positive charge of an arginine guanidinium group provides a stabilizing electrostatic interaction for the departing oxygen atom. On the proximal side of the heme, a histidine imidazole, that is hydrogen bonded to a glutamate, is ligated to the heme iron. This partially anionic histidine (histidinate) provides the electrons needed to stabilize the electron deficient oxygen atom that is coordinated to the heme iron.

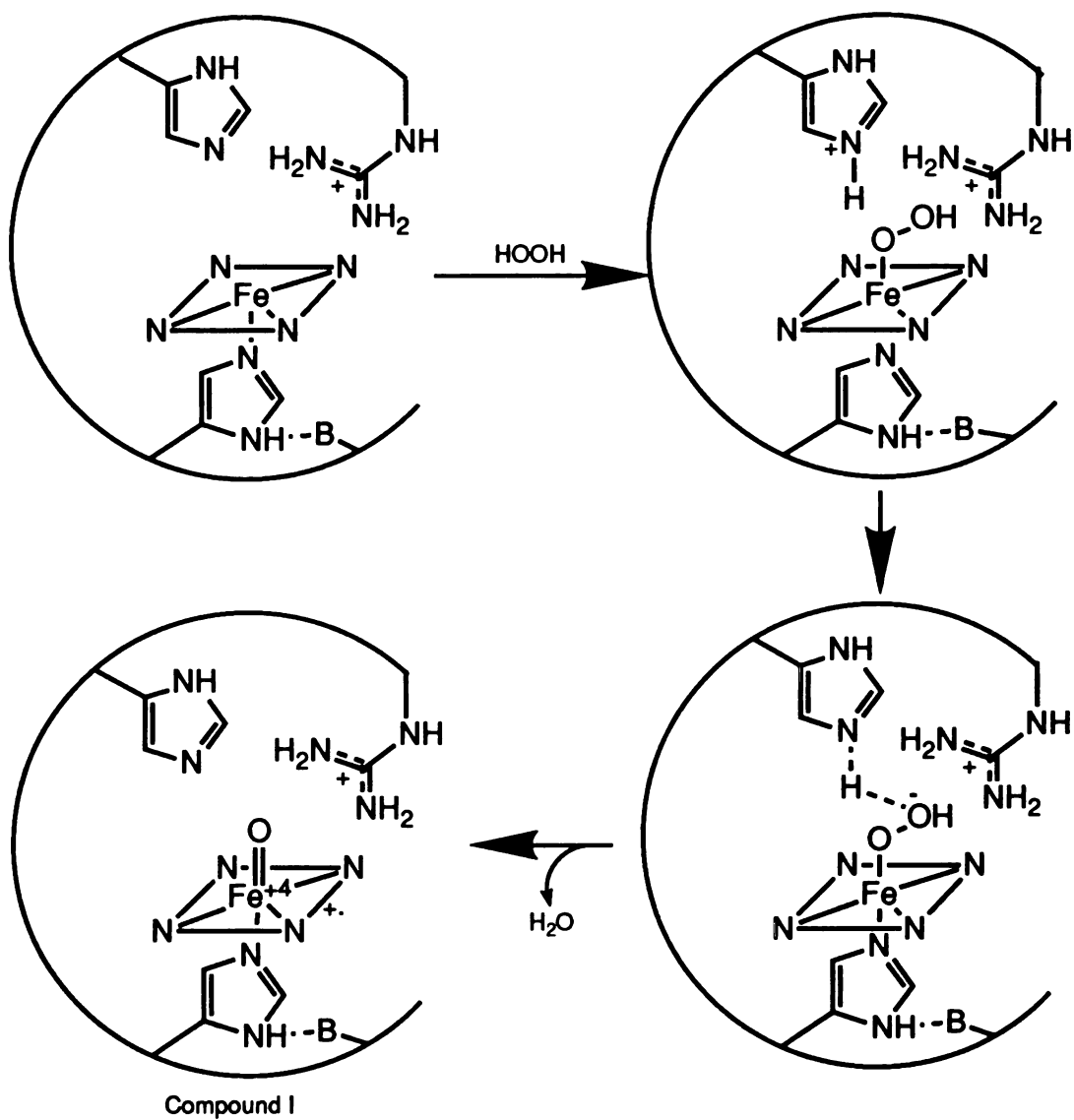


Figure 1.4.1. Formation of HRP Compound I. Adapted from Poulos and Kraut, 1980)

### 1.5. Structure and Reactivity of Compound I

The structure of HRP Compound I has been deduced by a variety of spectroscopic techniques. Mössbauer (Schultz et al., 1979), ENDOR (Roberts et al., 1981), resonance raman (Van Wart and Zimmer, 1985), and EXAFS (Penner-Hahn et al., 1986) studies have determined that one

of the two electron deficiencies is manifested as a ferryl iron that is double bonded to an oxygen atom ( $\text{Fe}^{\text{IV}}=\text{O}$ ). EPR (Schultz et al., 1984), and model studies (Dolphin et al., 1971) suggest that the second electron deficiency is manifested as a porphyrin radical cation (Figure 1.5.1), although recent NMR (Thanabal et al., 1988) and resonance Raman (Ogura and Kitagawa, 1987) spectroscopic studies suggest that a portion of the electron deficiency may also be localized on the proximal histidine residue. The porphyrin radical cation is believed to have an  $a_{2u}$  highest occupied molecular orbital (Dolphin and Felton, 1974). HRP Compound I has distinct UV-Vis spectroscopic characteristics (Figure 1.5.2).

The second electron deficiency in CCP Compound I, in contrast to that of HRP Compound I, is located on the protein, as evidenced by a detectable protein radical (Yonetani, 1965; Yonetani and Ray, 1965). EPR studies on CCP and CCP mutants suggest that most of the radical density is located on a tryptophan residue (Fishel et al., 1991). The significance of whether the second oxidative equivalent is located on the porphyrin or protein is unknown. It is interesting to note that in the case of lactoperoxidase, which initially forms a porphyrin radical cation that slowly decays to a protein radical, only the porphyrin radical cation form of Compound I is able to iodinate tyrosine (Cochran and Schultz, 1990). However, the existence of a porphyrin radical cation does not appear to be a requirement for classical peroxidase activity.

HRP Compound I is a fairly strong oxidizing agent with a half-cell potential of 0.96 V (Hayashi and Yamazaki, 1979). It is rapidly reduced

to Compound II by a variety of electron rich aromatic molecules (Job and Dunford, 1975; Marnett et al., 1986).

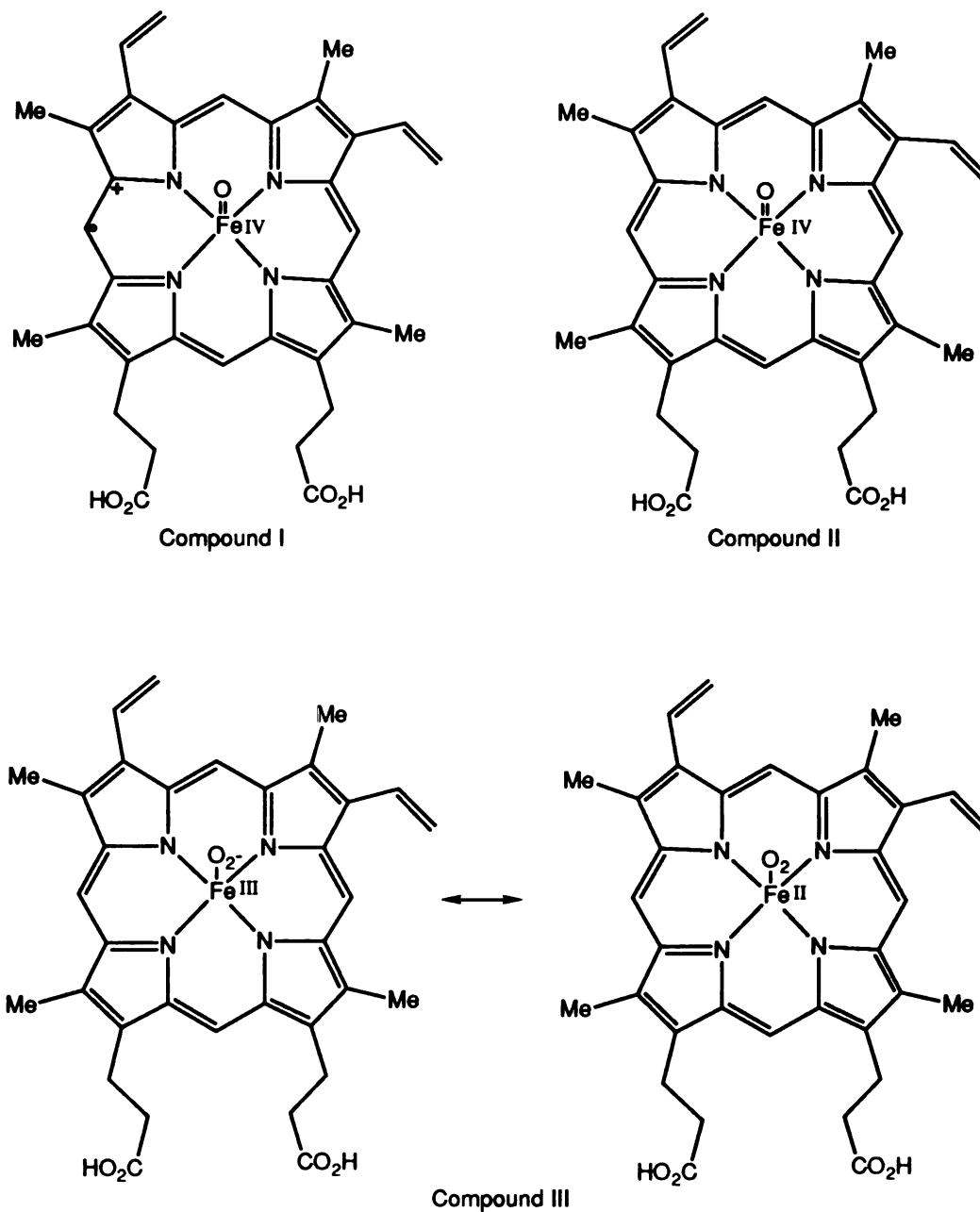


Figure 1.5.1. The heme structure of HRP Compounds I, II, and III.

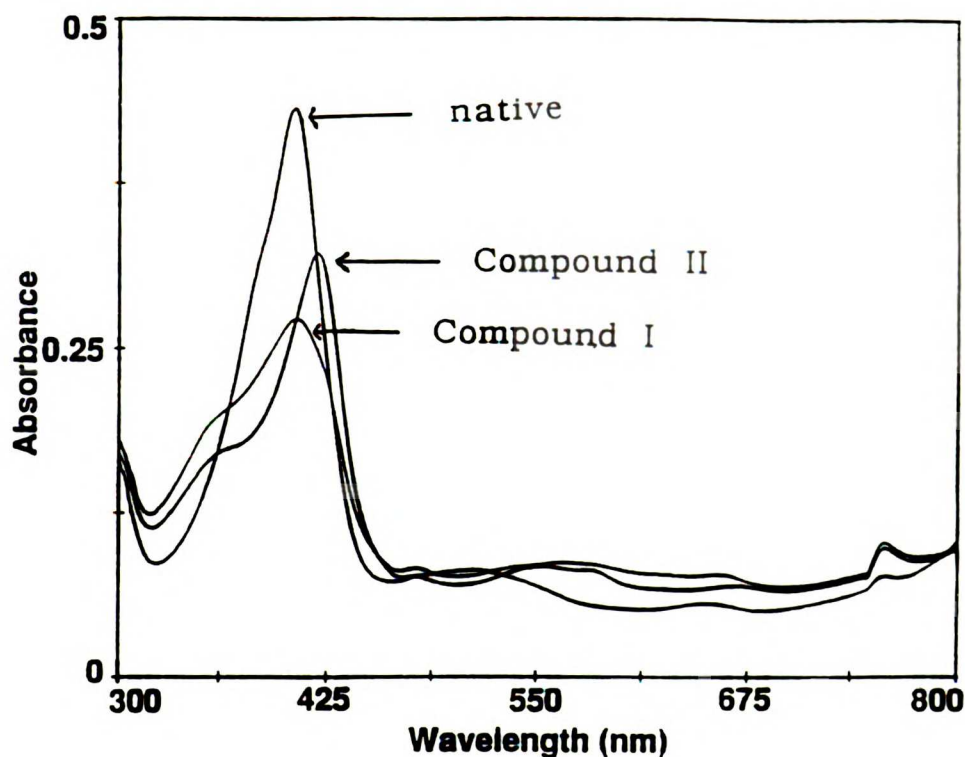


Figure 1.5.2. Spectra of native HRP, Compound I and Compound II.

### 1.6. Structure and Reactivity of Compound II.

Compound I is reduced by one electron to Compound II. The electron reduces the porphyrin radical cation (or the protein radical), leaving the ferryl iron-oxygen species (Penner-Hahn et al., 1986; Schultz et al., 1984), (Figure 1.5.1). Compound II has distinct spectral characteristics (Figure 1.5.2). HRP Compound II has a half-cell potential of 0.99 V (Hayashi and Yamazaki, 1979), nearly identical to that of Compound I. However, it is kinetically more stable toward most substrates (Dunford, 1991). Therefore, reduction of Compound II to native enzyme is usually rate limiting.

## **1.7 Structure of Compound III**

In the presence of a large excess of  $\text{H}_2\text{O}_2$ , HRP forms a species called Compound III. Compound III can also be formed by the reaction of ferrous HRP with molecular oxygen, or by the reaction with ferric HRP with superoxide (Dunford, 1991). The structure of Compound III is shown in Figure 1.5.1. It is a relatively inert species that does not take part in the normal catalytic cycle (Dunford, 1991).

## **1.8 Homologies Among Peroxidases**

As described in the preceding sections, a great deal is known about the catalytic mechanism of HRP and the structure of CCP. It is not clear, however, if it is justifiable to extrapolate the information on these peroxidases to other peroxidases.

All classical peroxidases characterized have a histidine residue as the proximal heme ligand, and all appear to react with hydrogen peroxide to form a Compound I species that is spectroscopically similar to the Compound I species of either HRP or CCP (Marnett et al., 1986; Ortiz de Montellano, 1992). Also, NMR and modeling studies suggest that the distal arginine and histidine residues are conserved in plant, animal, and fungal peroxidases (Dugad et al., 1990; Thanabal et al., 1987; Thanabal and La Mar, 1989). Thus, it seems reasonable to generalize, with caution, data on the heterolysis of the oxygen-oxygen bond and the electronic structure of Compounds I and II.

Plant peroxidases are approximately 50% identical in sequence. The 50% that is not identical appears to have a very similar secondary structure (Welinder, 1985). Thus, it has been predicted that the plant peroxidases have very similar tertiary structures (Welinder, 1985). This prediction is confirmed by circular dichroism studies (Job and Dunford, 1977; Strickland et al., 1968). Similarly, fungal and mammalian peroxidases appear to show a high degree of homology within their respective kingdoms.

Plant peroxidases and CCP have only 15% sequence identity (Takio et al., 1980). However, when the predicted secondary structure of HRP is aligned with the known structure of CCP, it appears that the two enzymes share many structural features (Welinder, 1985). This conclusion is supported by the recent low resolution crystal structure of HRP isozyme E5 which shows that HRP shares many structural features with CCP (Morita et al., 1991). Similarly, bacterial peroxidases appear to share many structural features with both plant and fungal peroxidases (Welinder, 1991). In contrast, it is nearly impossible to align the structures of the animal peroxidases with CCP (Kimura and Yamazaki, 1979). The difference in size between the fungal and mammalian peroxidases makes sequence alignments meaningless. Thus, extreme caution must be exercised when forming analogies between the active site topology of either plant or fungal peroxidases and the active site topology of mammalian peroxidases. Nevertheless, a recent low resolution crystal structure of myeloperoxidase suggests that this mammalian peroxidase has structural similarities to HRP (Zeng and Fenna, 1992).



## 1.9 Cytochrome P-450

The catalytic mechanism of cytochrome P-450 (P-450) has been extensively reviewed in the literature (Guengerich, 1987; Ortiz de Montellano, 1986). A brief description of the P-450 cycle is given below (Figure 1.9.1). P-450 reacts with oxygen and two electrons to form a Compound I-like species. This step is analogous to the first step of the peroxidase cycle: Oxygen plus 2 electrons is formally equivalent to hydrogen peroxide, and in some cases H<sub>2</sub>O<sub>2</sub> can replace the oxygen and 2 electrons used in P-450 catalysis (peroxide shunt). The Compound I-like species of P-450 can insert an oxygen atom into a substrate, giving hydroxylated substrate and native P450.

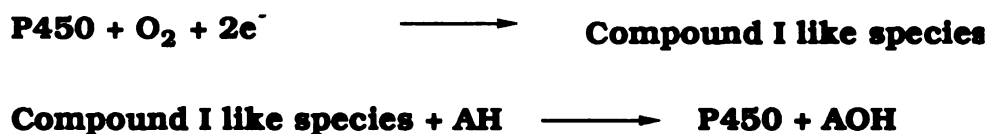


Figure 1.9.1. Catalytic cycle of cytochrome P-450.

The Compound I-like species of cytochrome P-450 has not been as well characterized as the Compound I species of HRP because it is very short-lived (McMurry and Groves, 1986). However, many studies suggest that it is similar in structure to HRP Compound I (Dawson, 1988; McMurry and Groves, 1986; Ortiz de Montellano, 1986). Both species appear to be 2 electrons oxidized relative to the ferric state and both

contain an iron-oxygen species. It is not known whether the Compound I-like species of P-450 contains an Fe(IV) or an Fe(V).

It should be noted that some studies suggest P-450s catalyze homolytic cleavage of the oxygen - oxygen bond, producing a Compound II-like species and a hydroxyl radical (Marnett et al., 1986; Poulos, 1986). If this mechanism is correct, it is somewhat more difficult to make direct comparisons between the Compound I species of peroxidase and the oxidized P-450 species. However, due to the reactivity of the hydroxyl radical, this mechanism is doubtful. Furthermore, a kinetic analysis suggests that homolysis, although catalyzed by P-450, is not involved in P-450 catalyzed hydroxylations (McCarthy and White, 1983).

### **1.10 An Intriguing Question**

An intriguing question is how cytochromes P-450 and peroxidases can be so similar and form such similar 2 electron deficient species, yet catalyze such different reactions. In other words, how does the protein direct the P-450 iron-oxygen species to insert its oxygen and the peroxidase iron-oxygen species to abstract electrons?

### **1.11 Oxygenase vs Peroxidase: The Effect of Proximal and Distal Residues**

Classical peroxidases have a histidine imidazole heme ligand, whereas P450s have a cysteine thiolate ligand. It is reasonable to hypothesize that the identity of the proximal ligand may determine

whether a hemoprotein behaves as a peroxidase or as an oxygenase. There is evidence, however, that the proximal ligand does not control hemoprotein reactivity in this fashion. CCP and chloroperoxidase contain an imidazole and a thiolate proximal ligand, respectively, yet each enzyme is able to catalyze both oxygenase and peroxidase reactions (Dawson et al., 1976; Miller et al., 1992). Likewise, model heme complexes, in which an imidazole is ligated to the heme iron, are able to catalyze oxygenase reactions (McMurry and Groves, 1986). Thus, it appears likely that the function of the proximal heme ligand is to provide the electron push needed to form and stabilize an iron-oxygen species. In the case of P-450, the large push of a thiolate is required, whereas in the case of peroxidases, the smaller push of an imidazole is required because there is also an electron pull provided by a distal arginine and a distal histidine residue. It is therefore likely that the distal and proximal residues affect the thermodynamic properties (redox potential) and kinetic stability of the electron deficient enzyme species, but they do not directly control the type of catalysis the species performs.

Again, it should be noted that there is evidence that suggests the thiolate ligand and the nonpolar distal residues of P-450 promote homolysis of the oxygen-oxygen bond, instead of the heterolysis observed with peroxidases (Marnett et al., 1986; Poulos, 1986). Furthermore, it has been suggested (Harold Van Wart, personal communication), that a *trans* effect (Doerge et al., 1991) may be important in determining whether a hemoprotein behaves as an oxygenase. The thiolate-iron bond is stronger than the imidazole-iron bond, thus the iron-oxygen bond of the thiolate ligated iron is weaker than the iron-oxygen bond of the

imidazole ligated iron (*trans* effect). The weaker bond is more easily broken and may thus facilitate oxygen insertion reactions. It is possible, therefore, that homolysis vs. heterolysis, or the *trans* effect, are key elements in determining whether a hemoprotein behaves as an oxygenase or a peroxidase. However, the results with CCP and chloroperoxidase clearly illustrate that if the above phenomena are factors in controlling hemoprotein reactivity, they are not the sole factors. Site directed mutagenesis studies may ultimately be the most useful tool in determining the role of the proximal ligand and the distal residues. To date, there have been no mutageneses that have provided conclusive results (Adachi et al., 1991; Smith et al., 1992; Vietch et al., 1992).

### **1.12 Oxygenase vs Peroxidase Activity: Miscellaneous Factors**

The polarity of the region surrounding the heme (Kassner, 1972) and the degree of exposure of the heme surface to solvent H<sub>2</sub>O (Stellwagen, 1978) are believed to influence the redox potential of a hemoprotein. There is no evidence, however, that these effects influence whether a hemoprotein behaves as a peroxidase or an oxygenase. Modifications of the heme structure may also influence hemoprotein reactivity, (see chapter 4), but this is not a general determinant because most hemoproteins do not contain modified prosthetic groups.

## 1.13 Oxygenase vs Peroxidase Activity: The Role of the $\delta$ -Meso Heme Edge

### 1.13.1 Inactivation by Phenylhydrazine and Phenyldiazene

Studies of the inactivation of hemoproteins by phenylhydrazine and phenyldiazene have provided valuable insights into the factors that control hemoprotein reactivity. Phenylhydrazine and phenyldiazene can each be oxidized to phenyl radicals (Figure 1.13.1).

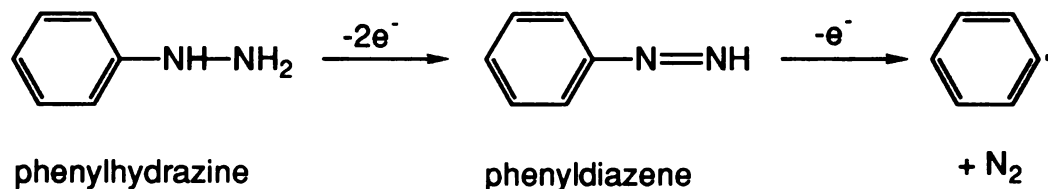


Figure 1.13.1. Formation of the phenyl radical via the oxidation of phenylhydrazine or phenyldiazene.

The phenyl radicals inactivate cytochrome P-450 by adding to the heme iron (Figure 1.13.2) (Raag et al., 1990; Swanson et al., 1991). The resulting iron-phenyl complex has distinct spectroscopic characteristics and has been detected in many types of hemoproteins (Augusto et al., 1982; Ortiz de Montellano and Kerr, 1983; Ringe et al., 1984). In contrast, when HRP is inactivated by phenylhydrazine or phenyldiazene, no iron-phenyl complex is observed. Instead, a small amount of heme arylated at the edge is found (Figure 1.13.2) (Ator and Ortiz de Montellano, 1987). This result led to the hypothesis that there is a large open area above the heme iron in P-450s. The substrate therefore has

access to the iron-oxygen species and oxygen insertion can occur. In contrast, the region above the heme iron in HRP is sheltered by the protein. The substrate does not have access to the iron-oxygen species and oxygen insertion does not occur. Instead, the substrate has access to the heme edge, and it is at this location that electron abstraction occurs. In cytochromes P-450, the protein buries the heme edge positions, preventing electron abstraction (Geigert et al., 1983).

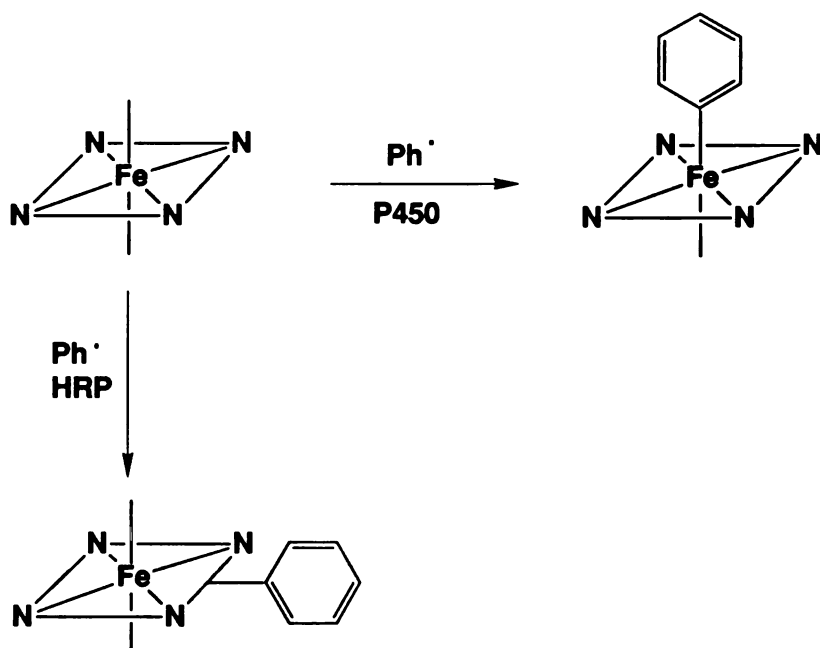


Figure 1.13.2. Addition of the phenyl radical to the heme iron of P-450 and to the heme edge of HRP.

### 1.13.2 Mechanism of $\delta$ -Meso Edge Modification

When the inactivation of HRP was characterized in detail, it was found that many other reagents, such as alkylhydrazines (Ator et al., 1987), azide (Ortiz de Montellano et al., 1988), and cyclopropanone

hydrate (Wiseman et al., 1982), behave as suicide substrates. A mechanism of inactivation was deduced (Figure 1.13.3): HRP Compound I oxidizes these substrates to reactive radicals that add to the *meso* position of the heme of Compound II. The porphyrin radical produced reduces the ferryl iron, yielding an isoporphyrin intermediate. The existence of this isoporphyrin intermediate is verified by an absorbance at approximately 840 nm that is predicted by model studies (Dolphin et al., 1970). The isoporphyrin decays via a loss of a proton to *meso*-substituted heme. Interestingly, only 1 of the 4 *meso* positions, the  $\delta$ -*meso* position, is modified. In addition, with certain suicide substrates, 100% inactivation correlates with 100% formation of  $\delta$ -*meso* substituted heme (Ator et al., 1989; Ortiz de Montellano et al., 1988). These results strongly suggest that substrates are oxidized in a region near the  $\delta$ -*meso* heme edge, and that the  $\delta$ -*meso* substituent inactivates the enzyme by denying the substrate access to this region.

The inactivation of HRP by phenylhydrazine differs from the inactivation by alkylhydrazines and azide in that 100% inactivation is accompanied by only a small amount of  $\delta$ -*meso* substituted heme. Instead, the major product of phenylhydrazine inactivation is arylated protein (Ator and Ortiz de Montellano, 1987). In addition, a modest amount of 8-hydroxymethylheme is formed during phenylhydrazine inactivation (Ator and Ortiz de Montellano, 1987), indicating that substrates also have access to the heme 8-methyl group. A mechanism for 8-hydroxymethylheme formation is shown in Figure 1.13.4.

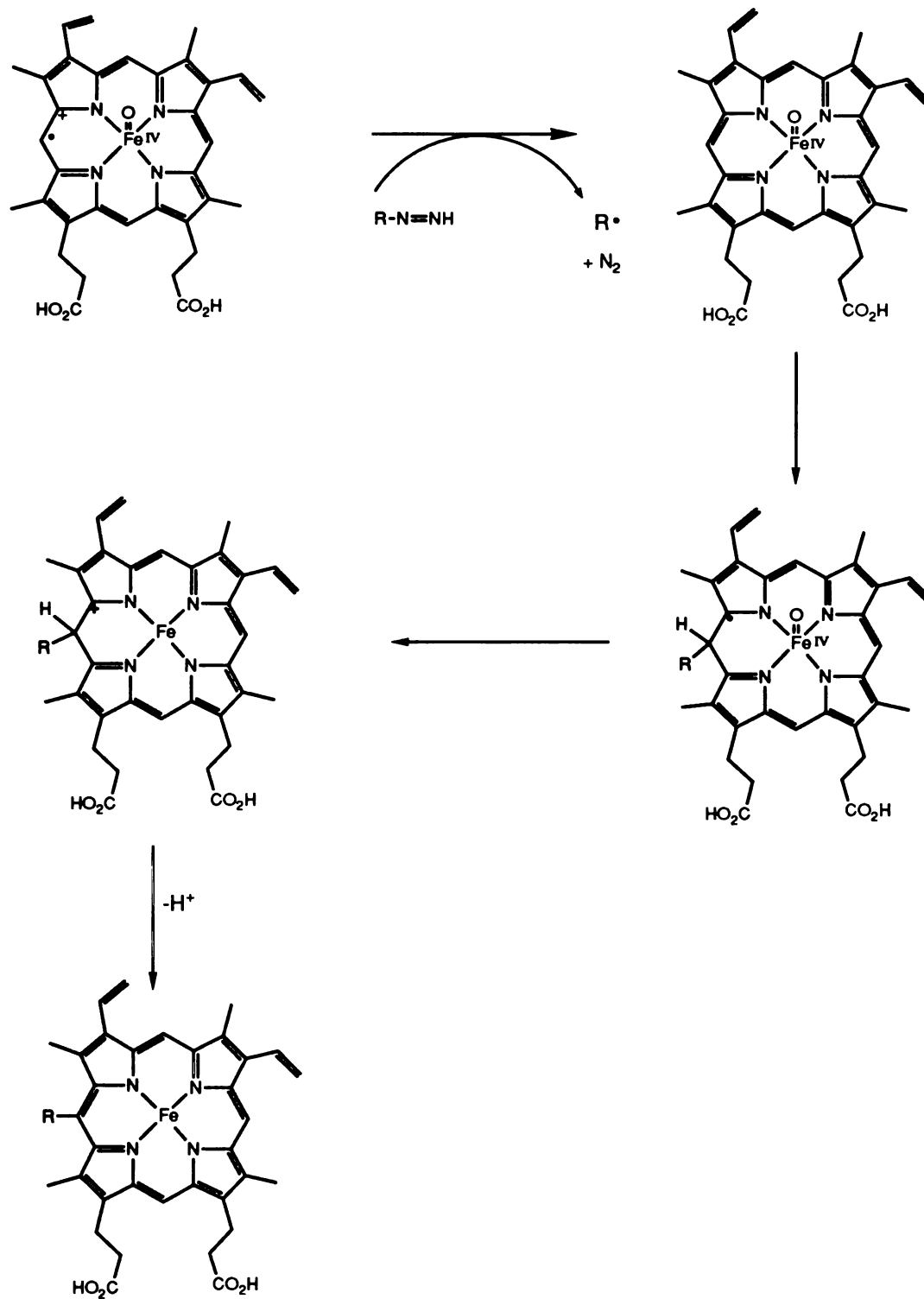


**Figure 1.13.3. Mechanism of HRP inactivation by alkylhydrazines. A similar mechanism applies for the other suicide substrates described in the text.**



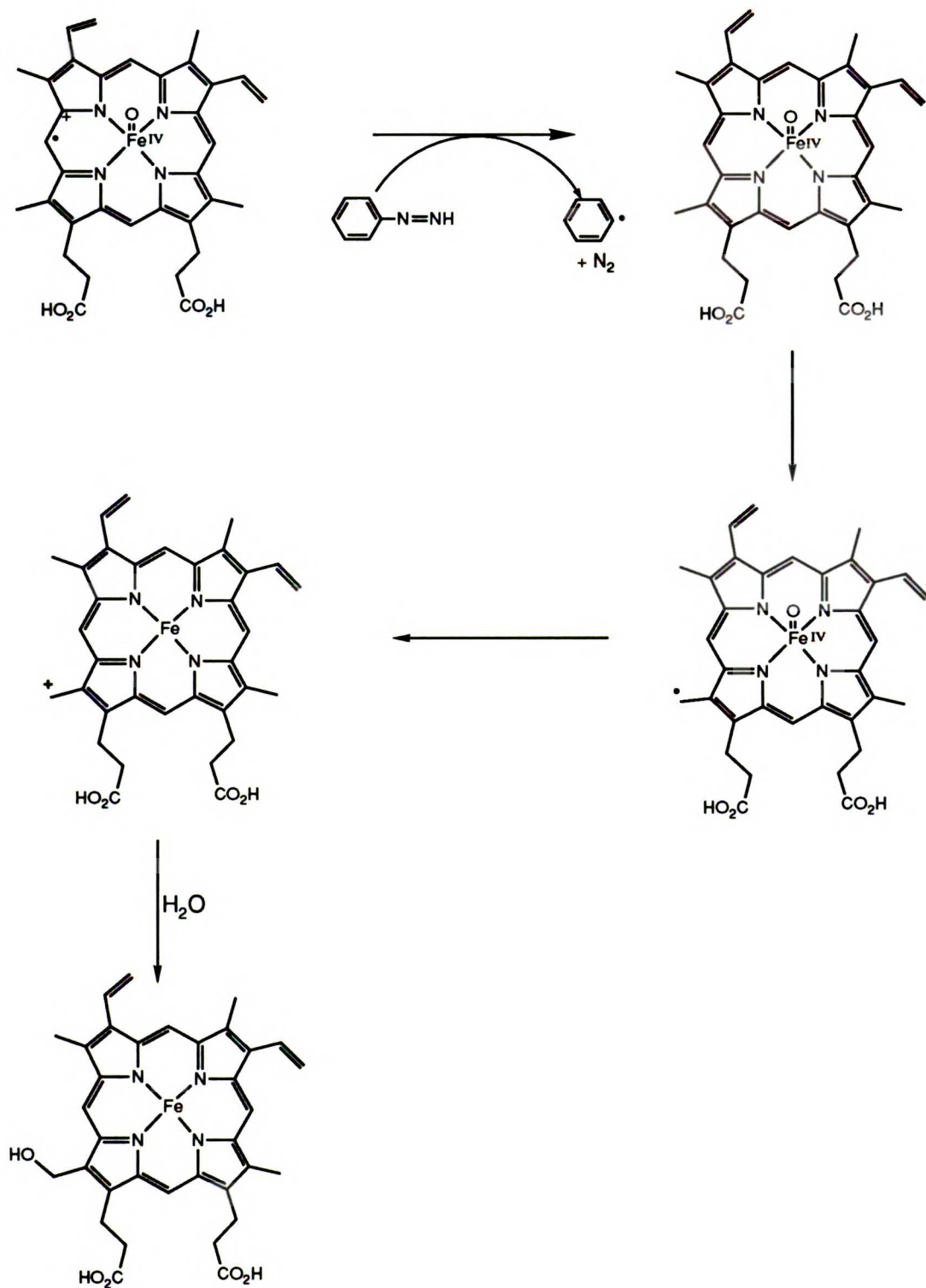


Figure 1.13.4. Mechanism of 8-hydroxymethylheme formation in HRP-phenyldiazene incubations.

### 1.13.3 Reconstitution Studies

To further examine the effect of heme substitution at the  $\delta$ -*meso* position, HRP was reconstituted with  $\delta$ -*meso*-methyheme,  $\delta$ -*meso*-ethylheme, and  $\delta$ -*meso*-azidoheme (Ator et al., 1987; Ortiz de Montellano et al., 1988). HRP reconstituted with  $\delta$ -*meso*-methyheme does not lose its ability to oxidize phenols. Thus, *meso* substitution *per se* does not inactivate HRP. In contrast, HRP reconstituted with  $\delta$ -*meso*-ethylheme or  $\delta$ -*meso*-azidoheme loses the ability to oxidize phenols, yet still reacts with H<sub>2</sub>O<sub>2</sub>. Thus, it appears that the larger substituent inactivates HRP by creating a steric barrier that denies phenols access to the  $\delta$ -*meso* edge.

### 1.13.4 NMR Studies

Nuclear Overhauser experiments (Modi et al., 1989; Sakurada et al., 1987) indicate that phenols bind to ferric HRP in a region near the heme 8-methyl group. NMR relaxation experiments (Saxena et al., 1990) suggest that the phenol is positioned approximately 8 Å from the heme iron. These studies suggest that phenolic substrates also bind to native HRP in a region near the  $\delta$ -*meso* heme edge.

## 1.14 A Hemoprotein Theory

The results of the preceding sections lead to the following hemoprotein theory: A hemoprotein that is able to form a Compound I-like species behaves as an oxygenase if its substrate has access to the

iron-oxygen species, and behaves as a peroxidase if its substrate only has access to the heme edge. In other words, the protein moiety controls hemoprotein reactivity by determining where the substrate binds relative to the heme group. This theory can be summarized by models of the peroxidase and the oxygenase active sites (Figure 1.14.1)

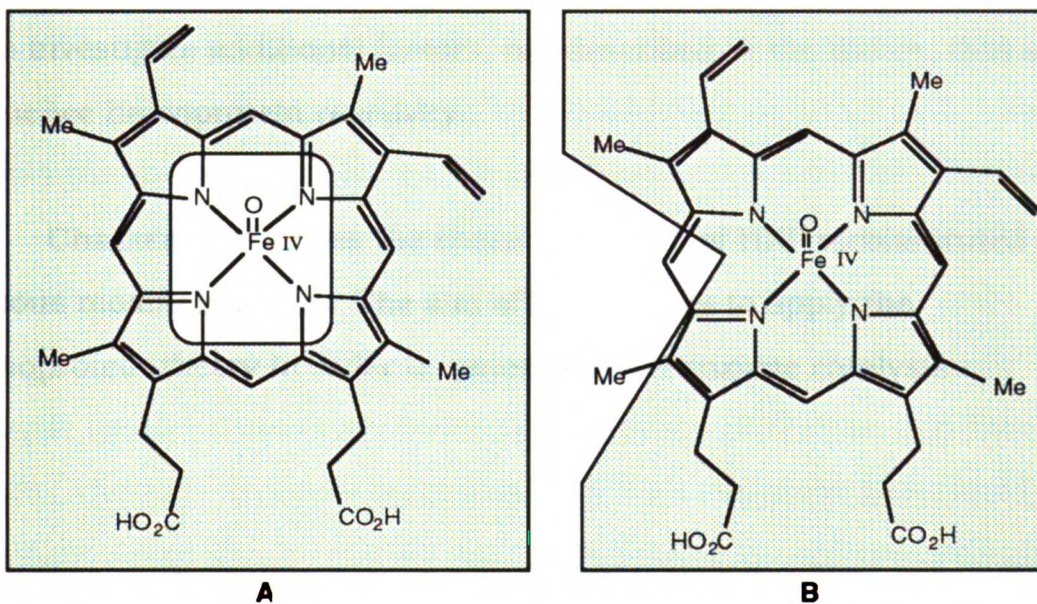


Figure 1.14.1. Models of A) oxygenase active site and B) peroxidase active site. The shaded region represents protein.

## 1.15 Thesis Overview

Chapter 2 describes the characterization of manganese peroxidase. The primary aim of this work is to test the generality of the hemoprotein theory.

**Chapter 3 describes the characterization of thioanisole oxidation by HRP. The primary aim of this work is to investigate a possible flaw in the hemoprotein theory.**

**Chapter 4 describes the characterization of HRP reconstituted with 8-hydroxymethylheme and 8-formylheme. The primary aim of this work is to investigate additional factors, not described in the theory, that may influence hemoprotein reactivity.**

**Chapter 5 describes the characterization of HRP reconstituted with various modified hemes. The aim of this work is to apply the hemoprotein theory in order to generate novel enzyme catalysts.**

## **2.0 Inactivation of Manganese Peroxidase by Azide and Hydrazines**

### **2.1 Introduction**

Lignin is a complex phenylpropanoid polymer that makes up approximately 25% of the mass of woody plants (Crawford, 1981; Gold et al., 1989; Kirk and Farrell, 1987). It is extremely degradation resistant, so its breakdown is a key element in the recycling of the earth's carbon supply (Bumpus et al., 1985; Gold et al., 1989; Kirk and Farrell, 1987). The white rot fungus *Phanerochaet chrysosporium* secretes 2 families of peroxidases that catalyze the H<sub>2</sub>O<sub>2</sub> dependent degradation of lignin. One family is comprised of the lignin peroxidase isozymes which directly degrade lignin (Glenn et al., 1983; Leisola et al., 1987; Tien and Kirk, 1983). The second family is comprised of the manganese peroxidase (MnP) isozymes which catalyze manganese-mediated lignin degradation.

MnP is a 46,000 Dalton glycoprotein that contains one heme prosthetic group (Glenn and Gold, 1985; Pascynski et al., 1986). Its amino acid sequence has been deduced through its cDNA (Pease et al., 1989; Pribnow et al., 1989) and it has recently been expressed in a baculovirus system (Pease et al., 1991). Recent NMR studies suggest that MnP shares the structural features found in other classical peroxidases (Banci et al., 1992). Electronic absorption, EPR, and resonance Raman studies suggest that the heme is coordinated to a histidine ligand (Mino et al., 1988). Sequence alignment studies suggest that MnP has the distal histidine and arginine residues that are believed to mediate peroxide bond cleavage (Pease et al., 1989; Poulos and Kraut,

1980). The oxidation-reduction potential of the ferric/ferrous couple has been estimated to be -88 mv compared to -278 mv for HRP, indicating that the heme environment of MnP does not stabilize positive charge as well as that of HRP (Millis et al., 1989).

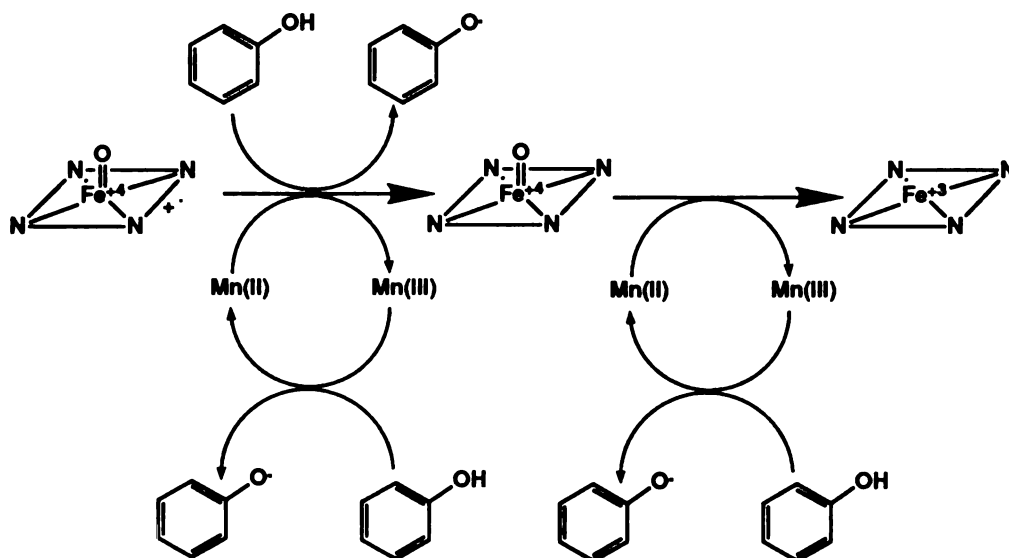


Figure 2.1.1 The catalytic cycle of MnP.

The catalytic cycle of MnP is very similar to that of HRP (Figure 2.1.1). MnP reacts with H<sub>2</sub>O<sub>2</sub> to form a 2 electron oxidized Compound I species. Like HRP Compound I, MnP Compound I appears to contain a ferryl iron-oxo species and a porphyrin radical cation (Wariishi et al., 1988; Wariishi and Gold, 1989). It also has an A<sub>2u</sub> electronic ground state (Wariishi et al., 1988). MnP Compound I is reduced by 1 electron to Compound II by Mn(II), ferrocyanide, or phenols (Wariishi et al., 1988; Wariishi and Gold, 1989). Like HRP, the porphyrin radical cation of MnP is reduced preferentially over the ferryl iron. Unlike HRP Compound II

however, the Compound II species of MnP is efficiently reduced only by Mn(II), which is oxidized to Mn(III), or by ferrocyanide (Pascynski et al., 1986; Wariishi et al., 1988; Wariishi and Gold, 1989). Therefore, Mn(II) (or ferrocyanide) is necessary for completion of the MnP catalytic cycle (Glenn et al., 1986; Pascynski et al., 1986). It is interesting to note that HRP does not efficiently oxidize manganese (Glenn and Gold, 1985). This difference in reactivity may be due to the relatively high oxidation potential of MnP Compounds I and II (Hammel et al., 1986; Millis et al., 1989) or to a steric effect.

The Mn(III) that is produced diffuses from the enzyme and mediates substrate oxidation (Aitken and Irvine, 1990). Mn(III) is a strong oxidizing agent capable of oxidizing a variety of molecules such as NADH, ABTS, phenols, and lignin model compounds (DiCosimo and Szabo, 1987; Hammel et al., 1989). The ability of MnP to oxidize most substrates in the presence of Mn(II) directly correlates with the ability of Mn(III) to oxidize the substrates (Aitken and Irvine, 1990; Glenn and Gold, 1985). For example, in the presence of pyrophosphate, which forms an inert complex with Mn(III), neither Mn(III) nor the MnP-Mn(II) system is capable of oxidizing phenols (Glenn and Gold, 1985). Thus, Mn(III) is believed to be the active agent that is involved in MnP mediated wood degradation (Gold et al., 1989; Hammel et al., 1989). A mechanism, based on model compound studies, for Mn(III) catalyzed lignin degradation has been proposed (DiCosimo and Szabo, 1987). Mn(III) is capable of abstracting electrons from the lignin polymer, producing radical cations that undergo various types of degradation reactions such as side chain cleavage and oxygen addition (Figure 2.1.2).

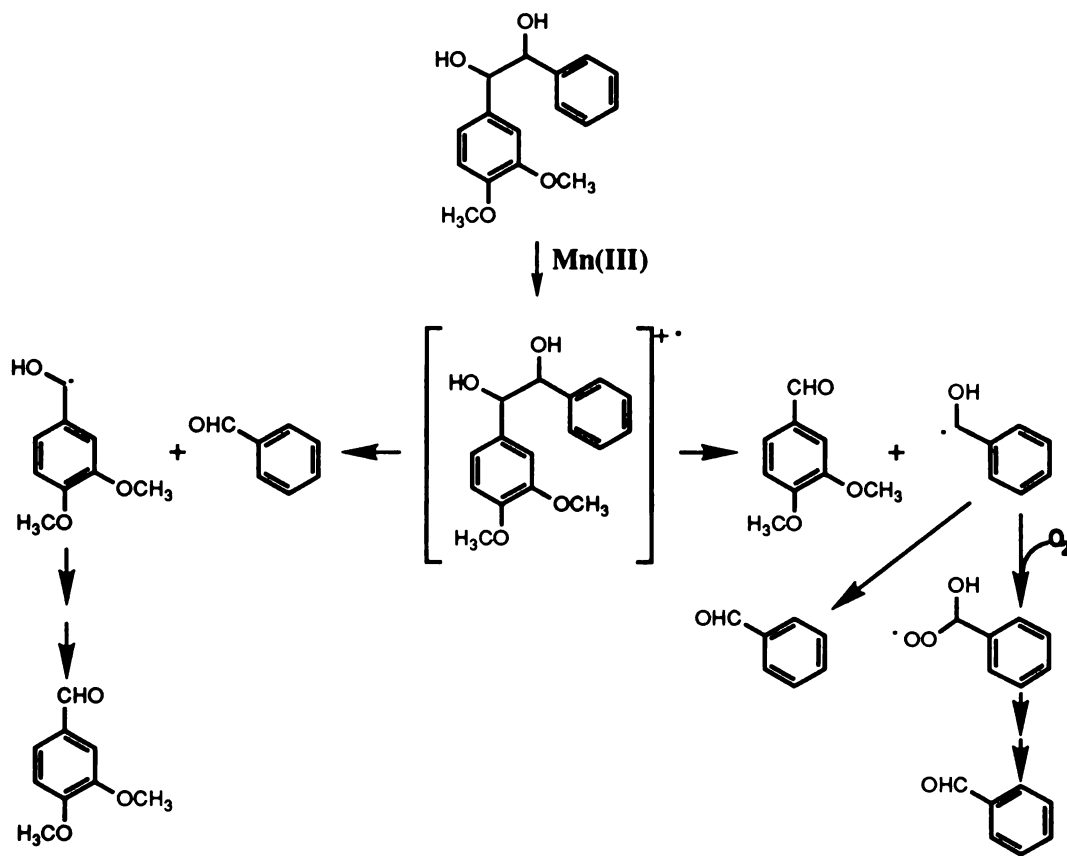


Figure 2.1.2 Degradation of a lignin model compound by Mn(III).

Recently, a theory has developed which describes how the protein moiety of a hemoprotein determines whether the hemoprotein catalyzes oxygen insertion (oxygenase activity) or electron abstraction (peroxidase activity) (Ator et al., 1987; Ator and Ortiz de Montellano, 1987; Ortiz de Montellano et al., 1987; Ortiz de Montellano et al., 1988). (Chapter 1 section 14). According to this theory, the location of substrate binding, relative to the heme group, determines the activity displayed. If a substrate binds near the iron-oxo species, oxygen insertion occurs; whereas if the substrate binds near the heme edge, electron abstraction occurs. There are numerous pieces of evidence that support this theory:



(1) HRP inactivation by azide, alkylhydrazines, and arylhydrazines results in substitution of the heme at the  $\delta$ -*meso* position (Ator et al., 1987; Ator and Ortiz de Montellano, 1987; Ortiz de Montellano et al., 1988), (2) HRP reconstituted with  $\delta$ -*meso*-ethylheme cannot catalyze substrate oxidation (Ator et al., 1987), (3) HRP, in contrast to cytochrome P-450, does not form an iron-phenyl complex when incubated with phenylhydrazine or phenyldiazene (Raag et al., 1990), (4) The crystal structure of P450<sub>CAM</sub> reveals that the heme edge is buried by protein (Poulos, 1986; Poulos et al., 1986), and (5) NMR studies suggest that phenols bind to native HRP near the heme 8-methyl group (Saxena et al., 1990).

It is likely that this hemoprotein theory applies to HRP, because the theory is based primarily on the results of HRP studies. However, the generality of the theory is not known. MnP was therefore examined to test the generality of the hemoprotein theory and to gain insights into the unique reactivity of MnP towards manganese.

## **4.2 Experimental Procedures**

### **Materials**

Ethylhydrazine oxalate and butylhydrazine oxalate were obtained from Fluka. Phenylhydrazine hydrochloride, tert-butylhydrazine hydrochloride, succinic acid disodium salt, malic acid, hematin, N-tert-butyl-phenylnitron (PBN), Sephadex G-25, methylhydrazine sulfate, manganese (III) acetate dihydrate and sodium hydrosulfite were obtained

from Aldrich. Phenylhydrazine·HCl and methylhydrazine·SO<sub>4</sub> were recrystallized from ethanol before use. Phenylethylhydrazine was obtained from ICN. Manganese sulfate monohydrate was obtained from Mallinckrodt. Ascorbic acid, HRP (type VI), bovine liver catalase, 2,2-azino-bis-(3-ethylbenzthiazoline sulfonic acid) (ABTS), hydrogen peroxide (nominal 10 M), Trizma HCl and Diethylenetriaminepentaacetic acid (DETAPAC) were purchased from Sigma. Methylhydrazine sulfate was from ICN. Cobaltous acetate was obtained from J. T. Baker Chemical Company. Methylphenyldiazene carboxylate azo ester was obtained from Research Organics. Phenyldiazene carboxylate was produced by delivering 3 μL of the azo ester into a vial containing 2 mL of 1.0 M sodium hydroxide that had been bubbled with argon for one hour. Phenyldiazene was generated *in-situ* when the phenyldiazene carboxylate was added to the pH 4.5 enzyme incubations. All phenyldiazene incubations were performed in buffer that had been bubbled with argon in order to remove oxygen.

Buffers were made with glass-distilled deionized water. Metals were removed by mixing with Chelex 100 (Biorad) 2.5 g/L for 12 hours. Unless otherwise noted, all MnP incubations were carried out in 50 mM succinate, 10 mM malate buffer, pH 4.5, and all HRP incubations were carried out in 50 mM phosphate buffer, pH 7.0. Stock solutions of hydrazines were prepared in 0.01 N HCl in order to lessen their autooxidation in solution. They were kept on ice and used within 6 hours after preparation.

MnP isozyme I was purified from the extracellular medium of an acetate-buffered agitated culture of *P. chrysosporium* strain OGC101 (Alic et al., 1987) as previously reported (Glenn and Gold, 1985). The purified enzyme was electrophoretically homogeneous and had a *pI* of 4.9. The protein concentration in the stock solution was estimated to be 10 mg/mL from the Lowry protein assay but 6.5 mg/mL from the extinction coefficient ( $\epsilon_{406\text{nm}} = 129 \text{ mM}^{-1} \text{ cm}^{-1}$ ). The difference in concentrations was probably due to heme loss because the R/Z (A406/A280) value for the enzyme was 4.7 rather than 6.1, the value for freshly prepared enzyme. The enzyme was stored at -80 °C.

$\delta$ -Meso-ethylheme and  $\delta$ -meso -azidoheme were obtained from HRP incubations (Ator et al., 1987; Ortiz de Montellano, 1987) and  $\gamma$ -meso-ethylheme was obtained from myoglobin incubations (Choe and Ortiz de Montellano, 1991) as already described.

Kinetic assays were performed on a Hewlett-Packard 8450A diode array spectrophotometer. Electronic absorption spectra were obtained with an Aminco DW-2000 spectrophotometer, (scan rate 3 nm/sec, slit width 3 nm). HPLC was performed on a Hewlett-Packard 1090 liquid chromatography system equipped with a diode array detector.

### **Manganese Peroxidase Assay**

MnP activity was measured by monitoring its ability to oxidize ABTS. MnP (1  $\mu\text{g}$ ) was added to a cuvette containing 1 mM manganous sulfate and 40  $\mu\text{g}$  (72  $\mu\text{M}$ ) ABTS in 1 mL of succinate-malate buffer, pH

4.5. ABTS oxidation was initiated by the addition of 2.5  $\mu\text{L}$  of 0.02 M  $\text{H}_2\text{O}_2$  (50  $\mu\text{M}$  final concentration). The rate of ABTS oxidation was calculated from the increase of absorbance at 415 nm. Because MnP directly oxidizes ABTS very slowly, the assay is a measure of the rate at which MnP oxidizes Mn(II) to Mn(III).

### **Kinetics of Inactivation by Alkylhydrazines**

Typical incubations contained 0.8  $\mu\text{M}$  MnP, 200  $\mu\text{M}$  hydrogen peroxide, and various concentrations of alkylhydrazine in a volume of 0.5 mL. All incubations were carried out at room temperature. At various times, a 20  $\mu\text{L}$  aliquot was removed and the activity was assayed as described.

### **Isolation and Characterization of Heme Adducts**

MnP (5  $\mu\text{M}$ ) in 3 mL of either pH 7.0 or pH 4.5 buffer was incubated with sodium azide (150  $\mu\text{M}$ ) and hydrogen peroxide (200  $\mu\text{M}$ ) for 10 min. Catalase (5  $\mu\text{L}$  of a 1 mg/mL solution) was added, and the mixture stood for 5 min to destroy any remaining hydrogen peroxide. Ascorbic acid (5  $\mu\text{L}$  of a 10 mg/mL solution) was then added to reduce all iron species to the ferric state. Similar incubations were performed with methylhydrazine (750  $\mu\text{M}$ ) and ethylhydrazine (500  $\mu\text{M}$ ) except that the reaction volume and incubation time were increased to 6 mL and 15 min. To pH 4.5 incubations, 12 mL of pH 7 phosphate buffer (1 M) was added

before the addition of catalase, because catalase has low activity at pH 4.5.

The incubations were acidified with 0.5 mL of acetic acid and the hemes were extracted twice with 3 mL of diethyl ether. When necessary, low speed centrifugation was used to break up emulsions. The ether fractions were pooled and washed twice with 3 mL of distilled water. The ether was removed under a stream of nitrogen gas and the heme residue was then dissolved in approximately 1 mL of HPLC solvent.

Reverse phase HPLC on a 5 mm column packed with Whatman Partisil ODS-3 was used to separate the heme products. The column was eluted with the gradient (solvent A: 60:40:0.1 MeOH:H<sub>2</sub>O:CF<sub>3</sub>CO<sub>2</sub>H; solvent B: 100:0.1 MeOH:CF<sub>3</sub>CO<sub>2</sub>H): 0-10 min 25% solvent B in solvent A, 10-25 min linear rise from 25% B to 100% B, and 25-30 min, 100% B. The flow rate was 1 mL/min and the column effluent was monitored at 406 nm.

### **Spin Trapping of the Azidyl Radical**

At room temperature, a 30  $\mu$ L aliquot of 100  $\mu$ M MnP was added to a solution of sodium azide (25 mM), PBN (70 mM), DETAPAC (10  $\mu$ M), and hydrogen peroxide (350  $\mu$ M) in 120  $\mu$ L of pH 4.5 buffer. The final peroxidase concentration was 26  $\mu$ M. A 50  $\mu$ L aliquot of the incubation was immediately transferred to a capillary tube and placed into a quartz EPR tube aligned in the sample cavity of the EPR. Scanning began approximately 20 seconds after the initiation of the reaction. EPR

spectrophotometer settings were: scan range 10 x 10 Gauss; time constant 0.25 sec.; field set 3400 Gauss; scan time 2 min; modulation amplitude 1 x 1; gain  $5 \times 10^4$ ; power 10 db = 20 mW; microwave frequency 9.51 GHz; second harmonic 100 KHz.

A similar experiment was performed with the Compound II species of MnP. A ten fold excess of hydrogen peroxide was added to the enzyme and the mixture was allowed to stand for two min to promote Compound II formation before it was added to the reaction mixture. Control experiments were carried out with HRP. Conditions were identical except that the incubations were performed in pH 7.0 phosphate buffer.

#### **Determination of Partition Ratios**

Manganese Peroxidase (0.8  $\mu\text{M}$ ) in 0.5 mL of pH 4.5 buffer was incubated for 6 min with  $\text{H}_2\text{O}_2$  (200  $\mu\text{M}$ ) and sodium azide (0.25 to 10.0  $\mu\text{M}$ ). A 20  $\mu\text{L}$  aliquot was then removed and assayed for its ability to oxidize ABTS. Phenyl diazene incubations were similarly performed except that phenyl diazene concentrations ranged from 20 to 120  $\mu\text{M}$  and the reaction time was decreased to three min. Activity was also assayed at later time points to ensure there was no further inactivation.

#### **Kinetics of Soret Absorbance Decrease**

Sodium azide (50  $\mu\text{M}$  final concentration) was added to a quartz cuvette containing 40  $\mu\text{g}$  MnP in 0.5 mL pH 4.5 buffer. Hydrogen peroxide was then added (200  $\mu\text{M}$  final concentration) to initiate the

reaction. The absorbance at 421 nm (Soret) - 700 nm (baseline) was then monitored for thirty min. The Soret wavelength (wavelength of maximal heme absorbance) remained at 421 nm over this time period.

Similar incubations were performed with methylhydrazine except that the methylhydrazine concentration was 700  $\mu\text{M}$ , the  $\text{H}_2\text{O}_2$  concentration was 250  $\mu\text{M}$ , and the absorbance was monitored at 419 nm - 700 nm.

### **Reconstitution of MnP with Hematin and $\delta$ -Meso -Ethylheme**

MnP apoprotein was reconstituted with hemin following a procedure similar to that already described (Ortiz de Montellano et al., 1988). In an ice bath, MnP (25 nmol) was dissolved in 0.5 mL of  $\text{H}_2\text{O}$  and the solution was acidified to pH 2.5 by the addition of 0.1 M HCl. The heme was extracted twice into 2 mL of butanone, resulting in the loss of most of the heme color from the aqueous layer. Low speed centrifugation was used to break up emulsions. The organic layer was discarded and the aqueous layer, containing apo-MnP, was dialyzed for 3 h against 2 liters of distilled  $\text{H}_2\text{O}$  and then 4 h against 2 liters sodium phosphate buffer, pH 7.0 (the optimal pH for reconstitution of this enzyme). The resulting apoprotein had no catalytic activity.

Hemin and  $\delta$ -meso -ethylheme were quantitated using the extinction coefficient  $\epsilon_{397} = 0.1 \mu\text{M}^{-1}$ . A four-fold excess of heme was dissolved in a few drops of NaOH and immediately added dropwise to the apoenzyme in pH 7.0 buffer. The resulting mixture was stirred for 12 h

at 4 °C and then run down a Sephadex G-25 column equilibrated with pH 4.5 buffer in order to remove excess heme. The solution was then vigorously bubbled with N<sub>2</sub> to remove, by precipitation, heme that was not properly reconstituted.

### **Formation of Ferrous-CO Complex**

Enzyme samples were placed in a septum covered cuvette and bubbled for 20 min with CO. A crystal of sodium sulfite was then added and the sample bubbled with CO for an additional 1 min. The reduced CO spectrum was immediately acquired.

### **Inhibition by Cobalt**

Cobalt was tested as a competitive inhibitor of manganese oxidation by MnP. MnP activity was measured as described above except that cobaltous acetate was present in the cuvette and the manganous ion concentration was varied (10 μM - 5 mM).

The kinetics of MnP inactivation by methylhydrazine (400 & 800 μM) and sodium azide (2.5 μM) in the presence of cobaltous acetate (4 mM) were measured as described above. Two control incubations were carried out, one of which contained MnP (0.8 mM), cobaltous acetate (1 mM), and H<sub>2</sub>O<sub>2</sub> (200 mM) and the other MnP (0.8 mM) and cobaltous acetate (8 mM).



## 2.3 Results

### Inactivation by Sodium Azide

Sodium azide caused fast (within 2 min)  $\text{H}_2\text{O}_2$  dependent inactivation of MnP (Figure. 2.3.1). Nearly 100% inactivation was observed when only 2 equivalents of azide were incubated with the enzyme (Figure 2.3.1).

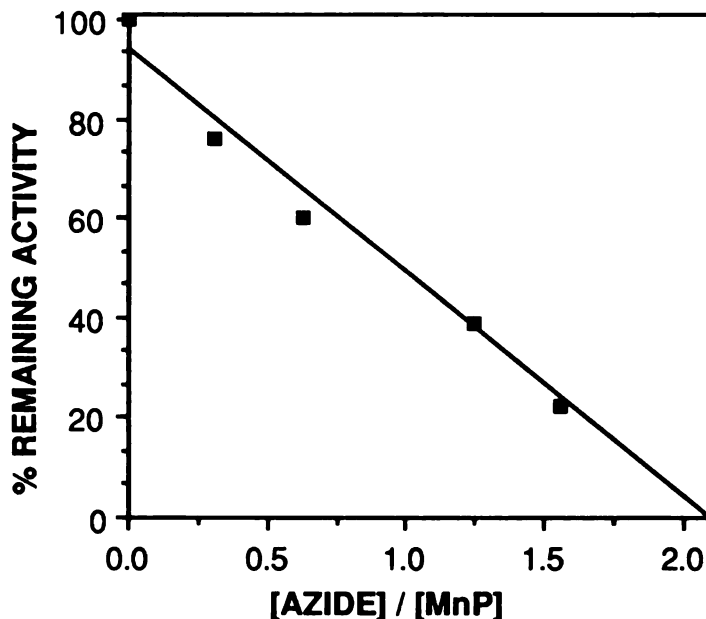
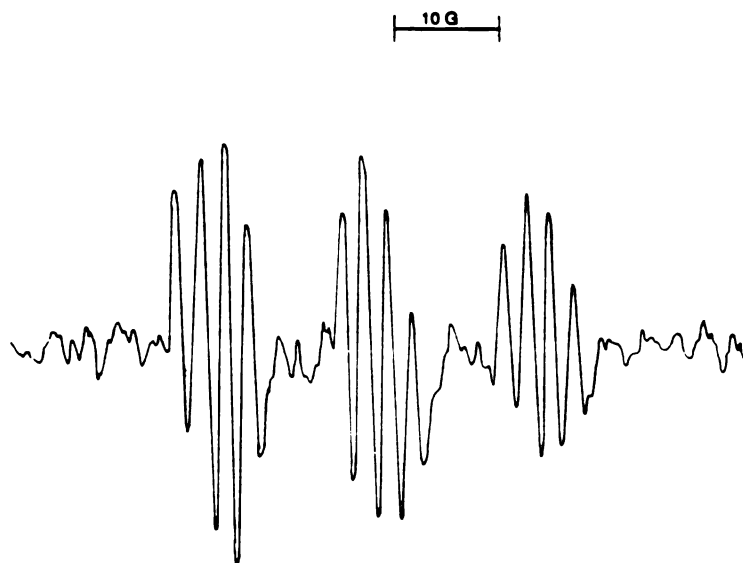


Figure 2.3.1. Partition ratio of azide mediated MnP inactivation.

Azidyl radicals that can be trapped by POBN were produced in MnP-azide incubations (Figure 2.3.2). The production of these radicals was both MnP and  $\text{H}_2\text{O}_2$  dependent. As expected, the EPR spectrum of the spin adduct formed in MnP-azide incubations was identical to the spectrum of the adduct formed in HRP azide incubations. MnP

Compound II also generated azidyl radicals, indicating that azide is capable of reducing the Compound II species of MnP.



**Figure 2.3.2.** EPR spectrum of the PBN trapped azidyl radical produced in an MnP-azide incubation.

No Fe-azide complex ( $\lambda_{\text{max}} = 417 \text{ nm}$ ) (Glenn and Gold, 1985) was observed during MnP - azide incubations. Instead, a Compound II spectrum having a 2 nm red-shifted Soret (relative to heme containing MnP) was observed, suggesting that a *meso*-modified heme was formed (Figure 2.3.3). The Soret decayed more rapidly over time (half-life = 2.3 h) than the Soret of unmodified MnP in the presence of  $\text{H}_2\text{O}_2$  (half-life = 4.8 h) indicating that the modified heme is more susceptible to peroxide mediated degradation than unmodified heme.

HPLC analysis of the heme extracted from an MnP incubation that contained sodium azide verified that a modified heme was produced (Figure 2.3.4). The modified heme, which was less polar than heme, had an HPLC retention time and an electronic absorption spectrum

(Figure 2.3.5) identical to that of a  $\delta$ -*meso*-azidoheme standard, although it is not certain that the  $\delta$ -*meso*-azido isomer was formed. However, because the HPLC system is capable of separating 2 *meso*-methylheme isomers (Choe and Ortiz de Montellano, 1991), it is likely the system can also separate *meso*-azido isomers. The small amount of sample available prevented unambiguous structural determination by NMR.

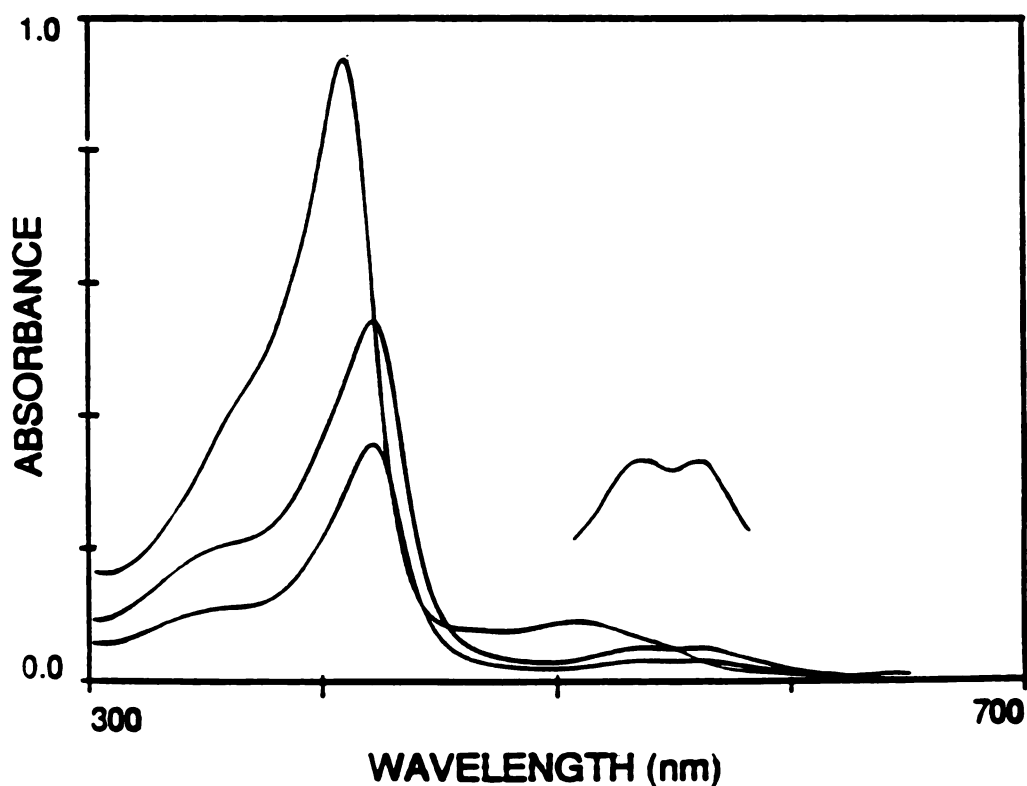


Figure 2.3.3. Spectrum of a MnP-azide incubation before addition of H<sub>2</sub>O<sub>2</sub> (top line), 5 min after addition of H<sub>2</sub>O<sub>2</sub> (middle line) and 30 min after addition of H<sub>2</sub>O<sub>2</sub> (bottom line). The expanded tracing shows long wavelength bands at 528 and 558 nm, characteristic of a Compound II species, that are observed in the bottom two traces.

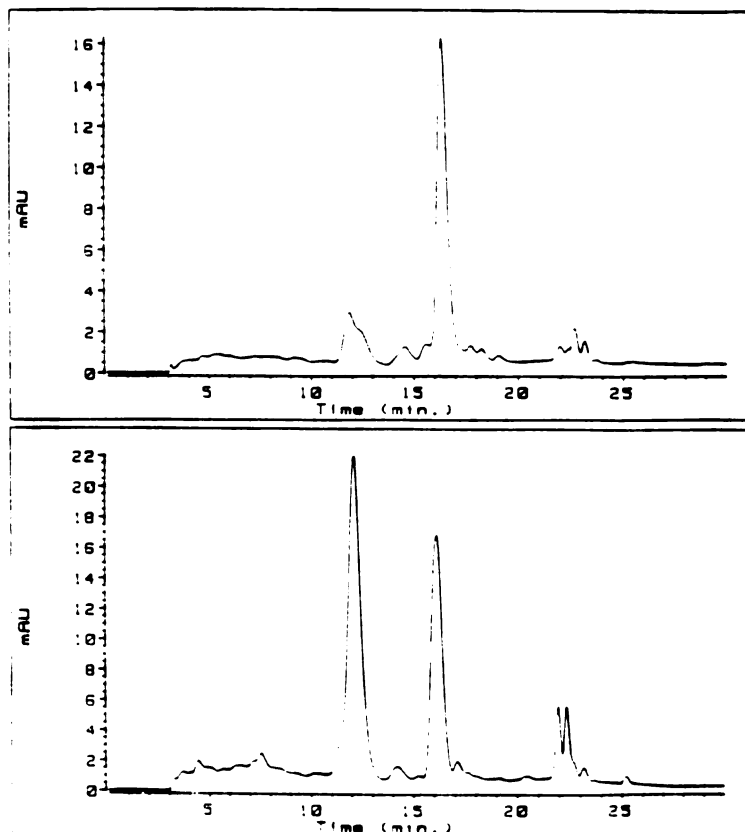


Figure 2.3.4. HPLC chromatogram of the prosthetic group extracted from azide-inactivated MnP (top) and partially azide-inactivated HRP (bottom). The peak at 12 min is heme. The peak at 16 min is  $\delta$ -meso-azidoheme.

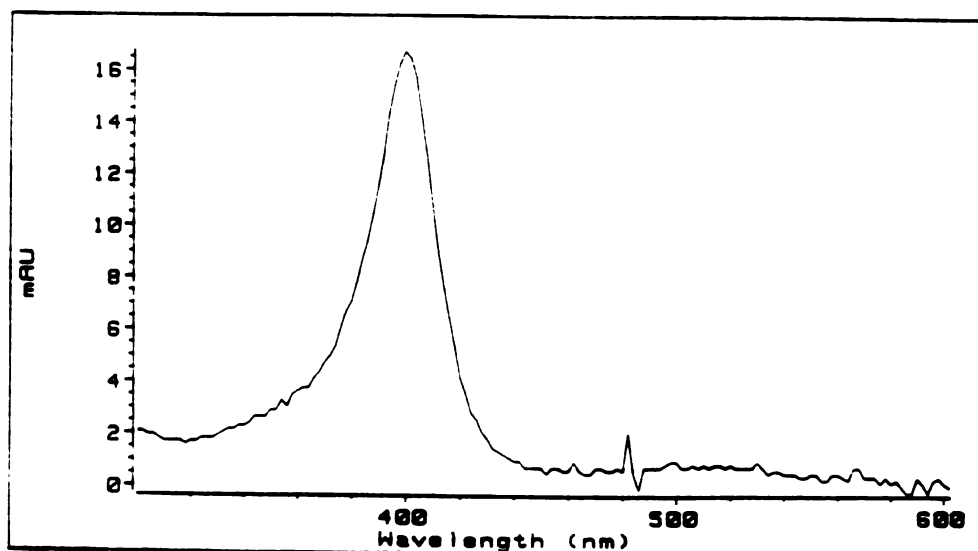


Figure 2.3.5. Electronic absorbance spectrum of  $\delta$ -meso-azidoheme obtained in an MnP-azide incubation. The Soret peak is at 402 nm.

## Alkylhydrazine Incubations

Methylhydrazine causes a slow, concentration dependent inactivation of MnP (Figure 2.3.6). The kinetics of inactivation are consistent with a suicide mechanism. A secondary plot (Figure 2.3.6, inset) yields  $K_I = 402 \mu\text{M}$  and  $k_{\text{inact}} = 0.22/\text{min}$  for MnP inactivation by methylhydrazine. Although MnP is most active at pH 4.5, it was inactivated slightly more rapidly at pH 7 (data not shown). This result may be due to the higher concentration of unprotonated hydrazine at pH 7 compared to pH 4.5. Ethylhydrazine also inactivates MnP, but a detailed kinetic profile of this inactivation was not obtained.

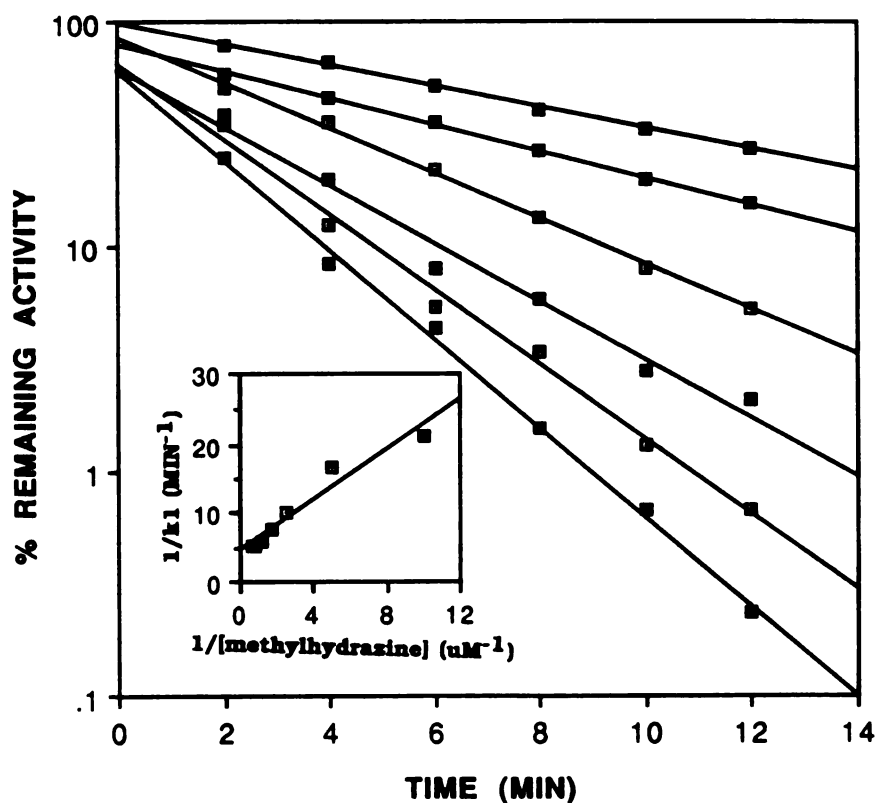


Figure 2.3.6. Time-dependence of methylhydrazine inactivation of MnP. The concentration of methylhydrazine was, from top to bottom, 100, 200, 400, 600, 800, and 1600  $\mu\text{M}$ . The inset shows the secondary plot used to calculate kinetic constants of inactivation.

The Soret absorbance of MnP Compound II decreases in the presence of  $\text{H}_2\text{O}_2$  and alkylhydrazines (half-life = 26 min) at a faster rate than in the presence of  $\text{H}_2\text{O}_2$  alone (half-life = 128 min; Figure 2.3.7), indicating that heme degradation occurs during alkylhydrazine inactivation. The rate of heme degradation, however, is considerably lower than the rate of inactivation (half-life = 9 min) (Figure 2.3.7). Both appeared to be first order process.

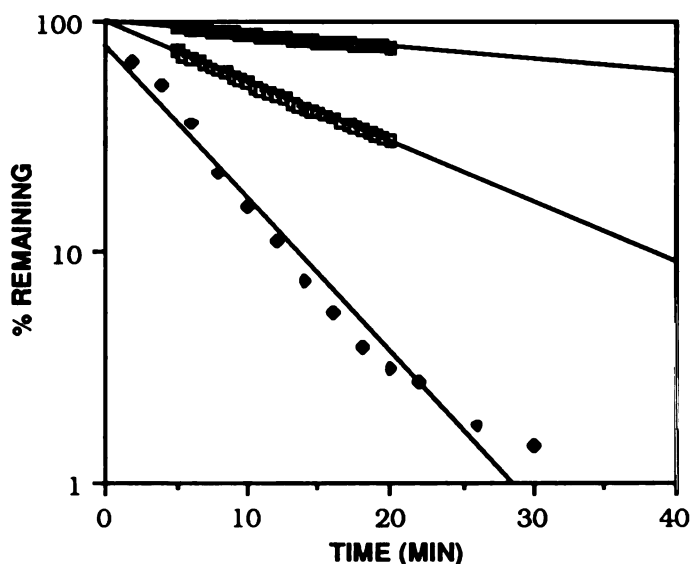


Figure 2.3.7. Time-dependence of Soret absorbance loss (middle line) and activity loss (bottom line) in an MnP methylhydrazine incubation. The top line is the Soret absorbance loss from a control incubation containing only enzyme and  $\text{H}_2\text{O}_2$ .

Heme products were isolated from pH 4.5 incubations that contained MnP and alkylhydrazine. HPLC analysis of the products revealed only unmodified heme and heme degradation products. However, at pH 4.5, HRP also only forms heme degradation products

when incubated with alkyhydrazines (Dr. Victor Samokyszyn, personal communication). Either alkylheme adducts are not formed, or the adducts are degraded rapidly at the low pH. An attempt was therefore made to isolate the heme products from a pH 7.0 MnP-ethylhydrazine incubation. A small amount of heme that coeluted with, and had the same electronic absorption spectrum as  $\delta$ -*meso*-ethylheme, was observed (Figure 2.3.8). The majority of the heme, however, was unmodified or degraded. Similar results were obtained with methylhydrazine, although a greater amount of heme degradation was observed.

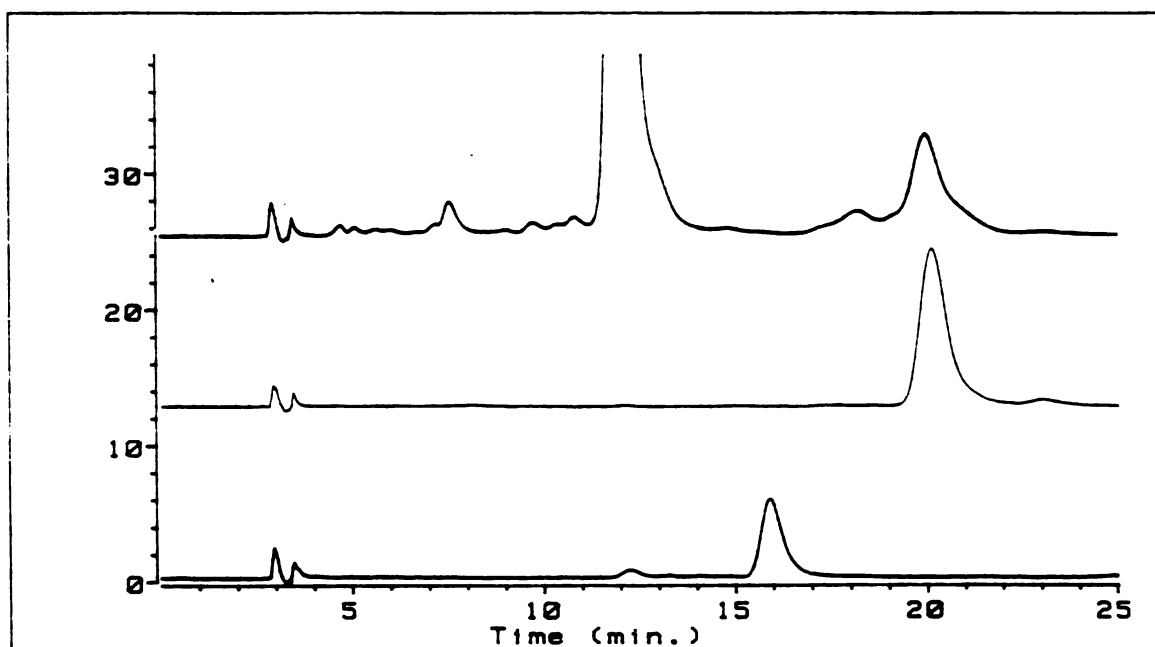


Figure 2.3.8. HPLC chromatogram of  $\gamma$ -*meso*-ethylheme standard (bottom),  $\delta$ -*meso*-ethylheme standard (middle), and  $\delta$ -*meso*-ethylheme produced in an MnP-ethylhydrazine incubation (top). The peak at 12 min is heme.

## Arylhydrazine Incubations

Phenylhydrazine and phenyldiazene both rapidly inactivate MnP in the presence of  $H_2O_2$  (Figure 2.3.9).  $H_2O_2$  is not required for phenyldiazene inactivation, presumably because phenyldiazene can autooxidize in solution. The partition ratio for inactivation is high, indicating inefficient inactivation. Importantly, the high wavelength electronic absorbance of the iron-phenyl complex is not observed during inactivation. Thus, it is unlikely that the inactivation is caused by the formation of an iron-phenyl complex.

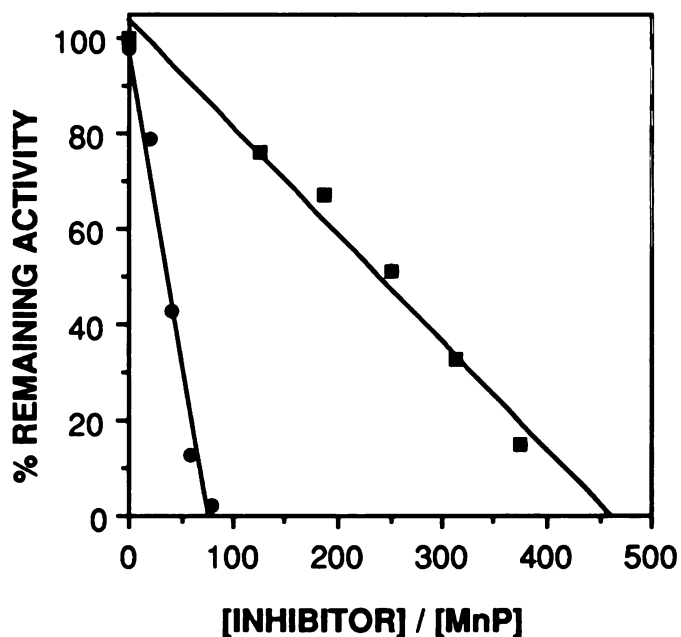


Figure 2.3.9 Partition ratios for the inactivation of MnP by phenylhydrazine (upper line) and phenyldiazene (lower line)



## Reconstitution Studies

MnP apoprotein displayed low heme absorbance and no catalytic activity. The spectrum of apo-MnP that had been reconstituted with hemin or  $\delta$ -*meso*-ethylheme had an extremely broad Soret (Figure 2.3.10), indicating improper heme reconstitution. Fortuitously, it was discovered that vigorous bubbling of the reconstituted enzyme with N<sub>2</sub> resulted in a considerable sharpening of the Soret peak (Figure 2.3.10). The bubbling caused the sharpening by removing incorrectly reconstituted protein rather than by causing protein to reconstitute correctly because a colored insoluble precipitate formed and neither the intensity of the Soret band (406 nm) nor the net catalytic activity of the solution increased during the bubbling process. The spectral characteristics and the catalytic activity of native MnP were not affected by bubbling.

The Soret band of heme reconstituted MnP was at 406 nm, identical to that of native MnP. The Soret band of  $\delta$ -*meso*-ethylheme containing MnP was 3 nm red-shifted to 409 nm. This red-shifting is expected in protein reconstituted with *meso*-modified heme. In order to determine if the reconstituted heme was incorporated correctly into the protein, the ferrous - CO complex was generated (Figure 2.3.11). Both reconstituted enzymes formed normal ferrous-CO complexes that have a sharp Soret band at 423 nm with an extinction coefficient larger than that of the ferric enzyme (Glenn and Gold, 1985).

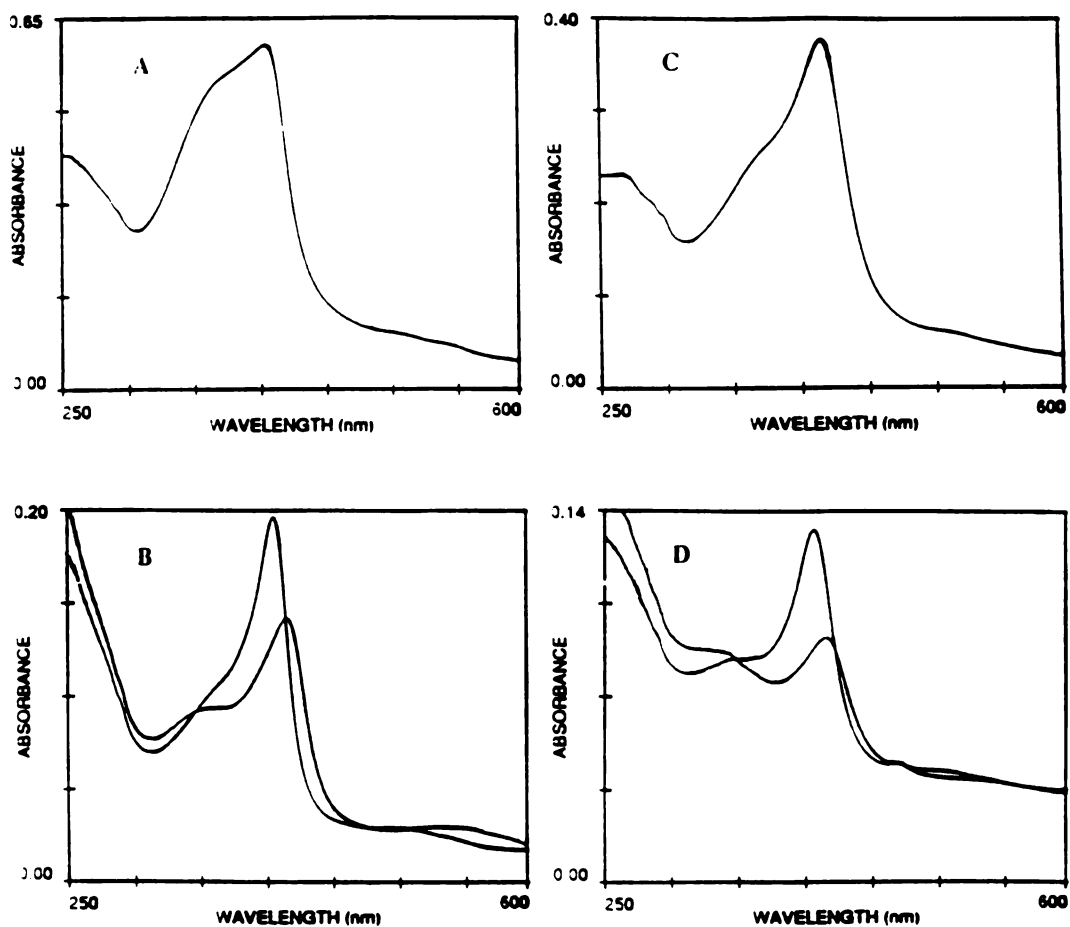


**Figure 2.3.10.** Electronic absorption spectra of MnP reconstituted with hemin (A, B) and with  $\delta$ -meso-ethylheme (C,D). Spectra A and C are of the reconstituted proteins before bubbling with  $N_2$ . The lower traces in B and D are the spectra after the addition of  $H_2O_2$ .

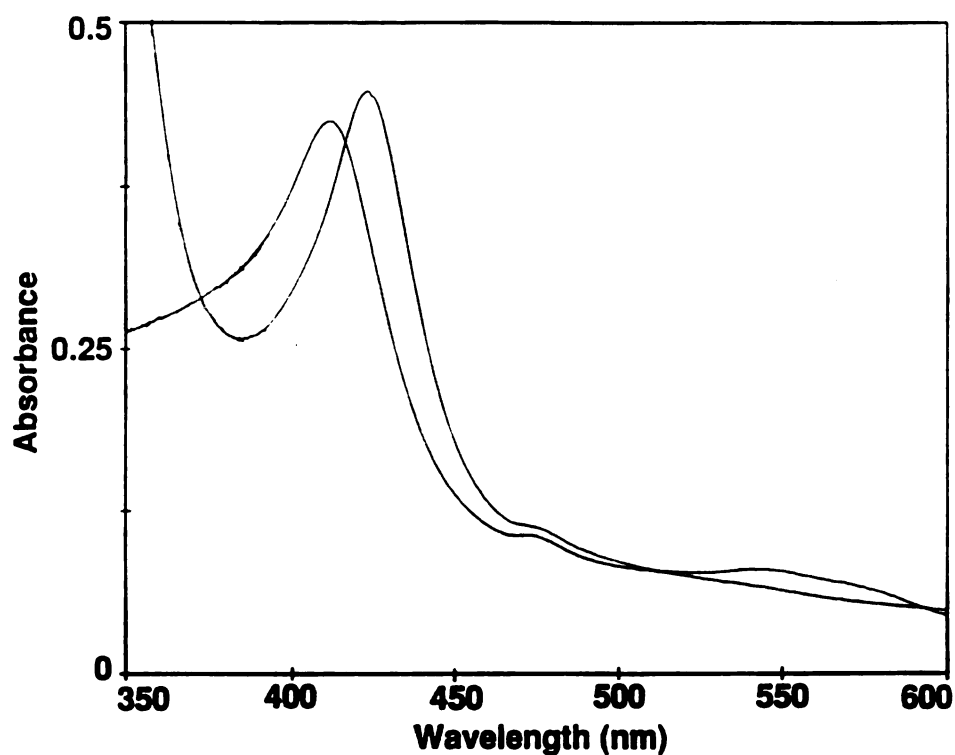


**Figure 2.3.11.** Electronic absorption spectrum of the ferric ( $\lambda_{\text{max}} = 409$  nm) and the reduced CO ( $\lambda_{\text{max}} = 423$  nm) complex of  $\delta$ -meso-ethylheme reconstituted MnP.

When  $\text{H}_2\text{O}_2$  was added to  $\delta$ -meso-ethylheme-reconstituted MnP, a decrease and red-shifting of the Soret band (to 419 nm) was observed (Figure 2.3.10). This decrease and red-shifting is virtually identical to the decrease and red-shifting observed when  $\text{H}_2\text{O}_2$  is added to hemin reconstituted MnP or native MnP.

The activities of equal amounts of hemin reconstituted,  $\delta$ -meso ethylheme reconstituted, and native MnP were compared (quantitation

based on magnitude of Soret absorbance). Hemin reconstituted MnP had half the activity of MnP (Table 2.3.1), whereas  $\delta$ -*meso*-ethylheme-reconstituted MnP had only 5% the activity of MnP. None of the enzyme species could oxidize ABTS or phenols at a significant rate in the absence of manganese.

<u>Enzyme</u>	<u>Relative Activity (%)</u>
native	100
reconstituted	
heme	50
$\delta$ - <i>meso</i> -ethylheme	5

Table 2.3.1. Catalytic activity of native, hemin reconstituted, and  $\delta$ -*meso*-ethylheme reconstituted MnP.

The 5% activity of  $\delta$ -*meso*-ethylheme-reconstituted MnP is rapidly eliminated when the modified enzyme is incubated with azide and H<sub>2</sub>O<sub>2</sub>. Control experiments indicate that this loss is not due to peroxide-mediated heme degradation. The heme products from  $\delta$ -*meso*-ethylheme containing MnP that had been inactivated by azide were analyzed by HPLC (Figure 2.3.12). Most of the *meso*-ethylheme was unaltered by azide. There was, however, a small amount of a new heme species. It was not possible to determine the structure of this new heme species because of the small amount available.

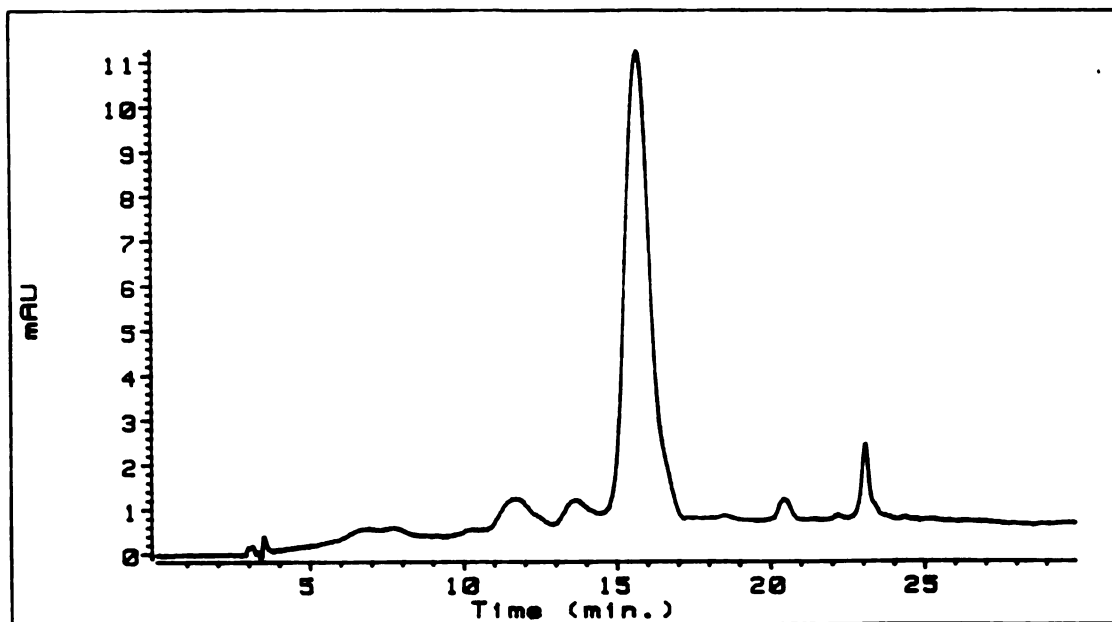


Figure 2.3.12. HPLC chromatogram of the heme extracted from a  $\delta$ -meso-ethylheme reconstituted MnP - azide incubation. The peak at 16 min is  $\delta$ -meso-ethylheme. The identity of the small peak at 23 min is unknown.

### Incubations Containing Cobalt

At concentrations below 4 mM, Co(II) was found to be a competitive inhibitor of Mn(II) oxidation ( $K_I = 1$  mM). At higher Co(II) concentrations, a greater amount of inhibition than would be expected from solely competitive inhibition was observed. In the presence of  $H_2O_2$ , cobalt also inactivated MnP in a time and  $H_2O_2$  dependent manner (Figure 2.3.14). This inactivation likely accounts for the unexpectedly high degree of MnP inhibition at high cobalt concentrations. At lower cobalt concentrations, simple competitive inhibition was observed because the rate of cobalt mediated inactivation was insignificant.

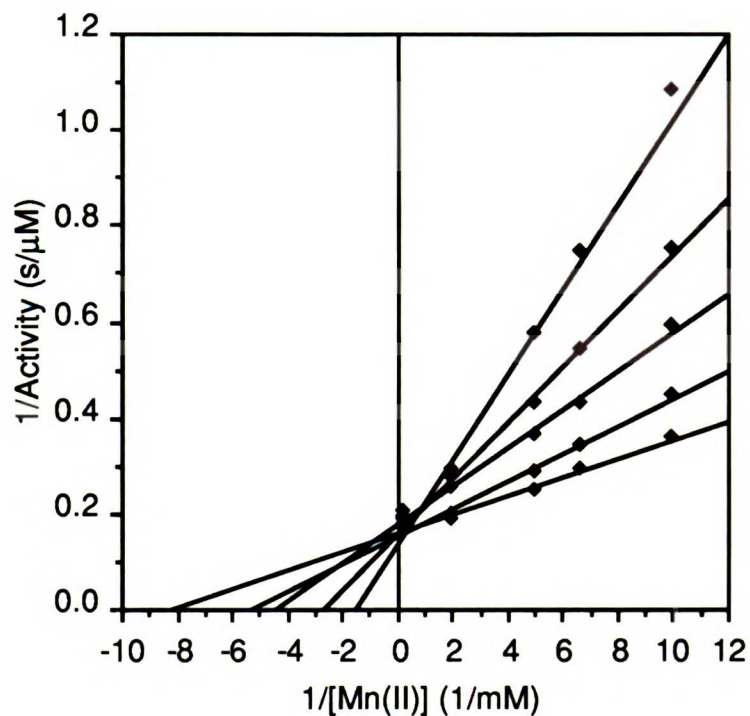


Figure 2.3.13. Competitive inhibition of manganese oxidation by cobalt. Cobalt concentrations were (from bottom to top) 0, 1, 2, 3, and 4 mM.

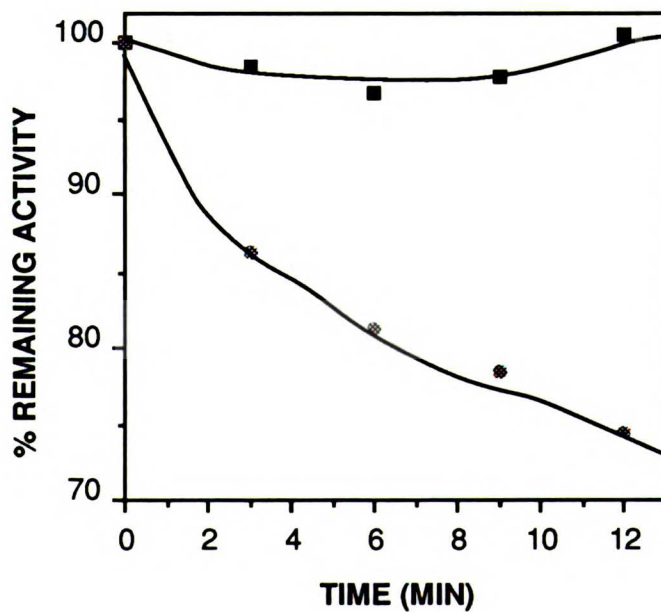


Figure 2.3.14. Inactivation of MnP by 1 mM cobalt in the presence (circles) or absence (squares) of H<sub>2</sub>O<sub>2</sub>.

Cobalt did not affect the rate of MnP inactivation by azide, and slightly accelerated the rate of inactivation by alkylhydrazines (Figure 2.3.15). This acceleration was likely due to the cobalt mediated inactivation described above because the rate of inactivation in the presence of both azide and methylhydrazine was approximately equal to the sum of the two individual rates of inactivation.

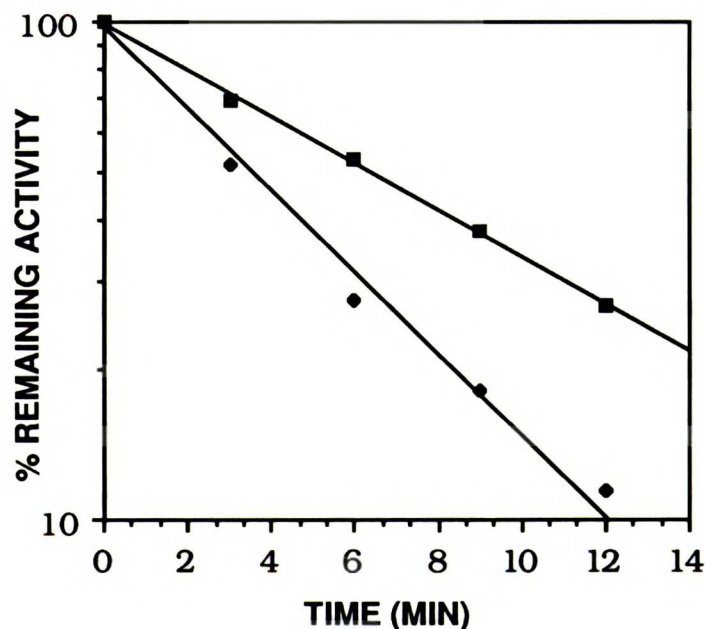


Figure 2.3.15. Ethylhydrazine inactivation of MnP in the presence (bottom line) and absence (top line) of cobalt.

## 2.4 Discussion

MnP is able to oxidize azide to the azidyl radical (Figure 2.3.2). Surprisingly, MnP Compound II, which is not capable of oxidizing classical peroxidase substrates, is also able to efficiently oxidize azide.

Presumably, the small azide molecule has access to a region that phenols cannot reach.

The azidyl radical that is produced can inactivate MnP. The inactivation is extremely efficient: only two molecules of azide per molecule of enzyme are required for complete inactivation (Figure 2.3.1). The fact that this number is greater than unity supports the conclusion that MnP Compound II can oxidize azide. The observed partition ratio of 1 is more than one order of magnitude lower than that observed for HRP inactivation by azide (Ortiz de Montellano et al., 1987). Therefore, the active site of MnP traps the azidyl radical more efficiently than does the active site of HRP.

The inactivation by azide results in the production of a modified heme that is likely  $\delta$ -*meso*-azidoheme. The fact that a spectroscopically normal Compound II species was present during the azide incubations illustrated that the *meso*-substituent did not inactivate MnP by preventing the enzyme from reacting normally with H<sub>2</sub>O<sub>2</sub>. Thus, MnP appears to react with azide in a manner similar to the way HRP reacts with azide (Ortiz de Montellano et al., 1988). Both enzymes oxidize azide in a region near the  $\delta$ -*meso* heme edge, and the azidyl radical produced adds to the heme  $\delta$ -*meso* position, resulting in enzyme inactivation. The *meso*-substituent likely inactivates MnP by denying manganese access to the region near the heme edge.

Alkylhydrazines also inactivate MnP. This inactivation is considerably slower than azide inactivation, so that the acquisition of



kinetic data was possible. The kinetic parameters for the inactivation of MnP by methylhydrazine are similar to the parameters for the inactivation of HRP by methylhydrazine. At pH 4.5, no  $\delta$ -*meso*-alkylheme adduct is obtained from MnP or HRP incubations. However, in MnP-alkylhydrazine incubations at pH 7, a small amount of  $\delta$ -*meso* adduct is isolated (Figure 2.3.8). There are at least 2 explanations as to why only a small amount of heme adduct is formed in these incubations. Either the *meso*-alkylheme adducts are unstable and degrade, or the alkylhydrazines inactivate primarily via protein modification. The fact that the rate of Soret band loss is significant, but lower than the rate of inactivation (Figure 2.3.7), suggests that both mechanisms are occurring. Incubations with radiolabeled methylhydrazine could be used to detect protein alkylation.

Phenylhydrazine and phenyldiazene also inactivate MnP (Figure 2.3.9). This inactivation was much less efficient than azide inactivation. Presumably, the inefficiency of arylhydrazine inactivation is related to the inability of MnP to efficiently oxidize aromatic compounds such as phenols. Importantly, no iron-phenyl complex was observed in MnP-arylhydrazine incubations. Therefore, there is likely a protein barrier above the heme iron that denies substrates access to the iron-oxygen species.

In order to determine more unambiguously if manganese is oxidized at the  $\delta$ -*meso* heme edge, MnP was reconstituted with  $\delta$ -*meso*-ethylheme. The  $\delta$ -*meso*-ethylheme reconstituted enzyme appeared to form a normal reduced carbon monoxide complex (Figure 2.3.11) and a

normal Compound II species (Figure 2.3.10) except that the *meso*-substituent causes a slight red-shifting of the Soret absorbance. However, the enzyme reconstituted with  $\delta$ -*meso*-ethylheme had only 10% of the activity of hemin-reconstituted enzyme (Table 2.3.1). The fact that  $\delta$ -*meso*-methylheme-reconstituted HRP retains activity illustrates that *meso* substitution *per se* does not eliminate peroxidase activity. It is thus likely that the  $\delta$ -*meso*-ethyl group inactivates MnP by denying Mn(II) access to the heme edge.

It is somewhat surprising that  $\delta$ -*meso*-ethylheme-reconstituted MnP retains 10% of the activity whereas the enzyme is completely inactivated by azide. There are at least 2 possible explanations of this phenomenon. First, manganese may be able to bind (though not in the optimal position for oxidation) near the  $\delta$ -*meso* heme edge when an ethyl, but not an azido group is linked to the heme edge. This possibility is reasonable because the ethyl group is bent whereas the azido group is linear and coplanar with the heme. Second, approximately 10% of the enzyme may have been reconstituted with the heme in an orientation flipped by 180° about the plane that bisects the  $\alpha$ - and  $\gamma$ -*meso* carbons. There is precedence for this type of heterogeneous reconstitution (La Mar et al., 1989; Levy et al., 1985). The fact that incubation with azide eliminated the activity of  $\delta$ -*meso*-ethylheme-reconstituted MnP supports the second explanation. If the enzyme was reconstituted with heme that was flipped, the  $\beta$ -*meso* position should have been catalytically active, and azide treatment should produce  $\delta$ -*meso*-ethyl- $\beta$ -*meso*-azidoheme. In fact, there was a novel heme produced in the incubations (2.3.12). However, lack of sample prevented structural characterization.

It appears that MnP substrates are oxidized near the  $\delta$ -meso heme edge. However, it is difficult to imagine molecules as different as azide and manganese binding at the same site. Thus, in order to determine if Mn(II) and azide or Mn(II) and ethylhydrazine bind at the same site, competition studies were performed. Direct competition studies could not be performed because MnP oxidizes Mn(II) extremely rapidly and the Mn(III) produced is capable of oxidizing azide and hydrazines. Therefore, an attempt was made to find a relatively inert metal that could replace Mn(II) in these studies.

Cobalt was found to be a competitive inhibitor of manganese oxidation by MnP (Figure 2.3.13). Therefore Co(II) and Mn(II) bind in the same region within the MnP active site. Cobalt is also oxidized by MnP in the presence of H<sub>2</sub>O<sub>2</sub>, but this oxidation is very slow compared to manganese oxidation (Glenn et al., 1986). The slow oxidation of cobalt appears to produce a species that inactivates MnP (Figure 2.3.14). The rate of this inactivation was negligible in incubations that contained manganese. The mechanism of this inactivation was not determined.

Cobalt did not affect the rate of azide inactivation and slightly increased the rate of ethylhydrazine inactivation of MnP (Figure 2.3.15). The increase in rate can be attributed to the slow peroxide dependent inactivation of MnP by cobalt. The rate of inactivation in the presence of cobalt and ethylhydrazine is approximately equal to the sum of the rate of cobalt mediated inactivation and the rate of ethylhydrazine mediated inactivation. (The rate of inactivation in the presence of azide and cobalt

equaled the rate in the presence of azide alone because azide inactivation is so fast that cobalt inactivation is negligible). If cobalt and azide or cobalt and ethylhydrazine compete for the same binding site, the rate of inactivation in the presence of the two reagents would be considerably lower than the sum of the individual rates. (This is true because high concentrations of cobalt, ethylhydrazine, and azide were used in these studies.) Thus, these results strongly suggest that cobalt and alkylhydrazines (or azide) do not compete for the same binding site. Therefore, manganese and alkylhydrazines (or azide) bind at separate sites in the MnP active site, although both are clearly oxidized near the  $\delta$ -*meso*-heme edge.

It should be noted that Aitken and Irvine have shown that Cu(II) catalyzes the decomposition of Mn(III) by hydrogen peroxide (Aitken and Irvine, 1990). They hypothesize that a similar mechanism may account for Co(II) inhibition of MnP. These results are not applicable to these competition studies because the Mn(III) produced was rapidly reduced by ABTS before it could react with hydrogen peroxide and cobalt. Also, no manganese was present in the hydrazine incubations containing cobalt, so the effect is not applicable to these incubations.

There is still some mystery as to why MnP Compound I can oxidize classical peroxidase substrates whereas Compound II cannot. One possibility is that the protein of Compound I is in a different conformation than the protein of Compound II. This is plausible, but a bit unlikely considering that crystallographic studies on CCP show that there is very little difference between the protein conformations of the

native enzyme and Compound I (Finzel et al., 1984). A second possibility is that classical peroxidase substrates bind to MnP at a site near to, but a bit removed from, the  $\delta$ -*meso* heme edge. This site is close enough to the heme edge for Compound I, which is typically very reactive, to perform an oxidation, but too far away from the heme for the less reactive Compound II to perform the oxidation.

A model of the MnP active site that is consistent with the results of these studies is shown below (Figure 2.4.1). There are 3 important features of this model. First, a protein barrier denies substrates access to the iron-oxygen species. Thus, MnP does not catalyze oxygenase reactions and does not form iron-phenyl complexes. Second, the protein directs substrates to bind near the  $\delta$ -*meso* heme edge. Thus, heme substitution at the  $\delta$ -*meso* position inactivates the enzyme. Third, manganese is oxidized below the plane of the heme whereas azide and the hydrazines are oxidized above the plane of the heme. Thus cobalt, which binds at the same site as manganese, competitively inhibits manganese oxidation but does not inhibit azide or alkylhydrazine inactivation. This model is in accord with the fact that azidyl or alkyl radicals must approach the heme edge from below or above the plane of the heme in order to add to the *meso* carbon. Finally, it should be noted that placement of the manganese below, as opposed to above, the plane of the heme is arbitrary and could be the reverse.

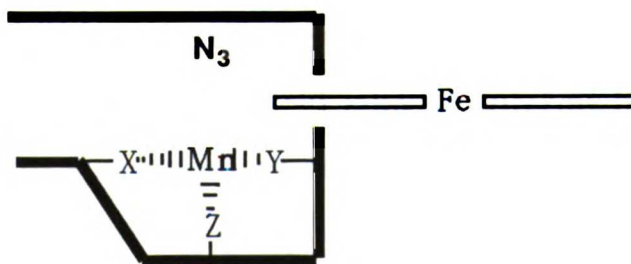
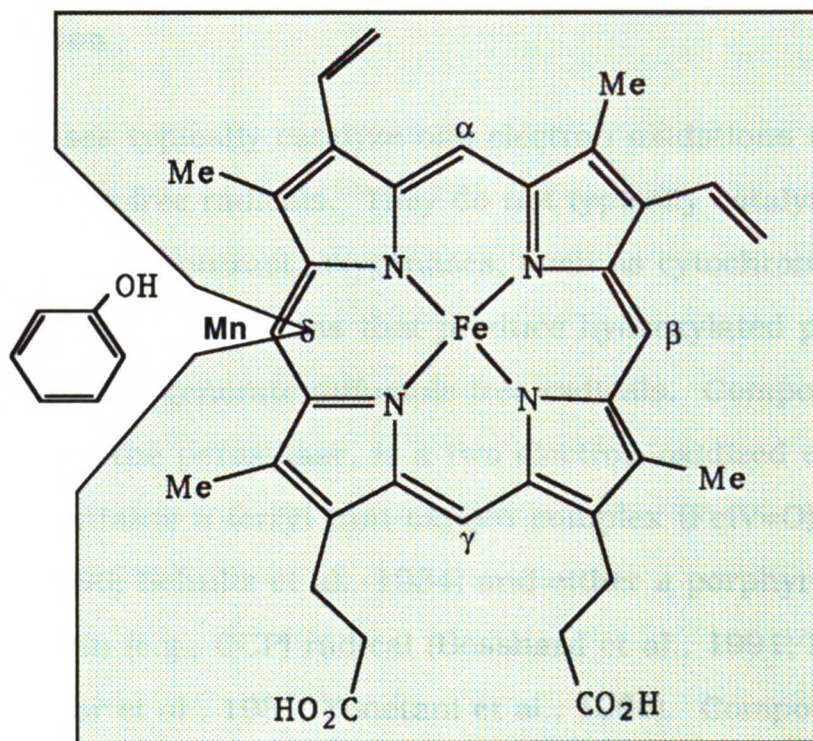


Figure 2.4.1. A model of the MnP active site. The shaded region represents protein.

### **3.0 HRP Catalyzed Thioanisole Sulfoxidation**

#### **3.1 Introduction**

Peroxidases typically catalyze one-electron oxidations that produce diffusible free radicals. They do not typically catalyze oxygen atom insertions. In contrast, oxygenases, such as cytochromes P-450, catalyze oxygen atom insertions that produce hydroxylated products, and do not typically generate diffusible free radicals. Compound I, the active oxidant of the peroxidase, is a two electron oxidized enzyme species that contains a ferryl iron-oxygen complex ( $\text{Fe}^{\text{IV}}=\text{O}$ ) (Penner-Hahn et al., 1986; Schultz et al., 1984) and either a porphyrin (e.g., HRP) or a protein (e.g., CCP) radical (Bosshard et al., 1991; Dolphin et al., 1971; La Mar et al., 1981; Yonetani et al., 1966). Compound I is normally reduced to native enzyme by oxidizing two substrate molecules via one-electron abstractions. The second electron abstraction is typically the rate limiting step in the peroxidase cycle, so Compound II, the one-electron oxidized enzyme intermediate, is normally the predominant species under steady state turnover conditions (Dunford, 1991; Marnett et al., 1986). In contrast to HRP, the electronic configuration of the active oxidant of cytochrome P-450 is not known. It does, however, contain some type of iron-oxygen species that is likely similar in structure to the Compound I species of peroxidases (Groves et al., 1981; Ortiz de Montellano, 1986). Thus, it is intriguing that P-450s and peroxidases form such similar two-electron deficient species, yet catalyze such different reactions. The protein must somehow direct the iron-oxygen species of P-450 to

insert its oxygen and the iron-oxygen species of peroxidase to abstract electrons.

Recently, a theory was developed which describes how the protein moiety of a hemoprotein determines whether the hemoprotein catalyzes oxygen insertion (oxygenase activity) or electron abstraction (peroxidase activity) (Ator, David et al. 1987; Ator and Ortiz de Montellano 1987; Ortiz de Montellano, Choe et al. 1987; Ortiz de Montellano, David et al. 1988; Chapter 1 section 13.). According to this theory, the location of substrate binding, relative to the heme group, determines the activity displayed. If a substrate binds near the iron-oxygen species, oxygen insertion occurs; whereas if the substrate binds near the heme edge, electron abstraction occurs. There are numerous pieces of evidence that support this theory: (1) HRP inactivation by azide, alkylhydrazines and arylhydrazines results in substitution of the heme at the  $\delta$ -*meso* position (Ator, David et al. 1987; Ator and Ortiz de Montellano 1987; Ortiz de Montellano, David et al. 1988). (2) HRP reconstituted with  $\delta$ -*meso*-ethylheme cannot catalyze substrate oxidation (Ator, David et al. 1987). (3) HRP, in contrast to P-450, does not form an iron-phenyl complex when incubated with phenylhydrazine or phenyldiazene (Raag, Swanson et al. 1990; Ator and Ortiz de Montellano 1987). (4) The crystal structure of P450<sub>CAM</sub> reveals that the heme edge is buried by protein (Poulos 1986; Poulos, Finzel et al. 1986). (5) NMR studies suggest that phenols bind to native HRP near the heme 8-methyl group (Saxena, Modi et al. 1990).



There are cases, however, in which HRP catalyzes oxygenase reactions such as hydroxylations, N-demethylations, and O-demethylations (Kedderis et al., 1986; Meunier, 1991; Miwa et al., 1983). However, in most of these cases it has been shown that the products are formed via a classical peroxidase electron abstraction mechanism. The primary piece of evidence that supports a classical peroxidase mechanism is that the oxygen in the product derives from H<sub>2</sub>O or O<sub>2</sub> and not from H<sub>2</sub>O<sub>2</sub> (i.e., not from the iron-oxygen species). For example, it has been shown that the product of HRP catalyzed O-demethylation of a 9-methoxyellipticine derivative contains oxygen that derives from H<sub>2</sub>O (Meunier, 1991)(Figure 2.1.1). Similarly, it has been shown that the HRP mediated hydroxylation of 2,4,6-trimethylphenol occurs through the addition of O<sub>2</sub> to a radical intermediate, and the addition of H<sub>2</sub>O to a cation intermediate, and not through direct incorporation of the ferryl oxygen (Ortiz de Montellano et al., 1987).

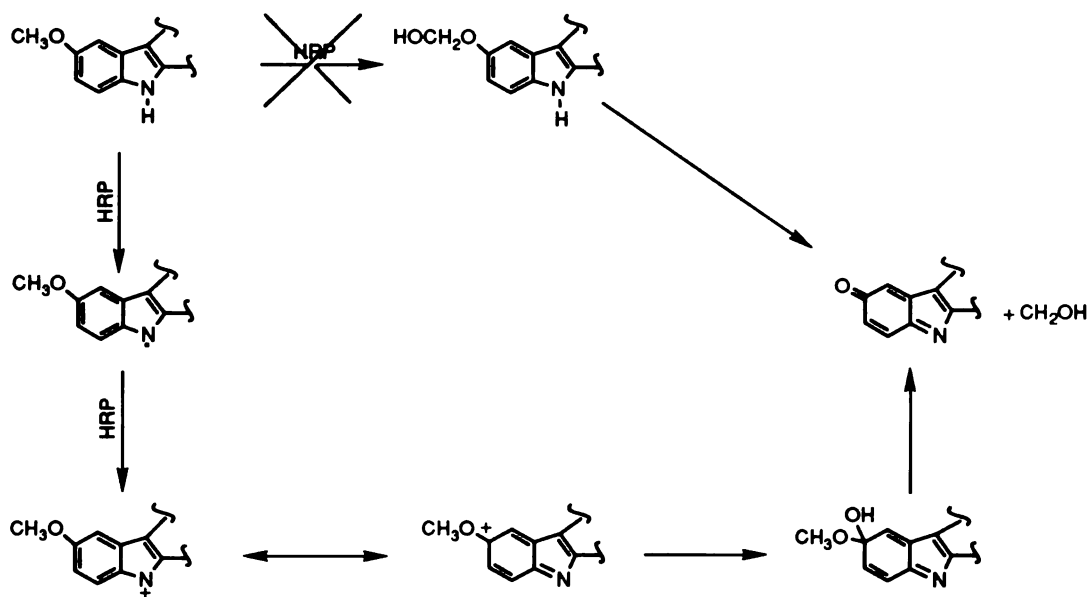
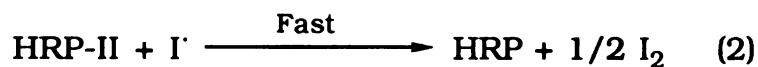
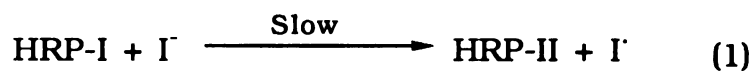
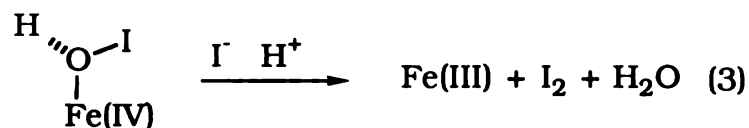


Figure 3.1.1 Mechanism of HRP oxidation of a 9-methoxyellipticine, an apparent oxygenase reaction that goes through a classical peroxidase mechanism. Adapted from Meunier and Meunier (1985).

There are, nevertheless, a few cases in which HRP performs what appears to be a direct two-electron oxidation. For example, HRP oxidizes iodide to iodine without the appearance of a Compound II species. This result suggests that Compound I directly oxidizes iodide by two electrons (Roman and Dunford, 1972; Roman et al., 1971; Sakurada et al., 1987). It is possible that iodide oxidation occurs via a classical peroxidase mechanism where the reduction of Compound I is rate limiting:



However, a detailed kinetic analysis of the reaction of HRP Compound II with iodide suggests that the above mechanism does not occur (Roman and Dunford, 1972). Instead, Compound I performs a direct two-electron oxidation of I<sup>-</sup> to generate I<sup>+</sup> or its equivalent. One possible mechanism for this oxidation invokes an iron-oxygen-iodide intermediate:



It should be noted, however, that there is no evidence that supports the existence of this intermediate, and the two-electron oxidation may occur at a location that is removed from the heme iron such as the heme edge.

There is, however, one case where HRP clearly behaves as a P-450 like oxygenase. Recent studies have shown that HRP oxidizes thioanisole to the sulfoxide and the sulfoxide oxygen derives primarily from H<sub>2</sub>O<sub>2</sub> (Doerge, 1988; Doerge et al., 1991; Kobayashi et al., 1986). Thus, HRP is able to insert its ferryl oxygen into thioanisole. This result clearly shows that thioanisole has access to the iron-oxygen species of HRP and argues against the theory that the peroxidase iron-oxygen species is sheltered by protein. Cytochrome P-450 and chloroperoxidase also oxidize thioanisole to the sulfoxide (Kobayashi et al., 1987; Watanabe et al., 1980).

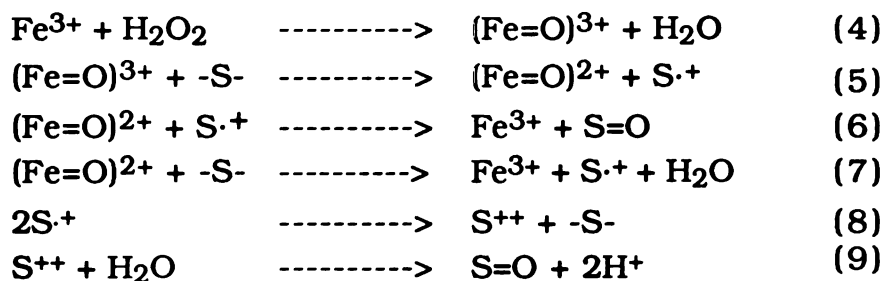
Unlike the oxidation of iodide, the oxidation of thioanisole by HRP proceeds with the formation of Compound II (Perez and Dunford, 1990a; Perez and Dunford, 1990b). Thus, thioanisole initially reduces Compound I by one electron. Electrochemical studies (Uneyama and Tori, 1971) and molecular orbital modeling (Doerge et al., 1991) indicate that the electron is removed from an orbital centered on the sulfur, resulting in a sulfur radical cation. The existence of a sulfur radical cation is further supported by EPR studies which show that the hydroxyl radical oxidizes sulfides to sulfur radical cation intermediates (Gilbert et al., 1973). The sulfur radical produced by HRP then combines with the ferryl oxygen of Compound II, producing native enzyme and the sulfoxide.

The thioanisole sulfoxide produced in these incubations is a chiral molecule. Surprisingly, it was reported that the oxidation proceeds without stereoselectivity (Colonna et al., 1990; Kobayashi et al., 1986). In contrast, stereoselectivity is observed in the oxidation of thioanisole by P-450 and chloroperoxidase (Kobayashi et al., 1987; Takata et al., 1980). Stereoselectivity is expected if thioanisole binds at a specific site near the iron-oxygen species. Typically, racemic products are formed during classical peroxidase reactions, because diffusible free radical intermediates are formed near the heme edge.

It is noteworthy that a Hammett analysis of the oxidation of substituted thioanisoles revealed that there is little correlation between the rate of HRP mediated oxidation and either  $\sigma^+$  or  $\sigma_p$  parameters (Kobayashi et al., 1987). In contrast, there is an excellent

correlation between the rate of oxidation by HRP Compound II and the  $\sigma^+$  parameter (Kobayashi et al., 1987). Based on this result, it has been suggested that thioanisole oxidation by HRP proceeds by more than one mechanism (Kobayashi et al., 1987). A simpler explanation is that the formation of the sulfur radical cation by HRP Compound I is relatively fast compared to its recombination with the ferryl oxygen, whereas the formation of the sulfur radical cation is the slow (and only) step of Compound II reduction by thioanisole.

A detailed kinetic analysis of the steady state and transient state kinetics of *p*-substituted thioanisole oxidation by HRP has been performed (Perez and Dunford, 1990a; Perez and Dunford, 1990b). The results of this analysis are consistent with the following mechanism:

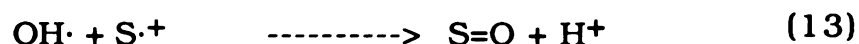
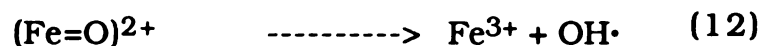
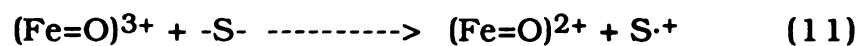
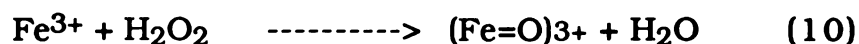


where  $\text{Fe}^{3+}$ ,  $(\text{Fe}=\text{O})^{3+}$  and  $(\text{Fe}=\text{O})^{2+}$  represent native HRP, Compound I, and Compound II, respectively, and  $\text{-S-}$ ,  $\text{S}\cdot^+$  and  $\text{S}^{++}$  represent the sulfide, sulfur radical cation, and dication, respectively.

According to this mechanism, HRP Compound I oxidizes thioanisole to the sulfur radical cation which can then either combine

with the ferryl oxygen (equation 6) or disproportionate in solution (equation 8). A key finding in support of this mechanism is that thioanisole competes with the thioanisole radical cation for oxidation by Compound II (Perez and Dunford, 1990b). Therefore, a lower incorporation of the H<sub>2</sub>O<sub>2</sub> oxygen into the sulfide would be predicted during catalysis at high thioanisole concentrations. The fact that approximately 90% of the sulfoxide oxygen derives from H<sub>2</sub>O<sub>2</sub> (Doerge, 1988; Kobayashi et al., 1986) illustrates that steps (8) and (9) are usually relatively minor pathways.

It is difficult to reconcile the above scheme with the apparent lack of stereoselectivity observed in thioanisole oxidation. It is even more difficult to reconcile the scheme with the theory that peroxidase substrates do not have access to the ferryl oxygen. One mechanism that reconciles the above results has been proposed (Perez and Dunford, 1990a; Perez and Dunford, 1990b):



According to this mechanism, HRP Compound II releases a hydroxyl radical that reacts with a sulfur radical cation that was formed at the heme edge. The invocation of the hydroxyl radical is not appealing, however, because of its high reactivity, and because there is no precedence for its existence in classical peroxidase reactions.

There are at least two explanations as to why the iron-oxygen species of HRP reacts directly with sulfur containing substrates but not with phenolic substrates. Either the sulfur containing compounds bind to the enzyme at a different location than do phenols, or the radical cation produced from the one electron oxidation of the sulfur compounds has a different reactivity than the radical produced by phenol oxidations. The studies described in this chapter provide insights into this issue and provide a partial explanation for the apparent inconsistencies observed in HRP mediated thioanisole oxidation. A summary of the oxygenase and peroxidase activities of HRP is shown in Figure 2.1.2.

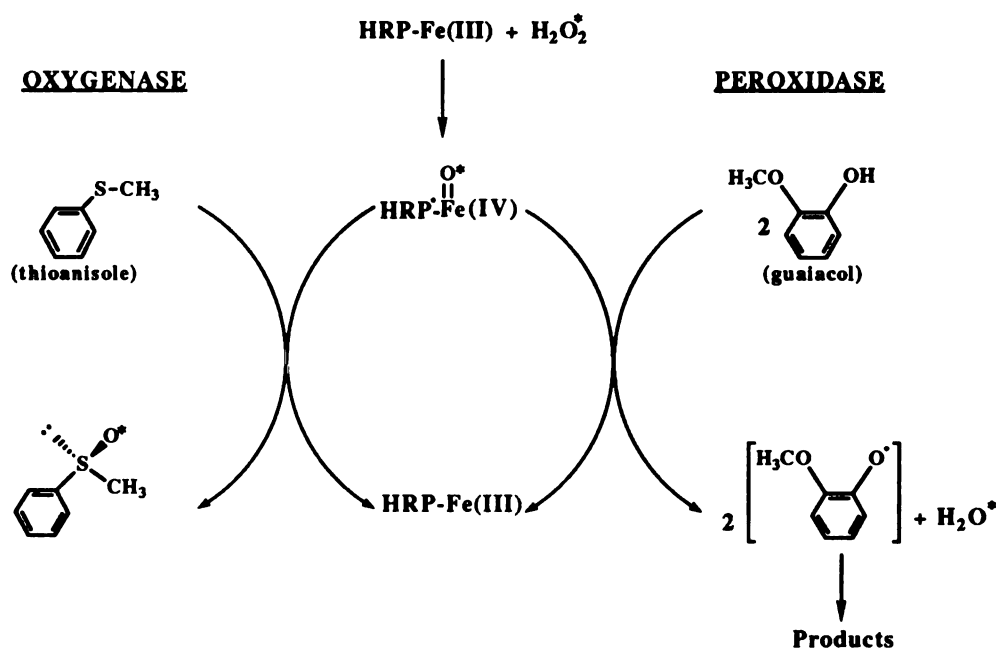


Figure 2.1.2. The peroxidase (electron abstraction) and oxygenase (oxygen insertion) activities of HRP.

### **3.1 Experimental**

#### **Materials**

Thioanisole, 4-methoxythioanisole, 4-methylthioanisole, 4-nitrothioanisole, hydrogen peroxide, thiophenol, 4-nitrobenzylchloride, chloroacetone, chloromethyl phenyl sulfide, phenylhydrazine·HCl, and *m*-chloroperoxybenzoic acid were purchased from Aldrich. Horseradish peroxidase (type IV), methemoglobin, and guaiacol were from Sigma. Cobaltous acetate was from J. T. Baker. Manganese sulfate monohydrate was from Mallinckrodt. 2-Mercaptoethanol was from Bio-Rad. <sup>18</sup>O labeled hydrogen peroxide was from ICON (lot #I063253485), and was found to be 98 atom-% <sup>18</sup>O by gas chromatography-mass spectrometry of the epoxide produced by reaction of the peroxide with menadione (Ortiz de Montellano and Catalano, 1985). Methylphenyldiazene carboxylate azo ester was from Research Organics Inc. Authentic samples of 4-methylthioanisole sulfoxide and 4-methoxythioanisole sulfoxide were provided by Ms. Julia Fruetel. Buffers were made with deionized, glass-distilled water that had been stirred overnight with 5 g/liter Chelex 100 beads (Bio-Rad). HRP incubations were carried out in 50 mM phosphate buffer, pH 7.0. Manganese peroxidase incubations were carried out in 50 mM succinate, 10 mM malate, pH 4.5.

HPLC was performed on a Hewlett Packard model 1040A system equipped with a diode array detector and a varian 9010 solvent pump. GC was performed on a Hewlett-Packard model 5890 gas



chromatograph equipped with a flame ionization detector and interfaced to a Hewlett-Packard 3365 Chemstation. GC/MS was performed on a similar system that was coupled to a VG-70 mass spectrometer. Guaiacol assays were performed on a Hewlett Packard model 8450A diode array spectrophotometer. Spectra were recorded on an Aminco DW-2000 spectrophotometer.

### **Synthesis of $p\text{-NO}_2\text{C}_6\text{H}_4\text{CH}_2\text{SC}_6\text{H}_5$ (1)**

To thiophenol (1.0 mL, 0.01 mol) in 20 mL dry DMF was added triethylamine (1.0 mL, 0.01 mol). *p*-Nitrobenzyl chloride (2.15 g, 0.01 mol) was then added and the mixture was stirred under argon at room temperature for 2 h. The reaction was quenched by addition of H<sub>2</sub>O, and the products were extracted into 100 mL of ether. The ether was washed successively with 100 mL of NaOH (1 M), HCl (1M), and brine, dried over magnesium sulfate, and evaporated. The product was purified by silica gel chromatography with 10% ethyl acetate in hexane. A yellowish solid was isolated. *R*<sub>f</sub> 0.49 in 80% hexane: 20% ethyl acetate, mp 76-77° C; <sup>1</sup>H NMR (CDCl<sub>3</sub>) δ 4.12 (2H, s), 7.22-7.26 (5H, m), 7.36 (2H, δ, *J* = 8.6 Hz), 8.09 (2H, δ, *J* = 8.6 Hz); <sup>13</sup>C NMR (CDCl<sub>3</sub>) δ 38.8, 123.5, 127.2, 129.0, 129.4, 129.8, 130.8, 134.5, 145.5. EI<sup>+</sup> MS: *m/e* = 245.

### **Synthesis of $\text{C}_6\text{H}_5\text{SCH}_2\text{COCH}_3$ (2)**

In a manner similar to the synthesis of **1**, chloroacetone was reacted with thiophenol in the presence of triethylamine. The

product was purified by silica gel chromatography with 10% ethyl acetate in hexane. A white crystalline solid was isolated.  $R_f$  0.40 in 80% hexane: 20% ethyl acetate, mp 35<sup>o</sup> C; <sup>1</sup>H NMR (CDCl<sub>3</sub>)  $\delta$  2.27 (3H, s), 3.67 (2H, s), 7.23-7.36 (5H, m); <sup>13</sup>C NMR (CDCl<sub>3</sub>)  $\delta$  27.9, 44.6, 126.9, 129.1, 129.5, 134.6, 203.5. EI<sup>+</sup> MS: m/e = 166.

### **Synthesis of methyl 4-nitrophenyl sulfoxide**

To methyl 4-nitrophenyl sulfide (100 mg = 0.52 mmol) dissolved in 10 mL of dry dichloromethane, was added KF (32 mg = .55 mmol). *m*-Chloroperoxybenzoic acid (87 mg = 0.50 mmol) dissolved in 10 mL dichloromethane was added, and the mixture was stirred at room temperature for 1 hour. An additional 32 mg of KF was then added, and the reaction was stirred another 1 hour. The solution was filtered to remove the potassium *m*-chlorobenzoate produced and washed once with 20 mL of 1 M sodium hydroxide and once with 20 mL of brine. The dichloromethane was then evaporated under a stream of argon and the resulting solid was redissolved in 80% hexane: 20% isopropyl alcohol and analyzed by HPLC.

### **Formation of Denatured HRP**

HRP (2 mg) was boiled in H<sub>2</sub>O for 2 hours in the presence of a large excess of 2-mercaptoethanol. A significant amount of heme bleaching was observed during the boiling. The sample was then run down a Sephadex G-25 column to remove 2-mercaptoethanol and any iron that may have been released.

### **Formation of Phenylhydrazine Modified HRP.**

HRP (50  $\mu\text{M}$ ) in 6 mL of pH 7.0 sodium phosphate buffer was incubated with phenylhydrazine (2 mM) and hydrogen peroxide (2 mM). The phenylhydrazine and hydrogen peroxide were added over 5 minutes. The mixture was stirred at room temperature for 10 minutes then run down a Sephadex G-25 column equilibrated in pH 7.0 phosphate buffer. The enzyme was collected and reincubated with phenylhydrazine and hydrogen peroxide in a similar manner. The second incubation was performed in order to insure a complete loss of guaiacol activity. After 10 minutes, 20  $\mu\text{L}$  of a 10 mg/mL solution of sodium ascorbate was added to reduce the heme iron to the ferric state, and the mixture was again run down a G-25 column to remove small molecules. The modified enzyme species was quantitated using the extinction coefficient of native HRP ( $\epsilon_{402} = 105 \text{ M}^{-1}\text{cm}^{-1}$ ). Previous studies indicate that phenylhydrazine modifies HRP predominantly through protein arylation (Ator and Ortiz de Montellano, 1987).

### **Reconstitution of HRP with $\delta$ -Meso-Methyl and $\delta$ -Meso-Ethylheme**

Formation of  $\delta$ -meso-alkylheme (Ator et al., 1987) and reconstitution of  $\delta$ -meso-alkylheme into HRP (Ator et al., 1989) were performed as already described.

## **Thioanisole Sulfoxidation**

To a solution of HRP or modified HRP (25  $\mu$ M) in pH 7.0 sodium phosphate buffer was added 10  $\mu$ L of a 1 M stock solution of thioanisole in methanol (giving a thioanisole concentration of 5 mM). Not all of the thioanisole dissolved in the buffer and thus 5 mM is an upper concentration limit. To this mixture, 100  $\mu$ L of a 0.04 M solution of hydrogen peroxide was added over 2 hours (2 mM final peroxide concentration). A standard (25  $\mu$ L of a 10 mM acetophenone solution in methanol) was added and the solution extracted with 3 mL of dichloromethane. When necessary, low speed centrifugation was used to separate the layers. The dichloromethane layer was removed and evaporated to near dryness under a stream of nitrogen. The resulting liquid was redissolved in 80% hexane, 20% isopropyl alcohol and analyzed by HPLC on a Diacel chiral column eluted with 80% hexane, 20% isopropyl alcohol, at a flow rate of 0.5 mL/min. In order to shorten the run time, the solvent system was changed to 60% hexane 40% isopropyl alcohol for *p*-nitro substituted samples. The runs were monitored at 254 nm with a bandwidth of 6 nm.

Identical incubations were performed except that thioanisole was replaced with *para*-substituted thioanisoles. Similar incubations were also carried out with hemoglobin and with MnP in pH 4.5 buffer.

## **Source of Sulfoxide Oxygen**

HRP and  $\delta$ -*meso*-ethylheme-containing HRP were incubated with thioanisole as described above except that hydrogen peroxide was replaced with  $^{18}\text{O}$  labeled hydrogen peroxide. The products were extracted into dichloromethane and analyzed by electron impact GLC-MS.

## **Incubation of $\delta$ -Meso-Ethylheme Reconstituted HRP with Phenyl diazene**

Methylphenyl diazene carboxylate azo ester (4  $\mu\text{L}$ ) was hydrolyzed to phenyl diazenecarboxylate in 400  $\mu\text{L}$  of argon saturated 0.1 M NaOH. A 2  $\mu\text{L}$  aliquot of this solution was added to 1 mL of 10  $\mu\text{M}$   $\delta$ -*meso*-ethylheme reconstituted HRP in pH 7.0 buffer and a spectrum was recorded. An additional aliquot of phenyl diazenecarboxylate was added every 5 minutes until a total of 4 aliquots had been added.

## **Inhibition of Guaiacol Oxidation by Thioanisole**

Solutions containing HRP (7.5 nM), guaiacol (10 mM - 100  $\mu\text{M}$ ) and thioanisole (0, 0.5, 1.0, or 1.5 mM) in 1 mL of pH 7.0 phosphate buffer were mixed for 10 minutes to allow complete dissolution of the thioanisole. The solutions were transferred to cuvettes and guaiacol oxidation was initiated by the addition of 6  $\mu\text{L}$  of 0.1 M  $\text{H}_2\text{O}_2$  (final peroxide concentration of 600  $\mu\text{M}$ ). Guaiacol oxidation was monitored at 470 nm for 20 s.

### **Incubation of 1 and 2 with HRP**

To a solution of HRP (25  $\mu\text{M}$ ) in pH 7.0 sodium phosphate buffer was added 20  $\mu\text{L}$  of a 0.5 M stock solution of **1** or **2** in methanol (5 mM substrate concentration). To this solution was added 50  $\mu\text{L}$  of 0.08 M  $\text{H}_2\text{O}_2$  over 2 hours (2 mM final peroxide concentration). The incubation was extracted with 2 mL dichloromethane or 2 mL ethylacetate and analyzed by either GC or HPLC.

### **Spectroscopic Binding Studies**

To a pair of matched cuvettes was added 1 mL of HRP (10  $\mu\text{M}$ ) in 50 mM phosphate buffer pH 7.0. Various amounts (5  $\mu\text{L}$  to 110  $\mu\text{L}$ ) of a 100 mM guaiacol solution were added to the sample cuvette and an equal amount of buffer was added to the reference cuvette. The solutions were mixed, and difference spectra were recorded. A value for  $K_d$  was computed from the relationship:

$$1/[S] = [E]\Delta\epsilon/K_d\Delta A - 1/K_d \quad (14)$$

where [S] is the concentration of substrate, [E] is the concentration of enzyme,  $K_d$  is the binding constant of the substrate to the enzyme,  $\Delta A$  is the absorbance of peak minus trough in the difference spectrum and  $\Delta\epsilon$  is the difference in molar absorptivity of the free and bound enzyme. (This relationship can be derived using the definition of a binding constant and Beers law). An identical experiment was carried out in the presence of 1.5 mM thioanisole.

A similar experiment was performed with thioanisole replacing guaiacol. The concentration of thioanisole ranged from 0.5 mM to 4 mM and was delivered from a stock solution in methanol. Similar experiments were also carried out with  $\delta$ -*meso*-ethylheme reconstituted HRP.

### **3.3 Results**

#### **Sulfoxide Formation**

HRP oxidizes thioanisole and *para*-substituted thioanisoles. Hydrogen peroxide alone also slowly oxidizes thioanisole, but the rate of this oxidation was usually negligible compared to the rate of enzymatic oxidation. A typical HPLC chromatogram from an incubation is shown in Figure 3.3.1.

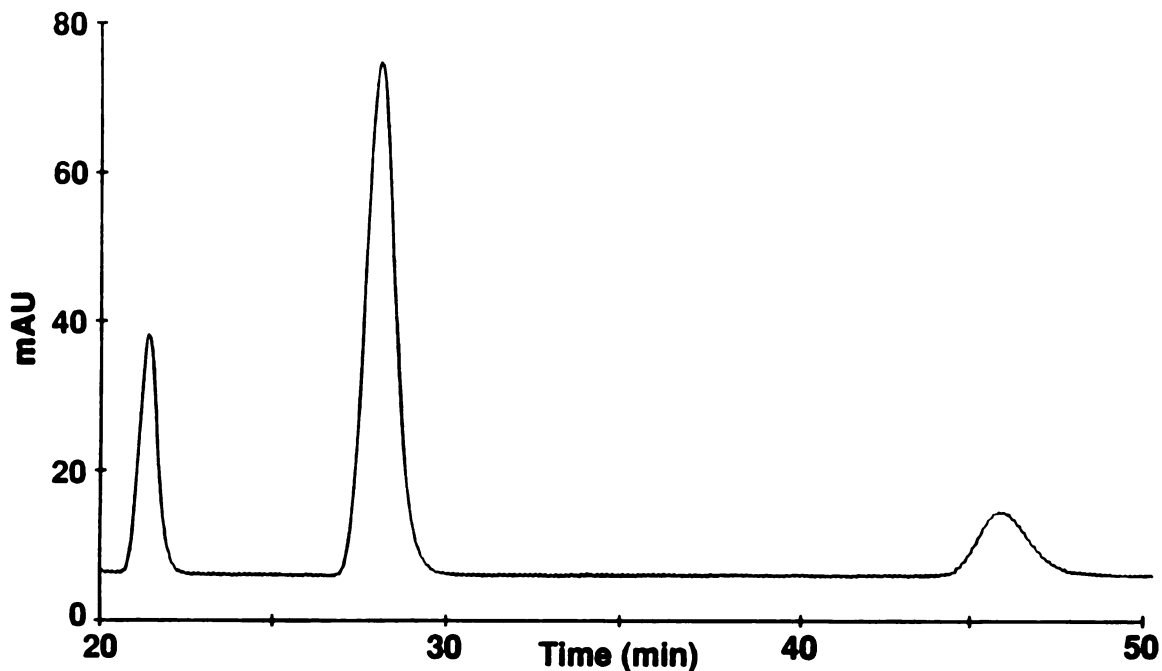
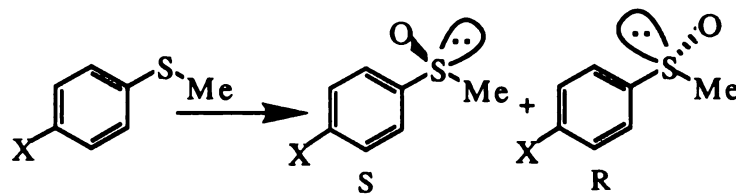


Figure 3.3.1. A typical HPLC chromatogram from an HRP incubation that contained thioanisole. The peak at 21 minutes is acetophenone, the peaks at 28 and 45 minutes are the sulfoxide ((S)-(-) and (R)-(+), respectively) enantiomers.

### Chirality of the Sulfoxide

Contrary to what has been reported (Colonna et al., 1990; Kobayashi et al., 1987), HRP asymmetrically oxidizes thioanisole and *p*-substituted thioanisoles (Figure 3.3.1; Table 3.3.1.). The enantiomeric excess of the product sulfoxide was not significantly affected by the nature of the *para*-substituent. The stereoselectivity was not significantly altered when the incubation pH was lowered to 4.5.





R	ee
H	70
Me	66
OMe	60
NO <sub>2</sub>	62

Table 3.3.1. Enantiomeric excess (ee) of sulfoxides produced in HRP-sulfide incubations at pH 7.0. Enantiomeric excess is defined as  $|\%R - \%S|$ .

### MnP and Myoglobin Mediated Sulfoxxygenation

MnP, in the absence of manganous ions, oxidizes thioanisole (Table 3.3.2). The oxidation is slower than the oxidation by HRP, but the stereoselectivity is much greater. Cobalt, which competes with manganese (Harris et al., 1991), lowered the amount of sulfoxide produced in an MnP incubation. The cobalt may compete with thioanisole for the MnP active site. However, because cobalt also inactivates MnP in the presence of peroxide, the decrease in activity may simply be due to inactivation. Hemoglobin oxidizes thioanisole more efficiently than HRP but the sulfoxide product was nearly racemic.

### **Activities of Phenylhydrazine-Modified and $\delta$ -Meso-Alkylheme-Reconstituted HRP**

HRP reconstituted with  $\delta$ -*meso*-ethylheme or arylated by phenylhydrazine had almost no guaiacol activity, yet had greater sulfoxxygenase activity than native HRP. The enantiomeric excess of the sulfoxide product was significantly decreased in incubations containing the modified enzymes (Table 3.3.2). The sulfoxide oxygen derived primarily (>90%) from hydrogen peroxide both in incubations containing HRP and  $\delta$ -*meso*-ethylheme reconstituted HRP, indicating the *meso*-substitution did not alter the mechanism of sulfoxidation. Control incubations containing no enzyme or heat denatured enzyme displayed low thioanisole and guaiacol activities. The small amount of sulfoxide produced in these control incubations was virtually racemic (Table 3.3.2).

Enzyme	ee	Thioanisole Activity	Guaiacol Activity
Native HRP	70	100 <sup>1</sup>	100
<i>Meso</i> -ethyl HRP	26	180	5
<i>Meso</i> -methyl HRP	22	70	120
Phenylhydrazine treated HRP	28	250	4
Heat denatured HRP	4.0	15	3
MnP	88	52	-
Hemoglobin <sup>2</sup>	4.0	439	-
No enzyme	0	4	0

Table 3.3.2. Oxidation of thioanisole and guaiacol by various enzyme species. See text for incubation conditions. <sup>1</sup>The concentration of thioanisole sulfoxide formed was approximately 197  $\mu\text{M}$ . <sup>2</sup>The concentration of hemoglobin used was 57  $\mu\text{M}$  instead of 25  $\mu\text{M}$ .

HRP reconstituted with  $\delta$ -*meso*-methylheme oxidized thioanisole at a lower rate and with lower enantioselectivity than native HRP (Table 3.3.2). The lower rate of sulfoxidation is probably due to the high susceptibility of  $\delta$ -*meso*-methylheme-reconstituted HRP to  $\text{H}_2\text{O}_2$  mediated degradation (Ator et al., 1989). During the relatively long thioanisole incubations, it is likely that much of the  $\delta$ -*meso*-methylheme degrades. This explanation is supported by the finding that the Soret band of  $\delta$ -*meso*-methylheme-reconstituted HRP decays considerably more rapidly than the Soret of native HRP or  $\delta$ -*meso*-ethylheme-reconstituted HRP in the presence of  $\text{H}_2\text{O}_2$ . This

degradation is not significant during the very short time period of the guaiacol assay.

### Formation of the Iron-Phenyl Complex

Neither HRP nor HRP reconstituted with  $\delta$ -*meso*-ethylheme formed an iron-phenyl complex when incubated with a large excess of phenyldiazene (Figure 3.3.3). Thus, the  $\delta$ -*meso*-ethylheme group does not perturb the region near above the heme iron in a manner that allows formation of an iron-phenyl complex.

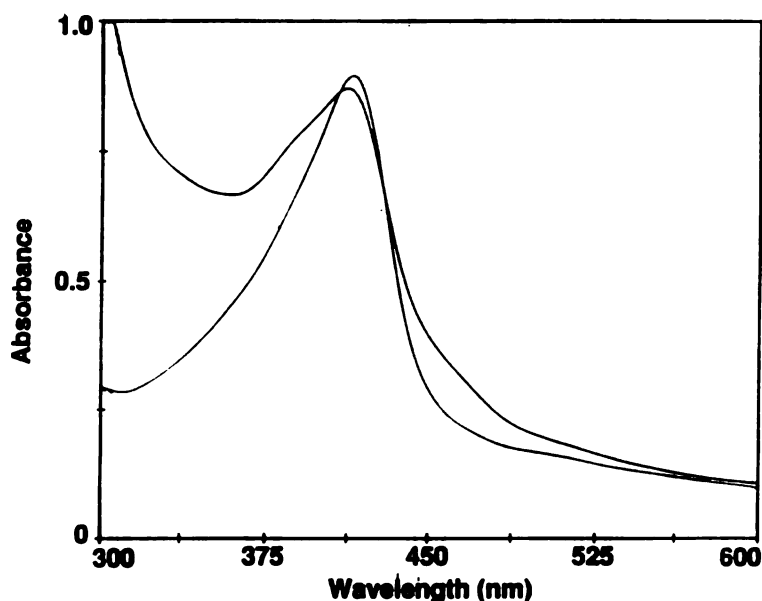


Figure 3.3.3. Spectrum of HRP reconstituted with  $\delta$ -*meso*-ethylheme after the addition of phenyldiazene. A. Before addition. B. After addition of a large excess of phenyldiazene. No significant change in the spectrum was observed over 30 minutes.

## Inhibition of Guaiacol Oxidation by Thioanisole

Thioanisole inhibits guaiacol oxidation by HRP. Kinetics that are consistent with mixed noncompetitive inhibition were observed (Figure 3.3.4).

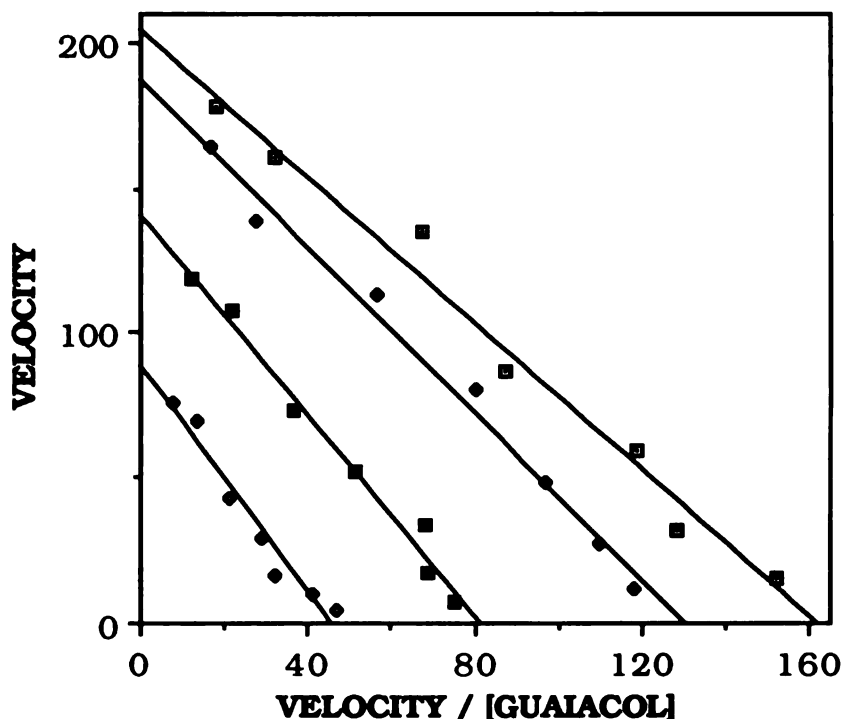


Figure 3.3.4. Mixed-type noncompetitive inhibition of guaiacol oxidation by thioanisole. The incubations contained 8 nM HRP, 600  $\mu$ M  $H_2O_2$ , and from top to bottom, 0, 0.5, 1.0, and 1.5 mM thioanisole.

Both the  $K_M$  and  $V_{max}$  were affected by the presence of thioanisole. The fact that the  $V_{max}$  of guaiacol oxidation was altered by the presence of thioanisole clearly establishes that thioanisole binds at a different site than guaiacol. The classical scheme for mixed kinetics is shown below (Figure 3.3.5) (Segel, 1986). Fitting the data to this scheme, the values for  $K_M$  and  $k_{cat}$  for guaiacol oxidation by HRP were found to be 1.2 mM and 112  $s^{-1}$ . The  $K_I$  and  $\alpha$  values for thioanisole

inhibition were found to be 0.41 mM and 2.4 (Figure 3.3.6). The  $K_i$  value of 0.41 mM is close to the  $K_M$  value of 0.56 mM found by Doerge (1986) for the oxidation of thioanisole by HRP. However, the data do not fit the lines well. Thus, the inhibition may not be classical mixed, perhaps due to thioanisole also being an HRP substrate.

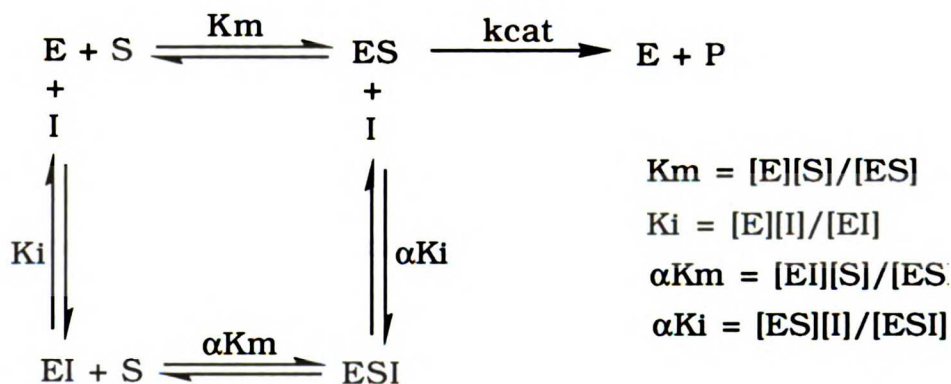


Figure 3.3.5. Classical mixed noncompetitive inhibition.

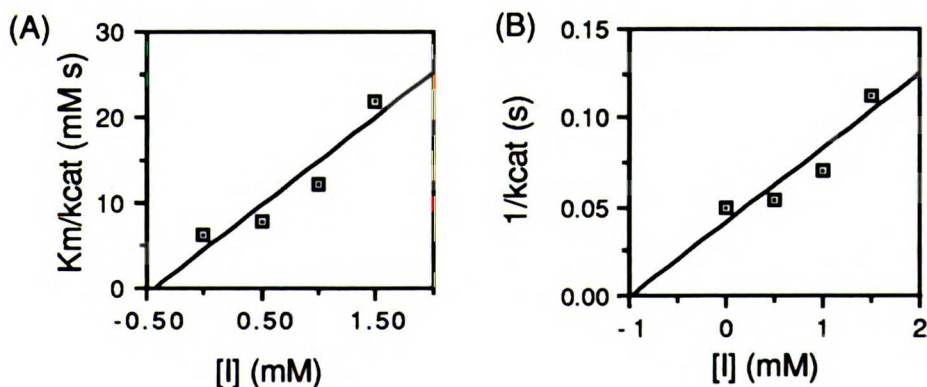
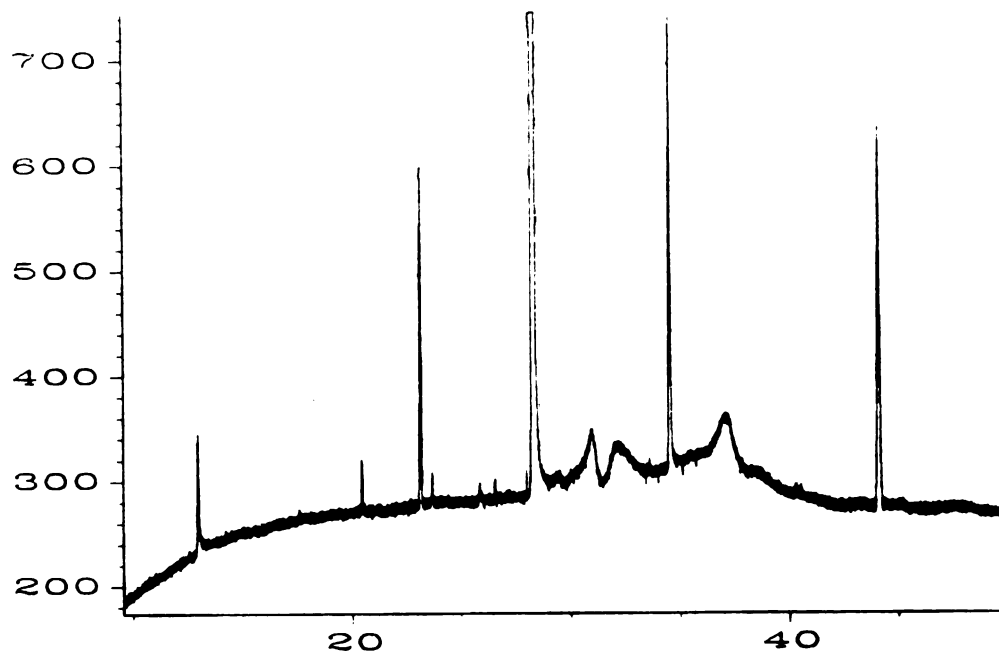


Figure 3.3.6. (A) Plot of apparent  $K_M$ /apparent  $k_{cat}$  for guaiacol oxidation by HRP vs thioanisole concentration. The value of the x intercept =  $-K_i$ . (B) Plot of  $1$ /apparent  $k_{cat}$  for guaiacol oxidation vs thioanisole concentration. The x intercept =  $-\alpha K_i = -0.96$ ,  $\alpha = 2.4$ .

### **Oxidation of Related Molecules:**

In order to determine whether HRP is able to insert its ferryl oxygen into an atom other than sulfur, the oxidation of *p*-NO<sub>2</sub>C<sub>6</sub>H<sub>4</sub>CH<sub>2</sub>SC<sub>6</sub>H<sub>5</sub> (**1**) and C<sub>6</sub>H<sub>5</sub>SCH<sub>2</sub>COCH<sub>3</sub> (**2**) was investigated. Molecule **1** was unable to reduce HRP Compound I at a significant rate. Furthermore, the HPLC chromatogram of the dichloromethane extract of an incubation that contained HRP and **1** was identical to the chromatogram of an extract from a control incubation that lacked enzyme (not shown). Therefore, molecule **1** is not oxidized by HRP.

Molecule **2** was turned over by the HRP. A GC chromatogram of the dichloromethane extract is shown below (Figure 3.3.7). Products were identified by their coelution with standards and by GC/MS. No product was formed in a control incubation that lacked enzyme. A scheme for the oxidation of **2** by HRP is shown in Figure 3.3.8. Because phenyl disulfide was produced in the incubation, pyruvic aldehyde should also have been produced. If the oxygen in the pyruvic aldehyde derives from H<sub>2</sub>O<sub>2</sub>, it would demonstrate that a carbon atom is able to react directly with the ferryl oxygen of HRP. However, pyruvic aldehyde was not detected. Based on the amount of phenyl disulfide produced in the incubation, the pyruvic aldehyde should have been easily detected. It remains unclear why no aldehyde was produced. Perhaps the pyruvic aldehyde reacted with arginine residues of the enzyme.



**Figure 3.3.7.** GC chromatogram of the extract from a HRP - **2** incubation. The peaks are: 13 minutes thiophenol; 29 minutes, **2**; 34 minutes, the sulfoxide of **2**; and 44 minutes, phenyl disulfide. The peak at 23 minutes was not identified but had a molecular ion at  $m/z = 152$  and a major fragment  $m/z = 110$  - the mass of thiophenol. Pyruvic aldehyde was not detected.



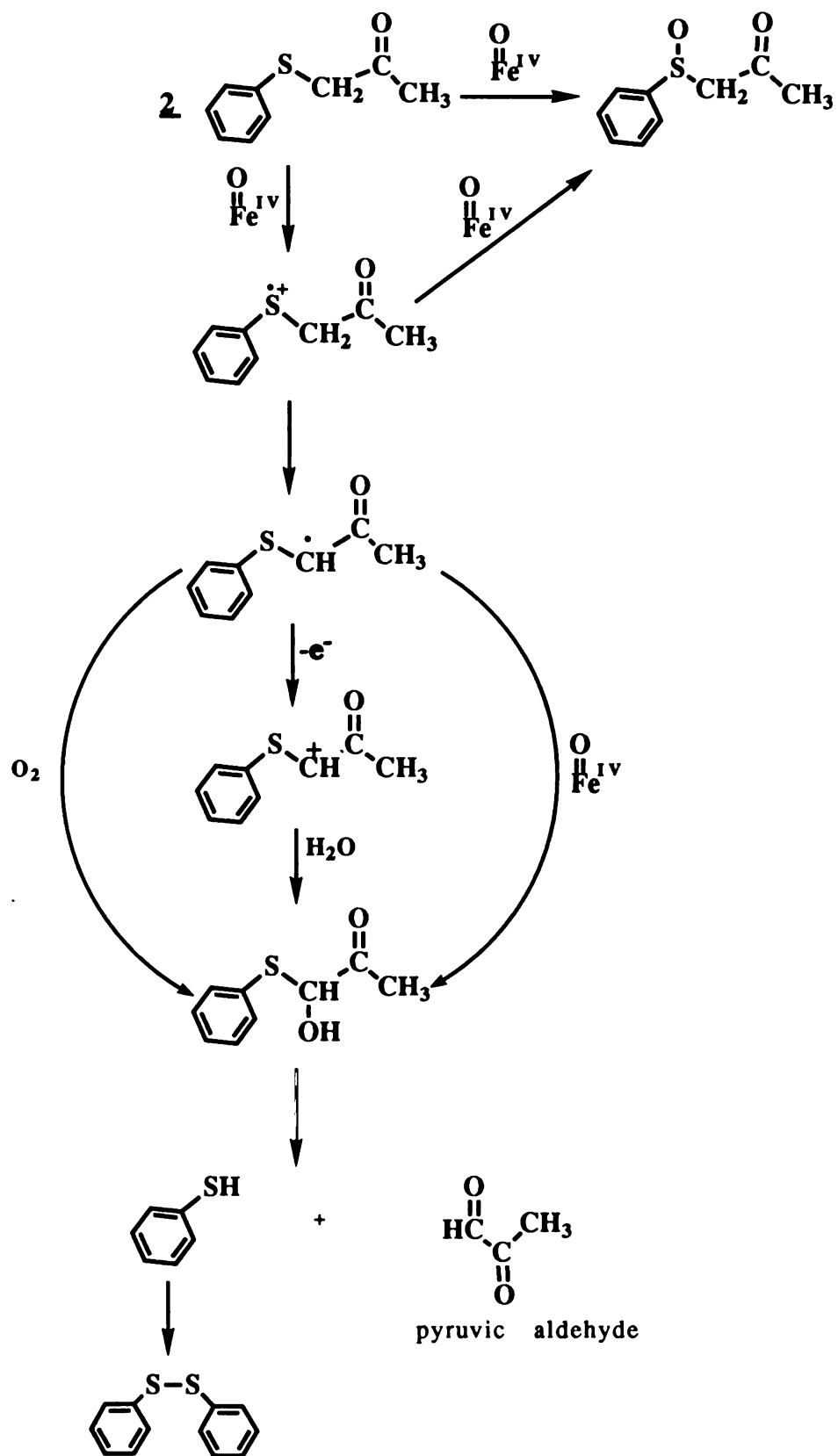


Figure 3.3.8. Possible pathways of oxidation of **2** by HRP.

## Binding Studies

The difference spectrum obtained when guaiacol binds to HRP ( $\lambda_{\max} = 408$  nm; Figure 3.3.9) is similar to that which has been reported (Hosoya et al., 1989). Interestingly, the difference spectrum obtained when thioanisole binds to HRP ( $\lambda_{\max} = 379, 421$  nm,  $\lambda_{\min} = 403$  nm) is very similar to the spectrum obtained with a number of molecules such as phenol, aniline, *p*-cresol and *p*-toluidine (Hosoya et al., 1989; Paul and Ohlsson, 1978; Schejter et al., 1975). The  $K_d$  value for guaiacol binding to HRP was found to be 11 mM from equation 14 (Figure 3.3.10). This result agrees well with the 10.8 mM value previously reported (Hosoya et al., 1989). The presence of thioanisole (1.5 mM) did not alter the form of the guaiacol difference spectrum but did increase the  $K_d$  value to 19 mM. The decrease in guaiacol binding in the presence of thioanisole is consistent with mixed noncompetitive inhibition of guaiacol oxidation by thioanisole. A  $K_d$  value for thioanisole binding to HRP could not be accurately determined due to the low solubility of thioanisole in water.

HRP reconstituted with  $\delta$ -*meso*-ethylheme displayed a significantly altered difference spectrum (Figure 3.3.9) for both guaiacol ( $\lambda_{\max} = 390$  nm) and thioanisole ( $\lambda_{\max} = 402$  nm,  $\lambda_{\min} = 444$  nm) binding. Surprisingly, the  $K_d$  of guaiacol binding to  $\delta$ -*meso*-ethylheme reconstituted HRP was found to be 4 mM (Figure 3.3.10), indicating that guaiacol actually binds more tightly to *meso*-ethylheme reconstituted HRP than to native enzyme. Thus, the  $\delta$ -*meso* ethyl

moiety likely blocks electron transfer by causing guaiacol to bind in an abnormal orientation relative to the heme group.

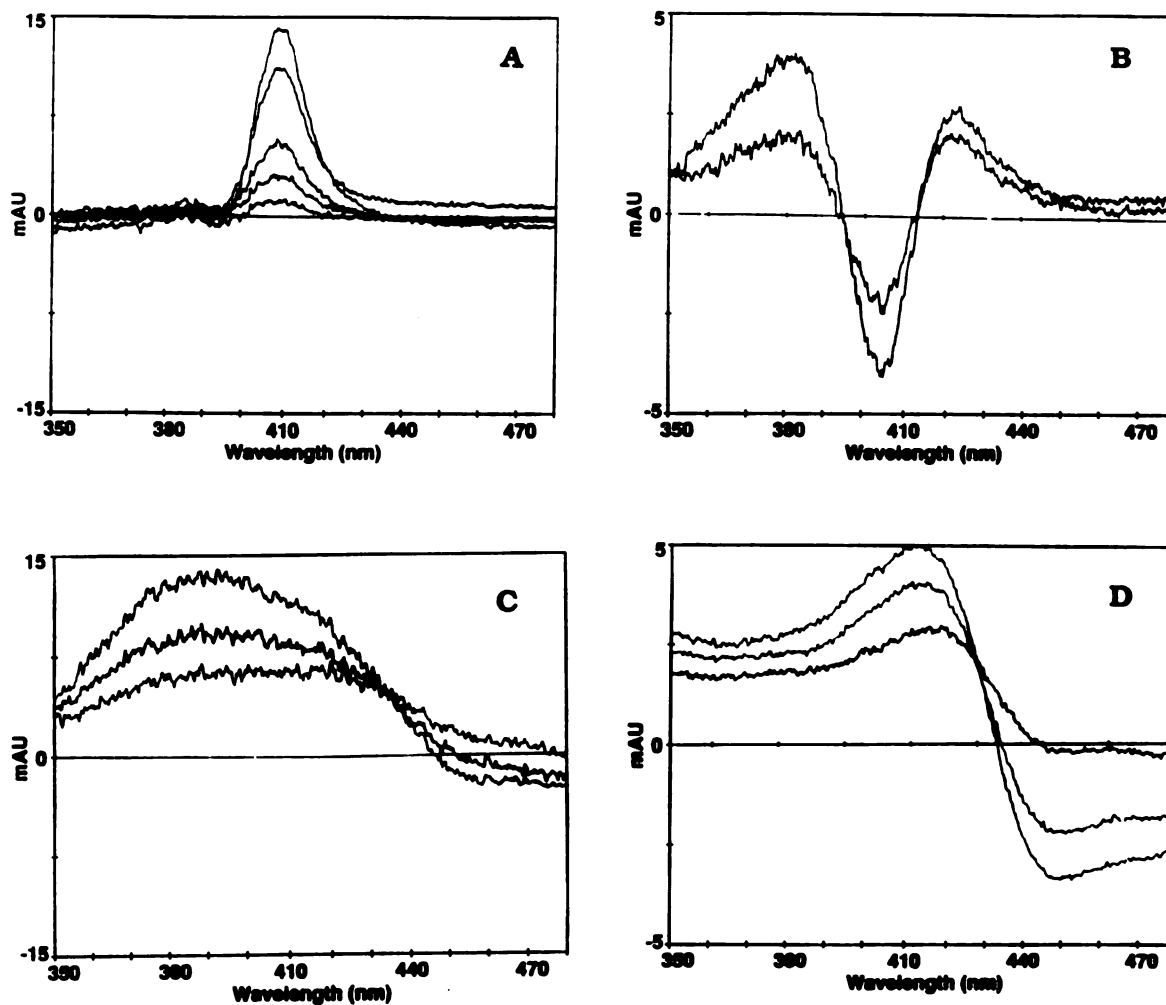


Figure 3.3.9. Difference spectra obtained for binding of (A) guaiacol, and (B) thioanisole to HRP; and (C) guaiacol and (D) thioanisole to  $\delta$ -meso-ethylheme reconstituted HRP.

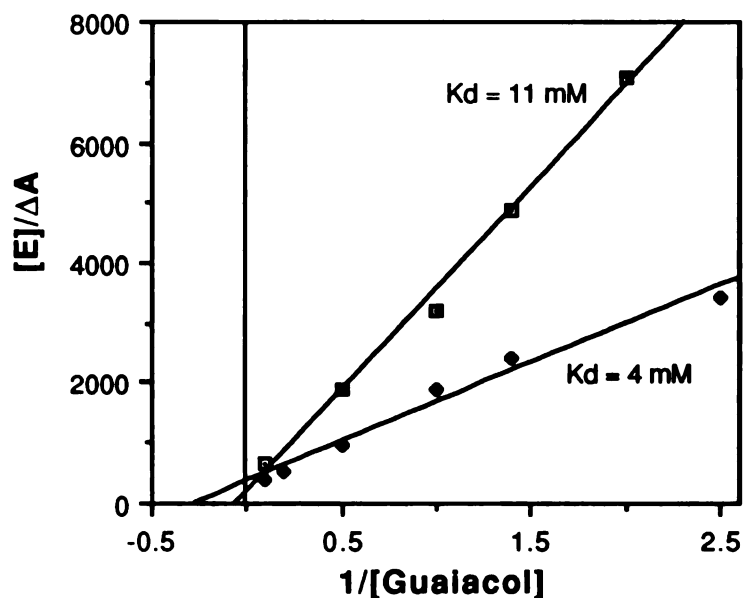


Figure 3.3.10. Determination of the binding constants for guaiacol binding to (A) HRP ( $K_d = 11$  mM) or (B)  $\delta$ -*meso*-ethylheme reconstituted HRP ( $K_d = 4$  mM).

### 3.4 Discussion

In agreement with what has been previously reported (Doerge et al., 1991; Kobayashi et al., 1986), HRP oxidizes thioanisole and *para*-substituted thioanisoles to the corresponding sulfoxides. However, in contrast to what has been reported (Colonna et al., 1990; Kobayashi et al., 1987), the oxidation proceeds with enantioselectively.

Approximately 5 times more (S) than (R) sulfoxide was produced (Figure 3.3.1, Table 3.1.1). Colonna et al. and Kobayashi et al. likely did not detect this stereoselectivity because they were primarily observing background oxidation during their prolonged incubations. Colonna et al. reported stereoselectivity in chloroperoxidase mediated oxidations,

but they found that the selectivity was dramatically influenced by the type of alkyl hydroperoxide used. Because the structures of Compounds I and II do not depend on the structure of the peroxide used to form them, it is likely that part of the activity they were observing with chloroperoxidase was also background oxidation. Very recently, Colonna et al. (1992) reported that they had changed their incubation conditions and observed stereoselectivity in thioanisole oxidation by HRP.

The finding that 93% of the sulfoxide oxygen derived from  $H_2O_2$  is consistent with values in the literature (Doerge et al., 1991; Kobayashi et al., 1986). The 7% not derived from peroxide could be due to a fraction of the sulfur radical cation diffusing out of the active site, or to the fairly rapid exchange of the HRP ferryl oxygen with  $H_2O$  at pH 7 (Hashimoto et al., 1986). In support of the first possibility, Kobayashi et al. (1986) found that the product of the more easily oxidized 4-methoxyphenyl methyl sulfide derives only 66% of its oxygen from hydrogen peroxide, whereas the product of the less easily oxidized methyl 4-methylphenyl sulfide derives 85% of its oxygen from peroxide. The sulfur radical cation of the more easily oxidized substrate should be less reactive and thus more likely to escape into solution rather than combining with the ferryl oxygen. This hypothesis conflicts, however, with the finding that the enantioselectivity of thioanisole oxidation is not significantly affected by *para*-substitution of the thioanisole. The second possibility does not seem very likely. If oxygen exchange between the iron-oxo species and solvent was responsible for the 7% incorporation of non-peroxide

oxygen, then a higher  $^{18}\text{O}$  incorporation into the more rapidly oxidized substrates would be expected because there would be less time for oxygen exchange between solvent and iron-oxo species to occur. However, this result is opposite of that reported by Kobayashi et al. (1986).

Although there is a correlation between the oxidation potential of *para*-substituted thioanisoles and the enantiomeric excess of the product sulfoxide formed in chloroperoxidase incubations (Kobayashi et al., 1987), no such effect was observed in HRP incubations (Table 3.3.1). On one hand, this result is not surprising because the enantioselectivity of sulfoxidation of substituted thioanisoles by a chiral metalloporphyrin is also not affected by the *para* substituent (Naruta et al., 1990). However, this result is not consistent with previous studies that show the nature of the *para* substituent strongly affects the percent of the sulfoxide oxygen that derives from  $\text{H}_2\text{O}_2$  (Kobayashi et al., 1986). Sulfoxide with an oxygen that does not derive from  $\text{H}_2\text{O}_2$  should be formed in solution and therefore be racemic. Thus, an increase in incorporation of non- $\text{H}_2\text{O}_2$  oxygen should directly correlate with a decrease in the enantiomeric excess of the sulfoxide. There is no obvious mechanism in which a *para* substituent can affect the source of oxygen and not affect the stereochemistry of the product. Perhaps, the conclusions of Kobayashi et al. are in error because they did not properly control for background oxidation.

MnP also oxidizes thioanisole (Table 3.3.2). The rate of oxidation by MnP is slightly lower than the rate of oxidation by HRP,

but the enantiomeric excess of the product is considerably higher. These findings are consistent with the fact that MnP is a far less promiscuous enzyme than HRP and probably has a more restrictive active site structure (Glenn et al., 1986; Glenn and Gold, 1985). Hemoglobin, in contrast, oxidizes thioanisole more rapidly than HRP, giving a nearly racemic product. This finding is consistent with the finding that hemoglobin has an open active site architecture that allows the formation of an iron-phenyl complex (Augusto et al., 1982).

HRP reconstituted with  $\delta$ -*meso*-ethylheme catalyzes the sulfoxidation of thioanisole (Table 3.3.2). Importantly,  $\delta$ -*meso*-ethylheme-reconstituted HRP does not oxidize guaiacol at a significant rate (Table 3.3.2). Similarly, HRP arylated by phenylhydrazine retains its sulfoxxygenase activity yet has almost no peroxidase activity. Previous studies indicate that these treatments block guaiacol activity by denying the substrate access to the heme edge (Ator et al., 1987; Ator and Ortiz de Montellano, 1987). Thus, these results suggest that thioanisole and guaiacol are oxidized at different sites on the enzyme.

There are at least two explanations for the finding that phenylhydrazine-treated HRP and  $\delta$ -*meso*-ethylheme-reconstituted HRP oxidize thioanisole at a greater rate and with less stereoselectivity than native HRP (Table 3.3.2). First, the modifications may perturb the conformation of the enzyme active site in a manner that makes the iron-oxygen species more accessible to thioanisole. Thus the rate of oxidation is increased, yet the stereoselectivity is decreased because the prochiral sulfide binds in a less specific fashion. If these

conformational changes occur, they do not open up the region near the iron-oxygen species enough to allow formation of an iron-phenyl complex (Figure 3.3.3). A second possibility is that the enzyme modifications destabilize HRP Compounds I and II thereby increasing the oxidation potential of the enzyme. The more powerful enzyme would be expected to oxidize thioanisole at a higher rate with a relatively lower stereoselectivity. This second possibility is contradicted by the finding that the stereoselectivity of *p*-substituted thioanisole oxidation is not affected by the nature of the *para* substituent (Table 3.3.1).

The mixed noncompetitive inhibition of guaiacol oxidation by thioanisole (Figure 3.3.4) strongly supports the notion that the two substrates bind at distinct sites. The fact that a small amount of thioanisole can lower the apparent  $V_{max}$  of guaiacol oxidation illustrates that at "infinitely" high guaiacol concentrations, thioanisole is still able to bind to HRP. This result strongly suggests that guaiacol is not able to bind in the thioanisole binding site.

Interestingly, the difference spectrum of thioanisole binding to HRP (Figure 3.3.9) is similar to the spectrum of a number of other aromatic molecules binding to HRP (Hosoya et al., 1989; Paul and Ohlsson, 1978; Schejter et al., 1975). Thus, it seemed possible that thioanisole binds in a phenol binding site that is unaffected by  $\delta$ -*meso* substitution, and that guaiacol binds at a different, anomalous site near the heme edge. To investigate this possibility, the oxidation of *p*-toluidine by  $\delta$ -*meso*-ethylheme reconstituted HRP was examined.  $\delta$ -



*Meso*-ethylheme reconstituted HRP lacked the ability to efficiently oxidize *p*-toluidine, suggesting that all classical peroxidase substrates, regardless of the nature of their difference spectra, are likely oxidized at the heme edge. This result is consistent with the finding of Hosoya et al. (1989) that molecules can display different types of difference spectra, yet still compete for the same binding site.

A model that rationalizes the results of these studies is shown in Figure 3.4.1. Unlike previous models (Perez and Dunford, 1990a; Perez and Dunford, 1990b), this model does not invoke a free hydroxyl radical as the active oxidant of thioanisole. The key aspect of this model is that thioanisole and guaiacol bind at separate sites. As described in the introduction of this chapter, the guaiacol binding site is located near the  $\delta$ -*meso* heme edge. The thioanisole site must be located near the iron-oxygen species in order for oxygen insertion to occur. It must also be sufficiently removed from the  $\delta$ -*meso* heme edge so that a  $\delta$ -*meso*-ethyl substituent does not hinder sulfoxxygenation. The existence of two separate substrate binding sites has also been suggested from laser-excited fluorescence (Fidy et al., 1989) and NMR (Morishima and Ogawa, 1979) studies.

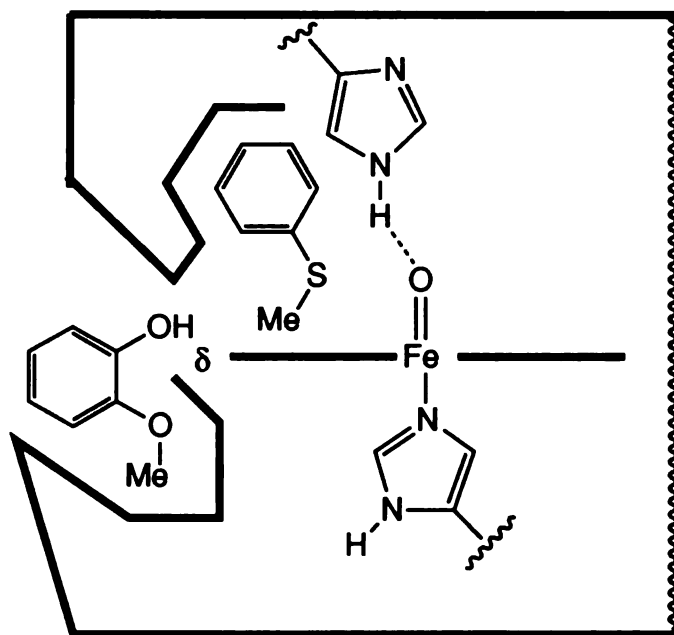


Figure 3.4.1. A model of the HRP active site.

The model also reconciles the fact that HRP behaves as an oxygenase with thioanisole, yet is unable to form an iron-phenyl complex or oxidize styrene to styrene oxide (Ortiz de Montellano, 1992). Because sulfoxidation requires only a single orbital overlap between the sulfur and the ferryl oxygen, thioanisole can bind laterally to the iron-oxygen species. Therefore, a protein barrier that prevents the formation of an iron-phenyl complex may exist directly above the heme iron. The steric restraints created by this barrier may also prevent HRP from carrying out the epoxidation of styrene because epoxidation, which requires the interaction of two carbons and the ferryl oxygen, is sterically more demanding than sulfoxxygenation.

The kinetic evidence clearly establishes that guaiacol, although similar in structure to thioanisole, does not bind at the site near the

iron-oxygen species. This conclusion is supported by the fact that catechol, the product of guaiacol O-demethylation (a classical oxygenase reaction), is not produced in HRP-guaiacol incubations (Dr. James DeVoss, personal communication). The kinetic results, however, do not preclude thioanisole from binding at the guaiacol site near the heme edge. An intriguing possibility is that thioanisole is oxidized at both sites. The 10 % sulfoxide whose oxygen does not derive from H<sub>2</sub>O<sub>2</sub> may be formed at the heme edge. This scheme nicely explains the fact that thioanisole and its radical cation compete for Compound II oxidation (Pérez and Dunford, 1990c). However, the finding that  $\delta$ -meso-ethylheme reconstituted HRP oxidizes thioanisole with a lower stereoselectivity than native HRP argues strongly against this possibility if it is assumed that the sulfoxide formed at the heme edge is racemic.

In summary, there are at least two explanations as to why the iron-oxygen species of HRP reacts directly with sulfur containing substrates and not with phenolic substrates. Either the sulfur containing compounds bind in a different region of the active site than do phenols, or the radical cation produced from the one-electron oxidation of the sulfur compounds has a different reactivity than the radical produced by phenol oxidation. The finding that HRP reconstituted with  $\delta$ -meso-ethylheme or modified with phenylhydrazine loses the ability to oxidize guaiacol yet retains the ability to oxidize thioanisole, along with the finding of mixed noncompetitive inhibition of guaiacol oxidation by thioanisole, clearly supports the first possibility. The results of these studies therefore

**strengthen the hemoprotein theory: Whether HRP behaves as an oxygenase or as a peroxidase is controlled, at least in part, by the location of substrate binding relative to the heme group.**

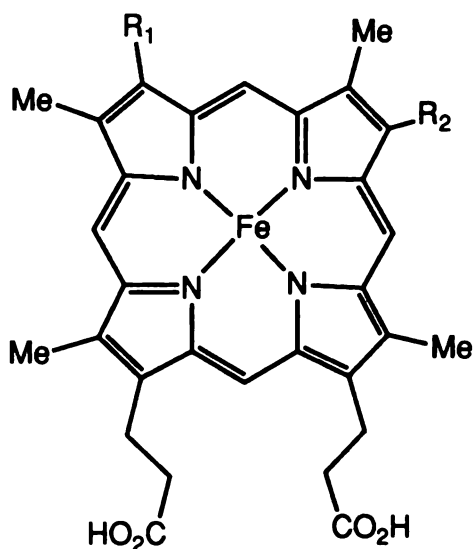
## **4.0 Reconstitution of HRP with 8-Hydroxymethylheme and 8-Formylheme**

### **4.1 Introduction**

Over fifty years ago, HRP became the first hemoprotein from which the heme was removed and the resulting apoprotein was reconstituted with hemin to fully active enzyme (Theorell, 1940). Since that time, a number of synthetic enzymes containing modified hemes have been prepared (Figures 4.1.1-4.1.3). These synthetic enzymes have provided many insights into hemoprotein structure and reactivity.

HRP reconstituted with deuteroheme, 2,4-dimethyldeuteroheme, or mesoheme (Figure 4.1.1) has chemical and enzymatic properties very similar to the properties of native enzyme (DiNello and Dolphin, 1981; Paul, 1959; Tamura et al., 1972). The only major difference is that the Compound I species of the deuteroheme containing enzyme has an  $^2A_{1u}$  electronic ground state instead of the  $^2A_{2u}$  ground state found in native HRP (DiNello and Dolphin, 1981), but this change in electronic configuration does not significantly alter enzyme activity (DiNello and Dolphin, 1981; Tamura et al., 1972). Thus, the side chains at positions 2 and 4 are not essential for normal peroxidase activity. However, if a relatively large group such as *p*-cresol is substituted at the 2 or 4 positions, the kinetics of reconstitution are slow and the modified enzyme reacts abnormally with H<sub>2</sub>O<sub>2</sub> and reducing substrates (DiNello and Dolphin, 1981). Based on these results, it has been suggested that the 2 and 4

positions of the heme are buried within the protein (DiNello and Dolphin, 1981; Tamura et al., 1972).

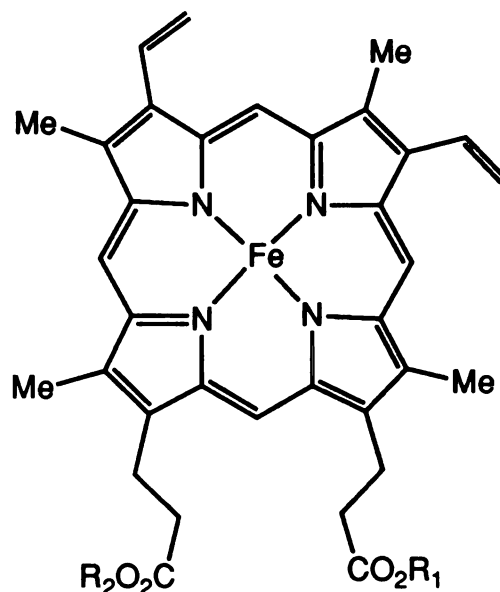


- 1  $R_1 = R_2 = -CHCH_2$  (protoheme)
- 2  $R_1 = R_2 = -H$  (deuteroheme)
- 3  $R_1 = R_2 = -CH_3$  (dimethyldeuteroheme)
- 4  $R_1 = R_2 = -CH_2CH_3$  (mesoheme)

Figure 4.1.1. Hemes modified at the 2 ( $R_1$ ) and 4 ( $R_2$ ) positions.

HRP reconstituted with hemes monomethylester or heme dimethylester (Figure 4.1.2) reacts with  $H_2O_2$  to form a normal Compound I species (Araiso and Dunford, 1981; Araiso et al., 1979; DiNello and Dolphin, 1981). Although the Compound I species of the monoester forms of HRP have normal stability in the absence of a reducing substrate (half life > 20 min), the Compound I of dimethylester HRP decays rapidly (half life = 30 s) (Araiso and Dunford, 1981). Thus, the negative charge of at least one carboxylate group is necessary for stabilization, but not formation of, Compound I.

The reconstitution efficiency of dimethylester heme into protein is low (1.5%) compared to the reconstitution efficiency of either of the possible monomethylester hemes into protein (25%) (Araiso et al., 1979), and if either propionate group is replaced with a butyrate group, reconstitution becomes extremely difficult (DiNello and Dolphin, 1981). Based on these results, it has been suggested that the main function of the propionate side chains is to stabilize heme orientation within the protein (Araiso and Dunford, 1981; Araiso et al., 1979). However, the fact that *o*-dianisidine treatment of HRP modifies a heme carboxylate demonstrates that one of the propionate side chains is solvent accessible (Ugarova et al., 1984).



- 5 R<sub>1</sub> = R<sub>2</sub> = -H (protoheme diacid)
- 6 R<sub>1</sub> = R<sub>2</sub> = -CH<sub>3</sub> (dimethylester)
- 7 R<sub>1</sub> = H, R<sub>2</sub> = -CH<sub>3</sub> (monoester)
- 8 R<sub>1</sub> = CH<sub>3</sub>, R<sub>2</sub> = -H (monoester)

Figure 4.1.2. Hemes modified at the 7 (R<sub>1</sub>) and 8 (R<sub>2</sub>) positions.

HRP has also been reconstituted with  $\delta$ -*meso* substituted hemes. HRP reconstituted with  $\delta$ -*meso*-methylheme reacts relatively normally with  $\text{H}_2\text{O}_2$  to form a species capable of oxidizing classical peroxidase substrates (Ator et al., 1987). Thus, a *meso* substitution does not, *per se*, eliminate normal peroxidase activity. In contrast, HRP reconstituted with  $\delta$ -*meso*-ethylheme reacts with  $\text{H}_2\text{O}_2$  yet does not efficiently oxidize classical peroxidase substrates (Ator et al., 1987). The relatively large ethyl group probably acts sterically to deny the substrates access to the  $\delta$ -*meso* heme edge. Based on these results, it has been hypothesized that classical peroxidase substrates are oxidized near the  $\delta$ -*meso* heme edge (Ator et al., 1987; Ortiz de Montellano, 1992). Many other pieces of evidence support this hypothesis (Chapter 1, section 13).

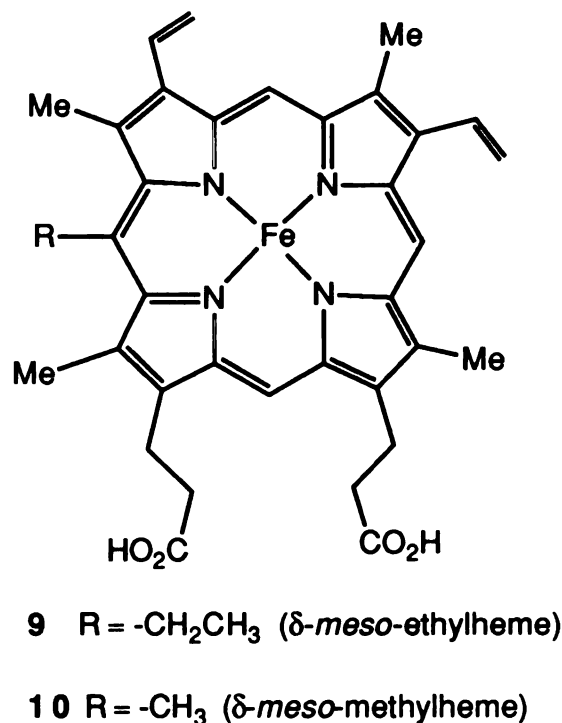


Figure 4.1.3. The structures of  $\delta$ -*meso* modified hemes.



As described above, heme modification can drastically alter hemoprotein reactivity. However, most hemoproteins do not contain modified hemes. Thus, it is the protein moiety that normally controls hemoprotein reactivity. There are, however, a few peroxidases that have modified heme prosthetic groups. The effects of the heme modifications on the reactivities of these hemoproteins are not understood. Reconstitution studies provide an excellent opportunity to model these proteins and to determine the effects of the heme modifications.

Myeloperoxidase (MPO) is a mammalian enzyme found in the cytoplasmic granules of polymorphonuclear leukocytes (Klebanoff, 1991). Leukocytes play a major role in the mammalian immune response by phagocytosing foreign microbes. It is generally believed that the primary function of myeloperoxidase is to oxidize  $\text{Cl}^-$  to HOCl (hypochlorous acid) (Harrison and Schultz, 1976; Klebanoff, 1991; Thomas and Learn, 1991), a powerful oxidizing agent that destroys phagocytized microbes (Hurst, 1991; Klebanoff, 1991; Thomas and Learn, 1991). The HOCl generated by myeloperoxidase may also mediate tissue degradation in inflammatory diseases (Weiss, 1989) and activate certain proteinases (Klebanoff, 1991). The ability of myeloperoxidase to oxidize chloride is quite unique. HRP, while capable of oxidizing iodide, cannot oxidize other halides.

Because MPO has a red-shifted spectrum (bathochromic shift) and relatively highly absorbing visible bands compared to other peroxidases (Wever and Plat, 1981), it is generally believed that MPO

contains a modified heme prosthetic group (Hurst, 1991). It has been impossible to determine the structure of this prosthetic group, however, because it can only be removed from the protein under harsh conditions that cause irreversible changes in its structure (Hurst, 1991). The unusual spectral characteristics of MPO may be due to the presence of a chlorin prosthetic group (Hurst, 1991). Chlorins are dihydroporphyrin derivatives that are produced by a reduction of one heme pyrrole ring (Figure 4.1.4). They can be formed by addition across the  $\beta$ -pyrrolic double bond. Resonance Raman studies suggest the presence of a chlorin prosthetic group in MPO (Babcock et al., 1985; Sibbett and Hurst, 1984), and a recent low resolution (3Å) crystal structure is consistent with this suggestion (Zeng and Fenna, 1992). However, neither study has provided conclusive evidence.

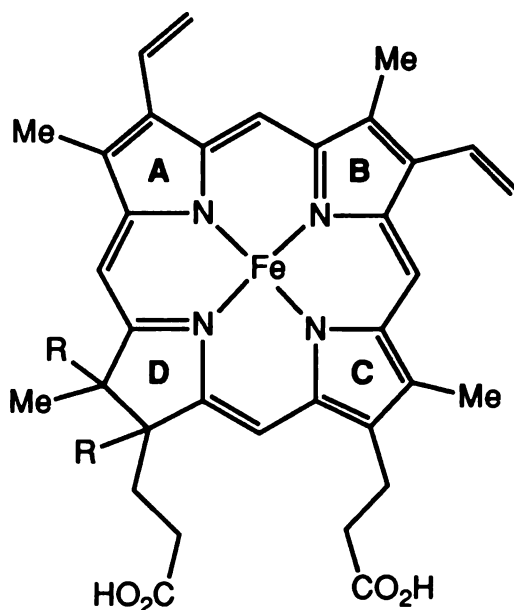


Figure 4.1.4. Structure of a chlorin isomer in which the D ring is reduced.

The unique spectral characteristics of MPO are also consistent with the presence of a heme that contains an electron-withdrawing moiety, such as a formyl group, at its periphery (Hurst, 1991). Heme *a* of cytochrome c oxidase provides precedence for this type of heme (Battersby et al., 1985) (Figure 4.1.5). A recent resonance Raman characterization of MPO that had been denatured with guanidine·HCl (Wever et al., 1991), and the fact that carbonyl reagents such as sodium cyanoborohydride blue-shift the MPO Soret band (Odajima, 1980), suggest the presence of a formylheme. Also, a comparison of the magnetic circular dichroism spectrum of MPO to that of myoglobin reconstituted with a formylheme strongly supports the existence of a formylheme in MPO (Sono et al., 1991). It should be noted, however, that a formyl modification of the heme is not apparent in the recent crystal structure of MPO (Zeng and Fenna, 1992). However, this result is ambiguous due to the low resolution of the structure.

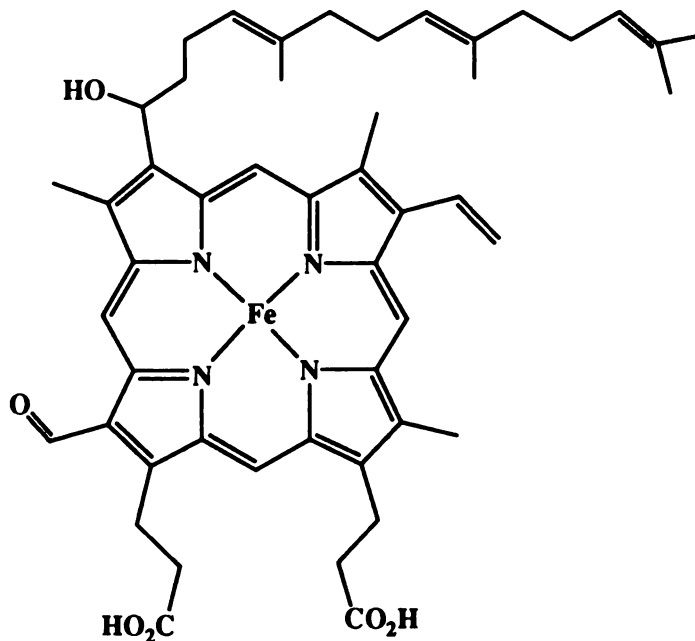


Figure 4.1.5. Structure of heme *a*.

A scheme that reconciles the existence of both a chlorin and a formylheme has been suggested (Hurst, 1991) (Figure 4.1.6). A formylheme is converted to a chlorin by the addition of a protein nucleophile. Thus, depending on the conditions, a formylheme or a chlorin may exist. However, further studies are needed to unambiguously determine the structure of the MPO prosthetic group.

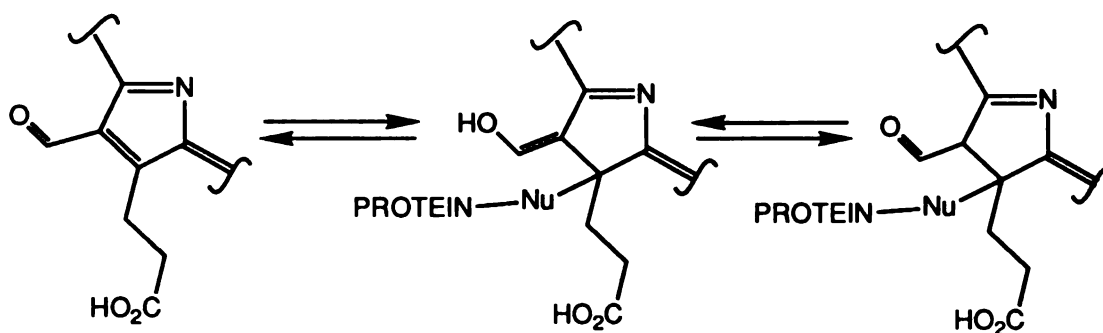
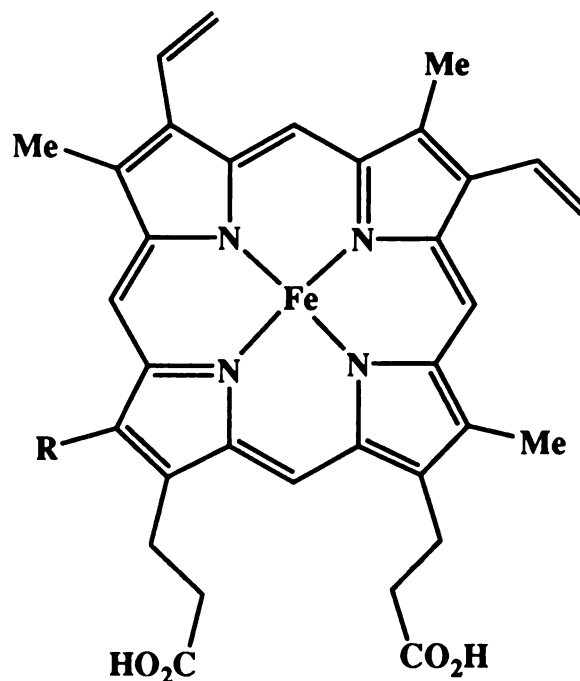


Figure 4.1.6. A possible structure of the MPO prosthetic group. Adapted from Hurst (1991).

Lactoperoxidase is a mammalian protein found in milk, tears, and saliva (Reiter and Perraudin, 1991; Thomas et al., 1991). It is believed to function to oxidize SCN<sup>-</sup> (thiocyanate) to OSCN<sup>-</sup> (hypothiocyanite) (Reiter and Perraudin, 1991; Thomas et al., 1991). Hypothiocyanite is a mild oxidizing agent that is believed to have bactericidal properties (Reiter and Perraudin, 1991; Thomas et al., 1991). Lactoperoxidase is also able to oxidize iodide, bromide, and phenols (Thomas et al., 1991). Like MPO, lactoperoxidase is believed to have a modified heme prosthetic group. The exact structure of this heme is unknown. Treatment of the enzyme with a reducing agent and denaturant causes the release of a species identical to protoporphyrin IX except that a thiol group is attached to the 1- or 8-

methyl group (Nichol et al., 1987). This result led to the hypothesis that the heme is attached to a cysteine residue via a disulfide or thioether linkage (Nichol et al., 1987; Thomas et al., 1991).

It is not known what effect the heme modifications have on myeloperoxidase and lactoperoxidase activities. It is conceivable, however, that the heme modifications impart to these enzymes their unique ability to oxidize halides and pseudohalides. Therefore, in order to investigate whether the prosthetic group structure can have such an effect, HRP was reconstituted with 8-hydroxymethylheme and 8-formylheme (Figure 4.1.7).



11 R = -CH<sub>2</sub>OH (8-hydroxymethylheme)

12 R = -CHO (8-formylheme)

Figure 4.1.7. Structures of 8-hydroxymethylheme and 8-formylheme.

## **4.1 Experimental Section**

### **Materials**

Thioanisole, hydrogen peroxide,  $\alpha$ -(4-pyridyl 1-oxide)-*N*-*tert*-butylnitrone (POBN), phenylhydrazine·HCl, styrene, tetrapropylammonium peruthenate, and 4-methylmorpholine N-oxide were purchased from Aldrich. Horseradish peroxidase (type VI), monochlorodimedon, and guaiacol were from Sigma. Sodium azide was from J.T. Baker. Ethylhydrazine oxalate was from Fluka. Phenyl *N*-*tert*-butylnitrone (PBN) was from Eastman. Stock solutions of ethylhydrazine were made in 0.01 N HCl to minimize autooxidation. Buffers were made with deionized, glass-distilled water that had been stirred overnight with 5 g/liter Chelex 100 beads (Bio-Rad). Incubations were carried out in 50 mM phosphate buffer, pH 7.0.

### **Analytical Methods**

HPLC was performed on a Hewlet Packard model 1040A system equipped with a diode array detector and a Varian 9010 solvent pump. Guaiacol assays were performed on a Hewlet Packard model 8450A diode array spectrophotometer. Absorption spectra were recorded on an Aminco DW-2000 spectrophotometer. Fast kinetics were measured on an Applied Photosystem stopped flow spectrometer model SF.17MV equipped with a xenon arc lamp and interfaced to an Acorn, Archimedes 400 series computer. EPR spectra were recorded on a

Varian E-104 instrument interfaced to an IBM XT computer. GC was performed on a Hewlett-Packard model 5890 gas chromatogram equipped with a flame ionization detector and interfaced to a Hewlett-Packard 3365 Chemstation.

### **Formation of 8-Hydroxymethylheme**

8-Hydroxymethylheme was kindly provided by Kevin Smith (Snow and Smith, 1989) or was formed from incubations containing phenylhydrazine and HRP essentially as previously described (Ator and Ortiz de Montellano, 1987) except that the incubation conditions were modified to increase the amount of 8-hydroxymethylheme produced: To HRP (30  $\mu$ M, 168 mg), and phenylhydrazine (750  $\mu$ M, 15 mg) in 140 mL of chelexed sodium phosphate buffer pH 7.0, was added an 18  $\mu$ L aliquot of 4 M hydrogen peroxide. The incubation stood at room temperature for 10 minutes before a second aliquot of hydrogen peroxide was added (1.0 mM final peroxide concentration). The incubation then sat an additional 15 minutes. Catalase (20  $\mu$ L of a 10 mg/mL solution) was added to destroy any remaining H<sub>2</sub>O<sub>2</sub> and after 5 minutes, sodium ascorbate (600  $\mu$ L of a 50 mM solution) was added to reduce any oxidized heme species. The mixture was acidified with acetic acid, extracted with diethyl ether, and analyzed by HPLC as already described (Ator and Ortiz de Montellano, 1987).

### **Formation of 8-Formylheme**

Tetrapropylammonium peruthenate (Griffith et al., 1987) was used to oxidize 8-hydroxymethylheme to 8-formylheme. In the dark, 8-hydroxymethylheme (1 mg, 1.5  $\mu\text{mol}$ ) was dissolved in a few drops of pyridine and then diluted with 1 mL of dichloromethane. The mixture was stirred at room temperature under argon and a small amount of tetrapropylammonium peruthenate was added. The shift of the Soret absorbance from 397 to 408 was used as a measure of the extent of the reaction. Additional tetrapropylammonium peruthenate or the peruthenate regenerator 4-methylmorpholine N-oxide was periodically added until the reaction was nearly complete. The total reaction time was approximately 2.5 h. The reaction mixture was then diluted with dichloromethane (20 mL) and sequentially washed with 20 mL of sodium sulfite solution, 20 mL of brine, and 20 mL of saturated copper(II) chloride solution. The dichloromethane was removed *in vacuo* and the sample was dissolved in HPLC solvent. The modified heme was purified by reversed-phase HPLC on a semi-prep column packed with Whatman Partisil ODS-3 and eluted with 55:45:10 acetonitrile : water : acetic acid at a flow of 3 mL/min. The HPLC effluent was monitored at 406 nm. Mass spectrometry revealed the expected molecular ion  $m/z = 632$ .

### **Reconstitution of Modified Hemes into HRP**

Reconstitution of modified hemes into apoprotein was performed as already described (Ator et al., 1989).



## **Kinetics of Compound I Formation and Decay**

The rate of formation and decay of Compound I was measured by stopped flow spectrophotometry. Equal volumes of 20  $\mu\text{M}$  8HM-HRP (20  $\mu\text{M}$ ) and hydrogen peroxide (200  $\mu\text{M}$ ) were delivered into the stopped flow mixing chamber to give final enzyme and peroxide concentrations of 10  $\mu\text{M}$  and 100  $\mu\text{M}$ , respectively. The absorbance was monitored at 412 nm, the isosbestic point of 8HM-HRP and its Compound II species so that only the formation and decay of Compound I were observed. The concentration of hydrogen peroxide was one order of magnitude greater than the concentration of enzyme so that Compound I was formed under pseudo first order conditions. The instrument settings were: monochromator = 412 nm, power = 150 W (current of 8 A x voltage of 19 V), slit widths = 1 nm, PM voltage = 700, and noise filtration = off. A similar experiment was performed with 8F-HRP except that the monochromator was set at 427 nm, the isosbestic point between 8F-HRP and its Compound I species.

## **Measurement of Guaiacol, Thioanisole and Iodide Activities**

The ability of HRP, 8F-HRP and 8HM-HRP to oxidize iodide, thioanisole and guaiacol was assayed as previously described (Harris et al., 1993). The ability of HRP, 8F-HRP and 8HM-HRP to oxidize chloride and bromide was determined by measuring the rate of enzyme-mediated monochlorodimedone halogenation (Hager et al., 1967). Peroxidase (0.4 nmol) was added to 50 mM sodium phosphate

buffer (pH 7.0) containing H<sub>2</sub>O<sub>2</sub> (200 μM), monochlorodimedone (100 μM) and NaCl or NaBr (100 mM). The rate of monochlorodimedone halogenation was determined from the decrease of monochlorodimedone absorbance at 290 nm ( $\epsilon = 18,000 \text{ M}^{-1}\text{cm}^{-1}$ ).

### **Characterization of the Products of Guaiacol Oxidation**

The aqueous solution of a peroxidase - guaiacol incubation was diluted with methanol and analyzed by HPLC. The products were separated on a 5-μM column packed with Whatman Partisil ODS-3 and eluted with the gradient (solvent A, 40:60:1 MeOH:H<sub>2</sub>O:CH<sub>3</sub>COOH; solvent B 100:1 MeOH:CH<sub>3</sub>COOH): 0-10 min. 100% A, 10-25 min. 100% A to 100% B in a linear gradient. The column effluent was monitored at 276 and 470 nm.

### **Spin-Trapping of Ethyl and Azidyl Radicals**

8HM-HRP (12 mM), in pH 7 chelexed sodium phosphate buffer that contained POBN (45 mM) and DETAPAC (5 μM), was incubated with hydrogen peroxide (175 μM) and either sodium azide (10 mM) or ethylhydrazine (20 mM). A 50 μL portion of the incubation was added by syringe into a capillary tube and dropped into a quartz tube aligned in the EPR cavity. The azide incubations were scanned immediately, whereas the ethylhydrazine incubations were scanned at various times after the reaction was initiated. Control incubations that lacked either enzyme or peroxide were performed. The EPR parameters were: field 3400 Gauss, scan range 10 x 10 Gauss, microwave frequency 9.52

GHz, power 20 mW, 2nd harmonic 100 KHz, modulation amplitude 1 x 1, scan time 2 minutes, and time constant 0.25.

### **Detection of a Protein Radical in 8F-HRP**

In a quartz EPR tube, 48  $\mu$ M hydrogen peroxide was added to 20  $\mu$ M 8F-HRP and the tube was immediately frozen in a liquid nitrogen bath. The sample was then inserted into a liquid nitrogen containing Dewar flask that was aligned in the EPR cavity and immediately scanned. EPR parameters were: field 3269 Gauss, scan range 5 x 100 Gauss, microwave frequency 9.07 GHz, power 2 mW, 2nd harmonic 100 KHz, modulation amplitude 0.8 x 10, scan time 2 minutes, and time constant 0.5.

### **Ethylhydrazine-Mediated Inactivation**

To a solution containing HRP, 8HM-HRP or 8F-HRP (1  $\mu$ M) in 1 mL of pH 7.0 sodium phosphate buffer was added 30  $\mu$ L of a 50 mM solution of ethylhydrazine oxalate in 0.01 M HCl, and 2  $\mu$ L of a 70 mM solution of hydrogen peroxide. The final ethylhydrazine and hydrogen peroxide concentrations were 1.5 mM and 140  $\mu$ M, respectively. The solution stood at room temperature, and at appropriate times 5  $\mu$ L aliquots were removed and assayed for guaiacol activity.

### **Azide Inactivation**

Hydrogen peroxide (120  $\mu\text{M}$ ) and sodium azide (2.5  $\mu\text{M}$  - 120  $\mu\text{M}$ ) were added to peroxidase (2.5  $\mu\text{M}$ ) in 0.5 mL of pH 7.0 phosphate buffer. The incubation stood at room temperature for 2 hr and was then assayed for guaiacol activity.

### **Detection of Iron-Phenyl Complex**

Methylphenyldiazene carboxylate azo ester (3  $\mu\text{L}$ ) was hydrolyzed to phenyldiazene carboxylate in 300  $\mu\text{L}$  of argon-saturated 0.1 M NaOH. A 2  $\mu\text{L}$  aliquot of this solution was added to 1 mL of 8F-HRP (4  $\mu\text{M}$ ) in pH 7 phosphate buffer. An additional aliquot of phenyldiazene carboxylate was added every 5 minutes until a total of 4 aliquots had been added. The electronic absorption spectrum of the solution was monitored over the 20 minute incubation.

### **Styrene Oxidation**

Styrene oxidation was analyzed as previously described (Ortiz de Montellano and Catalano, 1985; Ortiz de Montellano and Grab, 1987). A 2  $\mu\text{L}$  aliquot of styrene (neat) was added to enzyme (4  $\mu\text{M}$ ) in 0.5 mL of sodium phosphate. The solution was mixed for 5 minutes and then  $\text{H}_2\text{O}_2$  (100  $\mu\text{L}$  of a 10 mM solution) was added over 1 hr, giving a nominal 2 mM peroxide concentration. The solution was extracted with 0.5 mL of dichloromethane and analyzed by GC chromatography. The following temperature gradient was used: 0 to 3 minutes 80°C; 3

to 12.5 minutes linear rise from 80°C to 130°C; 12.5 to 20 minutes linear rise from 130°C to 300°C.

### **Isolation of Heme Adduct From Azide Inactivated 8HM-HRP**

In pH 7.0 sodium phosphate buffer (4ml), 8HM-HRP (20 µM), sodium azide (2 mM), and hydrogen peroxide (1.5 mM) were incubated for 10 minutes. Catalase was then added, and after 5 minutes, the solution was acidified with acetic acid and extracted with diethyl ether. The ether was removed under vacuum and the resulting heme residue was analyzed by HPLC. An Alltech Partisil ODS-3, 5µ HPLC column was utilized with the following gradient: 0 to 20 minutes 95 % A, 5 % B; 20 to 30 minutes linear rise from 5% B to 100% B; 30 to 35 minutes 100% B; where solvent A was 60:40:10, methanol : water : acetic acid and solvent B was 100:0.1, methanol : acetic acid.

## **4.3 Results**

### **4.3.1 Formation of 8-Hydroxymethylheme from Phenylhydrazine Incubations**

An HPLC chromatogram of the heme products extracted from an HRP - phenylhydrazine incubation is shown in Figure 4.3.1. The Soret of 8-hydroxymethylheme under the HPLC conditions was 397, nearly identical to that of heme. Assuming the extinction coefficient of 8-

hydroxymethylheme is equal to that of unmodified heme ( $\epsilon_{397} = 0.1 \mu\text{M}^{-1}\text{cm}^{-1}$ ), 800 nmol of 8-hydroxymethylheme was produced from 4200 nmol HRP, giving a yield of just under 20%. This yield is higher than that achieved in incubations performed under the conditions previously reported (Ator and Ortiz de Montellano, 1987).

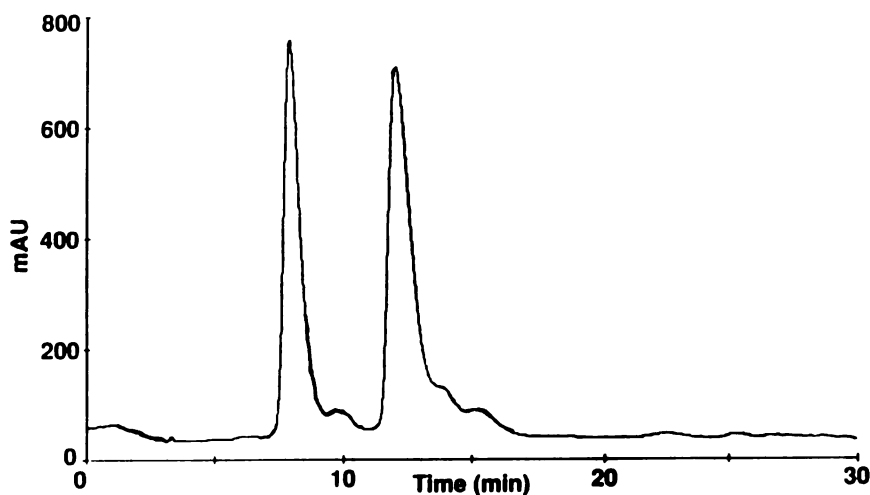


Figure 4.3.1. HPLC chromatogram of the heme products extracted from an HRP incubation with phenylhydrazine. The peak at 8 minutes is 8-hydroxymethylheme and that at 13 minutes is heme.

### **Formation of 8-Formylheme from 8-Hydroxymethylheme**

Many attempts to oxidize 8-hydroxymethylheme to 8-formylheme were carried out. However, many reagents, including pyridinium chlorochromate, activated DMSO, periodinane, and manganese dioxide caused a great amount of heme degradation and failed to produce a significant amount of the desired product.

Tetrapropylammonium peruthenate was the only agent that proved effective, affording a 20% yield of the product aldehyde. An HPLC chromatogram of the reaction is shown below (Figure 4.3.2). The HPLC system provided excellent separation of 8-hydroxymethylheme and 8-formylheme. The Soret of 8-formylheme was at 408 nm, 12 nm red-shifted from that of heme (Figure 4.3.3). This red-shift is expected of a heme having a conjugated formyl group at its periphery. The molecular ion  $m/z = 632$  is also consistent with the formation of 8-formylheme. (NMR could not be performed due to low amounts of material available.)

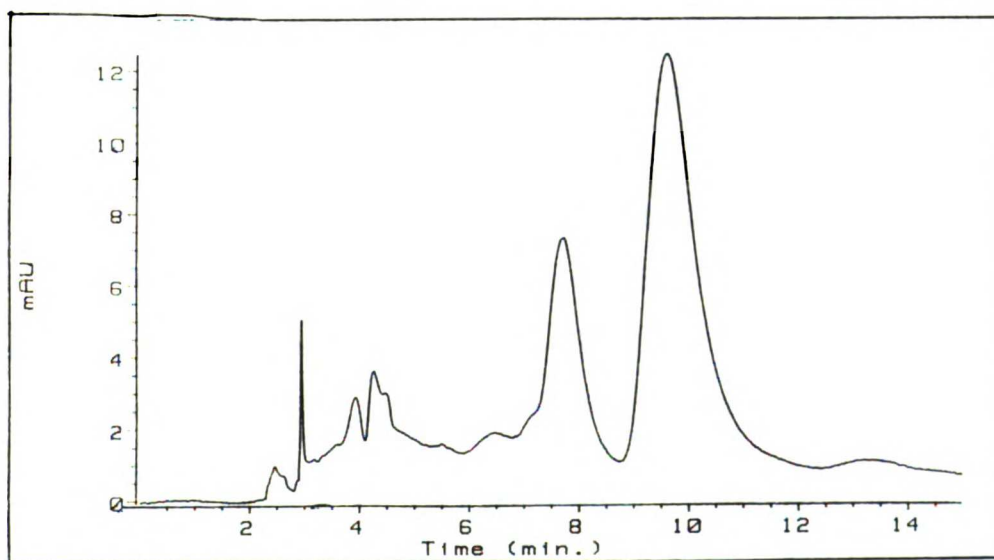


Figure 4.3.2. HPLC chromatogram of the products of a tetrapropylammonium peruthenate oxidation of 8-hydroxymethylheme. The peak at 7.8 minutes is 8-hydroxymethylheme and the peak at 9.5 minutes is 8-formylheme.

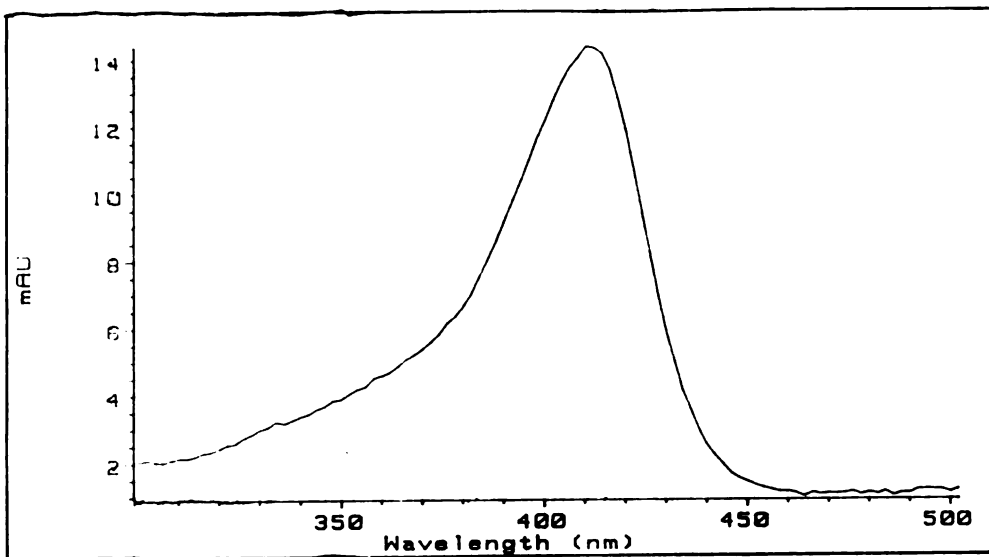


Figure 4.3.3. Electronic absorption spectrum of 8-formylheme.

### **Spectral Characterization of the Reconstituted Enzymes**

The spectra of HRP reconstituted with 8-hydroxymethylheme (8HM-HRP) and with 8-formylheme (8F-HRP) are shown in Figure 4.3.4. The Soret band of the 8HM-HRP is at 402 nm, identical to that of native enzyme. The spectra of 8HM-HRP Compounds I and II are also identical to those of native HRP. The Soret band of 8F-HRP is red-shifted to 417 nm. The Compound II species of 8F-HRP has a Soret absorbance of 436 nm, 20 nm red-shifted from that of native or 8HM-HRP. The Soret band of the Compound I species of 8F-HRP could not be measured (see below). Quantitation of the enzyme in all of the studies described below was performed using the extinction coefficient of native HRP ( $\epsilon_{404\text{nm}} = 1.02 \times 10^5 \text{ M}^{-1}\text{cm}^{-1}$ ).



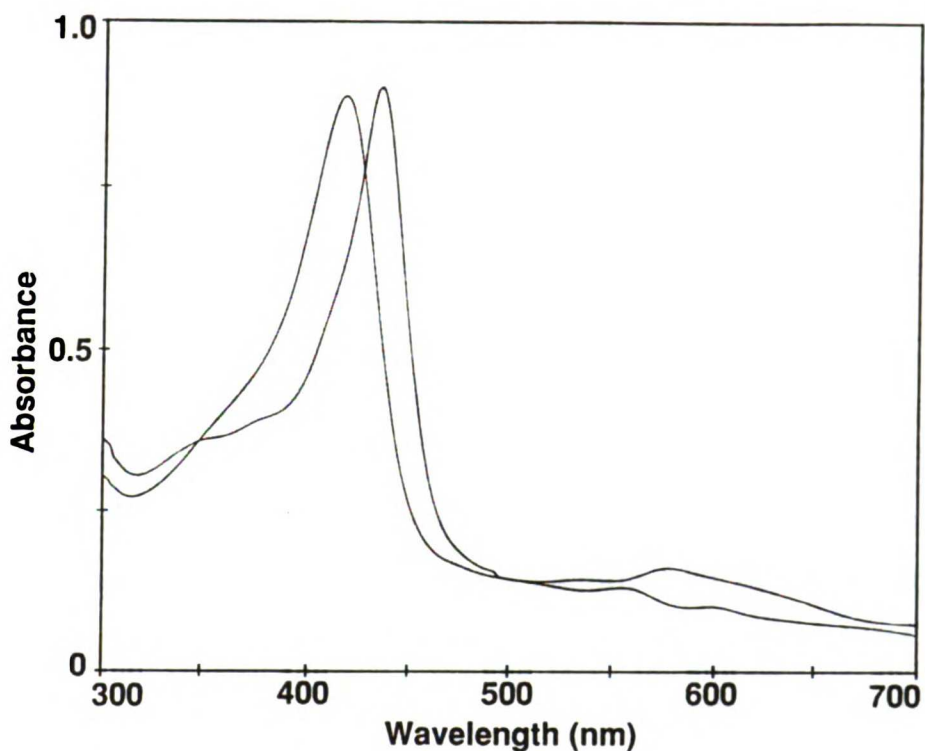


Figure 4.3.4. Electronic absorption spectrum of 8HM-HRP (Soret = 402 nm) and 8F-HRP (Soret = 417 nm).

### Rate of Compound I Formation and Decay

The rate of formation and decay of 8HM-HRP Compound I was measured by stopped flow spectrophotometry. The absorbance was measured at 412 nm, the isosbestic point between HRP reconstituted with 8-hydroxymethylheme and the Compound II species of the reconstituted enzyme. Therefore, only the formation and decay of 8HM-HRP Compound I were observed. The kinetic traces for the decay and formation of Compound I are shown in Figure 4.3.5. Compound I formation ( $V_1$ ) is described by the equation  $V_1 = k_1[\text{HRP}][\text{H}_2\text{O}_2] = k_1'[\text{HRP}]$ , where  $k_1'$  is a pseudo first order rate constant. Note that if  $[\text{H}_2\text{O}_2]$  is too high,  $k_1'$  gets too large and the

reaction becomes too fast to measure (the dead time of the machine is approximately 1 ms). The value of  $k_1'$  was found to be approximately  $860 \text{ s}^{-1}$  for both native and 8HM-HRP (Figure 4.3.5). This gives a second order rate constant of  $8 \times 10^6 \text{ M}^{-1}\text{s}^{-1}$  which agrees well with the literature value of  $1.8 \times 10^7 \text{ M}^{-1}\text{s}^{-1}$  (Marnett et al., 1986).

The rate of Compound I decay to Compound II ( $V_2$ ) is described by the equation  $V_2 = k_2[\text{HRP}][\text{reducing substrate}]$ . In these studies the reducing substrate is impurities in the buffer, or the enzyme itself. Thus,  $V_2 = k_2'[\text{HRP}]$ , where  $k_2'$  is a pseudo first order rate constant. For native HRP,  $k_2'$  was found to be  $0.010 \text{ s}^{-1}$ , and for 8HM-HRP,  $k_2'$  was found to be  $0.021 \text{ s}^{-1}$  (Figure 4.3.5). Therefore Compound I of 8HM-HRP forms at an equal rate to that of native HRP, and is reduced approximately 2 times faster than that of native enzyme.

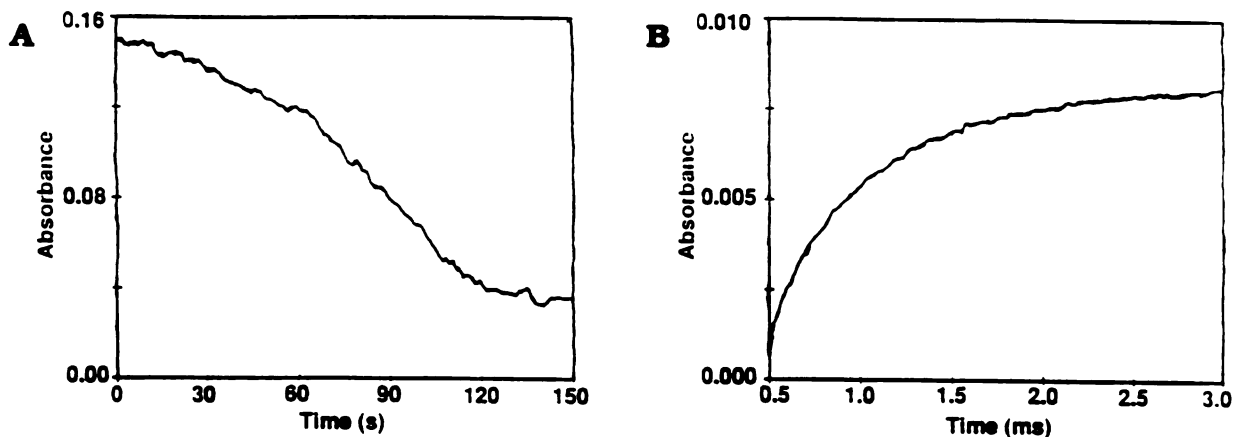


Figure 4.3.5. Stopped flow chromatograms of 8HM-HRP Compound I formation (A) and decay (B).

## **8F-HRP Compound I Formation**

When native HRP was incubated with a 20-fold excess of hydrogen peroxide, a Compound I species that was stable for approximately 1 minute could be observed. When 8F-HRP was incubated with hydrogen peroxide under identical conditions, only Compound II could be observed. Thus, under these conditions, the Compound I species of 8F-HRP decays in less than 5 seconds. When HRP was incubated with a 2-fold excess of peroxide, the resulting Compound I species took over 7 minutes to decay to Compound II. Under identical conditions, a mixture of Compounds I and II were observed immediately after the addition of peroxide to 8F-HRP, and only Compound II could be observed 15 seconds later. However, if the incubation was performed at 5 °C, a Compound I species, that was contaminated with only a small amount of Compound II, could be transiently detected (Figure 4.3.6). Due to the lack of sample, the kinetic constants for the formation and decay of 8F-HRP Compound I could not be determined by stopped flow spectroscopy.

In the absence of substrate, the protein is most likely the reductant of Compound I. Therefore, not surprisingly, a small, yet reproducible protein radical signal ( $g = 2.0$ ) was detected by EPR when 8F-HRP was incubated with hydrogen peroxide (Figure 4.3.7).

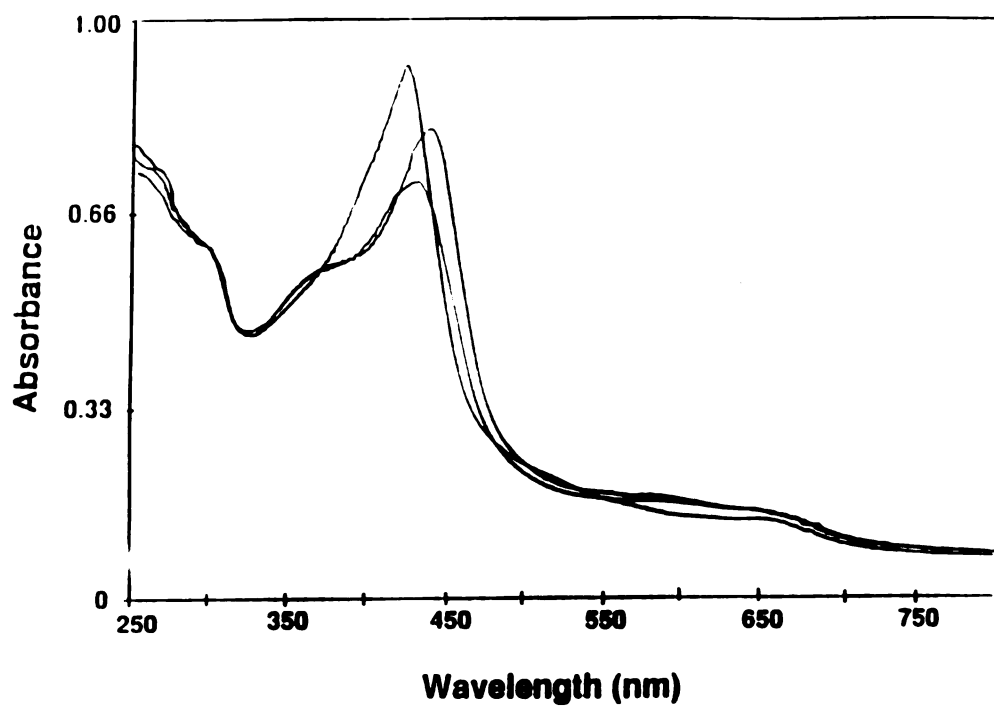


Figure 4.3.6. Spectrum of 8F-HRP (large Soret), its Compound I (small Soret), and its Compound II (medium Soret) species. The Compound I species is contaminated with a small amount of Compound II.



Figure 4.3.7. EPR spectrum of 8F-HRP upon addition of hydrogen peroxide.

## Catalytic Activity

HRP reconstituted with 8-hydroxymethylheme oxidized guaiacol, iodide, and thioanisole at rates nearly identical to those of native enzyme. The enantiomeric excess of the product sulfoxide in 8HM-HRP- and native HRP- thioanisole incubations were also identical. Furthermore, like native HRP, 8HM-HRP lacked the ability to oxidize chloride and bromide ions.

HRP reconstituted with 8-formylheme oxidized guaiacol, iodide, and thioanisole at rates significantly lower than the rates of oxidation catalyzed by native HRP. The  $k_{cat}$  and  $K_M$  values for guaiacol oxidation by 8F-HRP are  $33.4 \text{ s}^{-1}$  and  $2.3 \text{ mM}$  compared to  $104 \text{ s}^{-1}$  and  $1.8 \text{ mM}$  for HRP (Figure 4.3.8). Thus the decrease in guaiacol activity is primarily due to a decrease in  $k_{cat}$ .

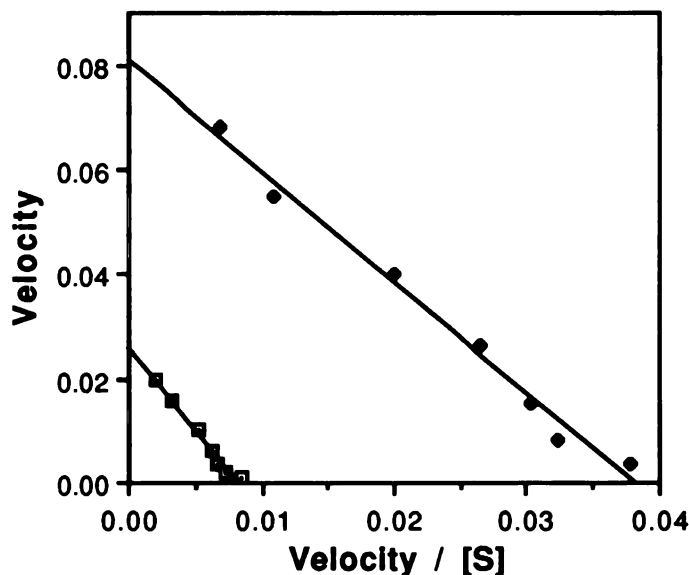


Figure 4.3.8. Eadie Hofstee plot of guaiacol oxidation by HRP (top line), and by 8F-HRP (bottom line).

The product profile from an 8F-HRP incubation with guaiacol (Figure 4.3.9) is virtually identical to the product profile from an HRP incubation with guaiacol.

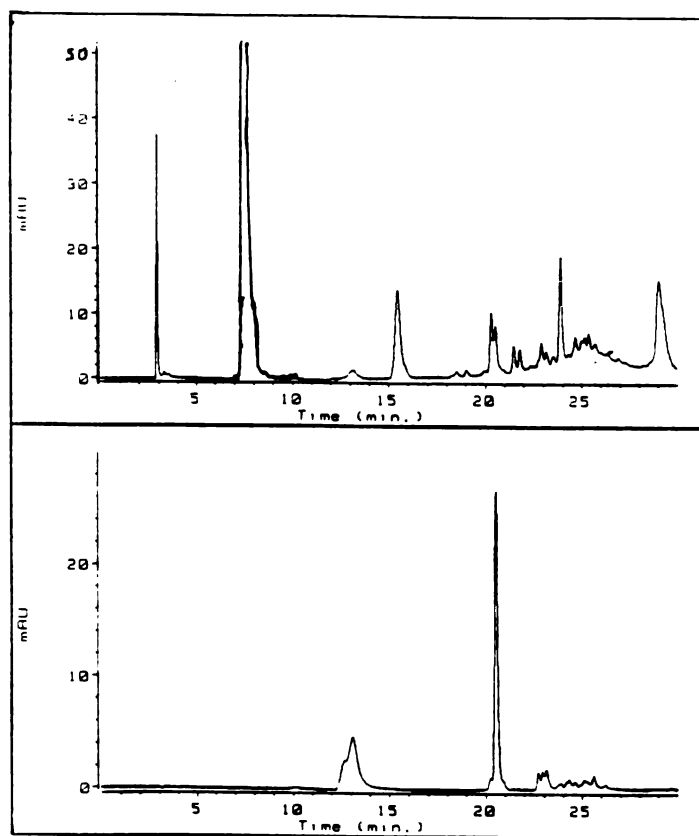


Figure 4.3.9. HPLC chromatogram of the products from a guaiacol incubation with 8F-HRP monitored at 276 nm (top) and 470 nm (bottom). The peak at 8 min is guaiacol.

## Inactivation by Ethylhydrazine

8HM-HRP is inactivated by ethylhydrazine (Figure 4.3.10). Ethyl radicals that can be trapped by POBN are produced during the inactivation (Figure 4.3.11). (Surprisingly, the ethyl radical could not be trapped by PBN. This result was reproducible and not due to bad PBN because azide radicals could be trapped by the same PBN solution that could not trap ethyl radicals. Perhaps the PBN ethyl adduct is oxidized by HRP, whereas the POBN adduct is not.) Interestingly, the inactivation of 8HM-HRP by ethylhydrazine is approximately half as fast as the inactivation of native HRP by ethylhydrazine (Figure 4.3.10). Thus, the hydroxymethyl group provides moderate protection from ethylhydrazine inactivation.

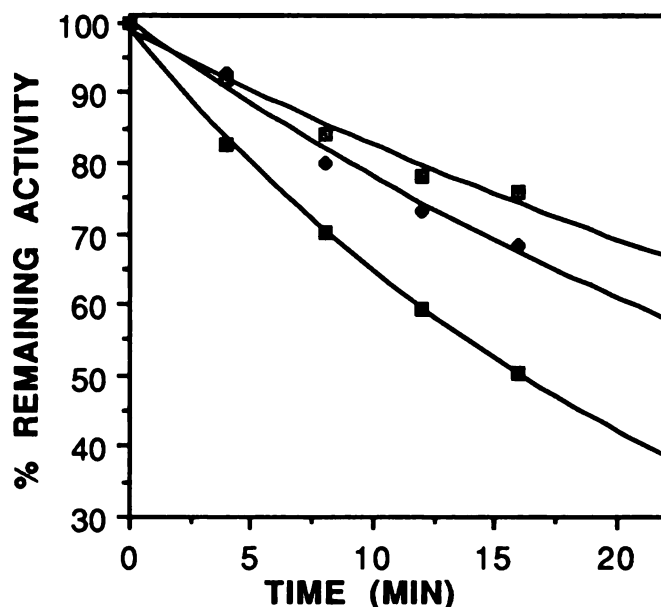


Figure 4.3.10. Inactivation of (A) HRP, (B) 8HM-HRP, and (C) 8F-HRP by ethylhydrazine. The half lives for inactivation were 15, 28, and 89 minutes for HRP, 8HM-HRP and 8F-HRP, respectively.

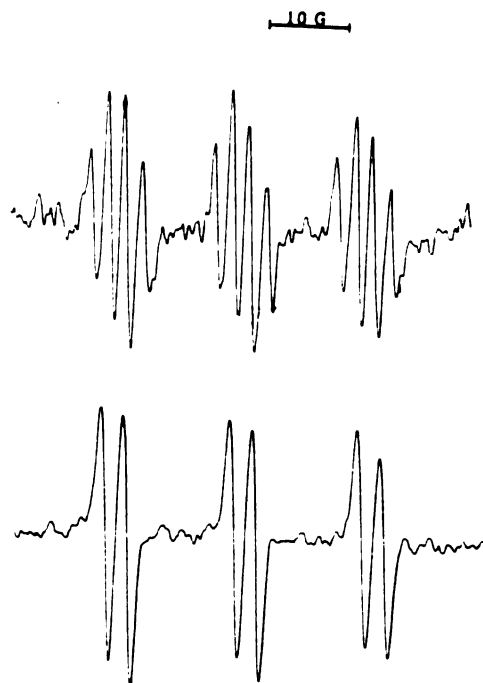


Figure 4.3.11. Generation of (A) azide radicals and (B) ethyl radicals by 8HM-HRP. The azide radicals were trapped with PBN, the ethyl radicals were trapped with POBN.

8-Formyl-HRP is inactivated very slowly by ethylhydrazine (Figure 4.3.10). This result is not surprising considering that ethylhydrazine is a suicide substrate and that 8F-HRP oxidizes substrates at a relatively slow rate.

#### **Inactivation by Sodium Azide**

8HM-HRP oxidizes azide to the azidyl radical (Figure 4.3.9). The rate of inactivation of 8HM-HRP by sodium azide is too fast to measure, but appears to be significantly faster than the rate of HRP inactivation. The partition ratio (rate of inactivation divided by the rate of product formation) for 8HM-HRP inactivation by azide is 16, compared to 58



for native HRP (Figure 4.3.11). Thus, the 8-hydroxymethyl group at the heme edge makes azide inactivation faster and more efficient.

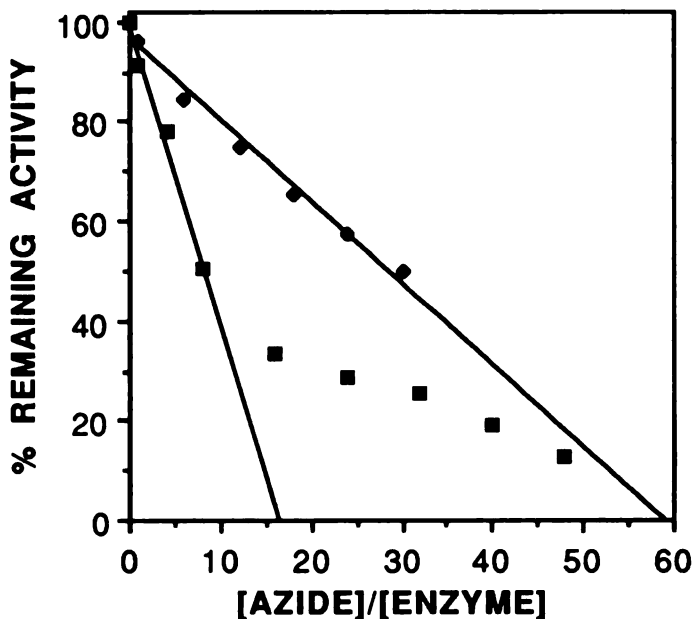


Figure 4.3.12. Inactivation of HRP and 8HM-HRP by sodium azide. The leveling of the inactivation at approximately 20% is a phenomenon previously observed (Ortiz de Montellano et al., 1988)

Heme modification occurs during azide inactivation (Figure 4.3.13). The Soret of the modified heme is at 403 nm, suggesting *meso* modification. Thus, the azidyl radical likely adds to the  $\delta$ -*meso* position of the heme yielding 8-hydroxymethyl-*meso*-azidylheme. Consistent with this prediction is the HPLC - electrospray MS which shows the expected molecular ion at  $m/z = 673$  (Figure 4.3.14). NMR could not be carried out due to lack of sample.

8F-HRP is also inactivated by azide, but at a very slow rate. The partition ratio could not be determined due to this slow rate of inactivation.

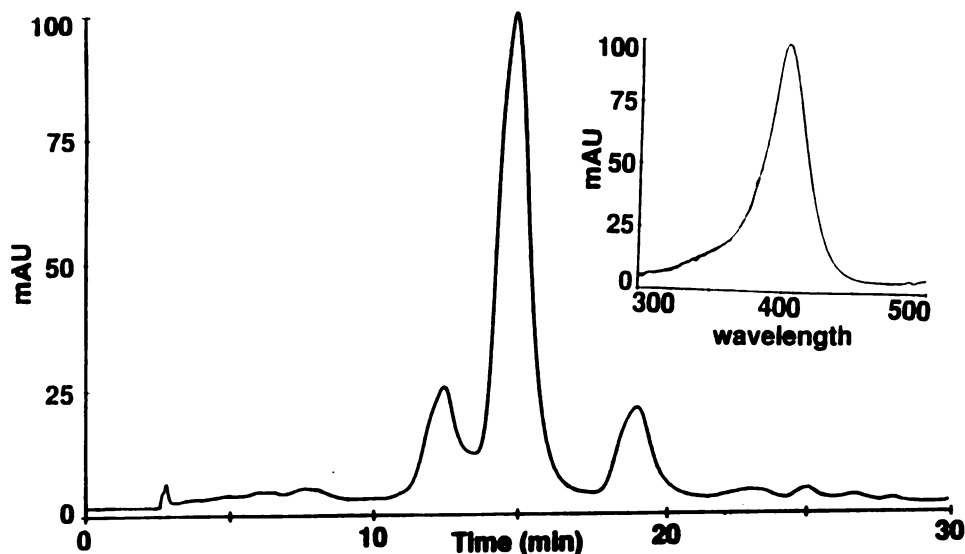


Figure 4.3.13 HPLC chromatogram of hemes produced in the reaction of 8HM-HRP with sodium azide. The peak at 12 minutes coelutes with 8-hydroxymethylheme, the peak at 18 coelutes with heme. The peak at 15 minutes is a new peak not present in a control incubation containing only 8HM-HRP and hydrogen peroxide. This peak is likely the double adduct 8-hydroxymethyl- $\delta$ -*meso*-azidoheme. The inset is the electronic absorption spectrum of the peak at 18 minutes. The Soret band is at 406 nm.

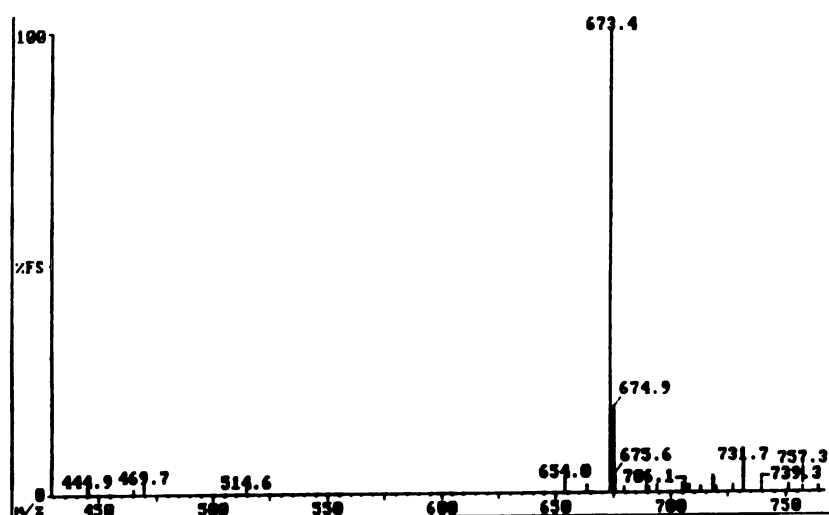


Figure 4.3.14. Mass spectrum of the heme product at 15 minutes in Figure 4.3.13. A molecular ion of  $m/z = 673$  is consistent with a double adduct.

## **Other Reactions**

Native HRP, 8HM-HRP, and 8F-HRP do not form iron-phenyl complexes from phenyldiazene, and do not oxidize styrene to styrene oxide. Also, none of the enzymes were able to oxidize chloride or bromide ions at a significant rate.

## **4.4 DISCUSSION**

HRP containing heme and HRP reconstituted with 8-hydroxymethylheme behave very similarly. Their native, Compound I, and Compound II species have virtually identical electronic absorption spectra and both enzymes react with peroxide at similar rates. A minor difference between the two enzymes is that in the absence of exogenous substrate, Compound I is reduced to Compound II twice as rapidly in 8HM-HRP than in HRP (Figure 4.3.5). Therefore, the hydroxyl group at the heme 8-position slightly destabilizes the Compound I species of HRP. This effect may be due to a steric perturbation or to the electron-withdrawing character of the hydroxyl group.

HRP and 8HM-HRP also have similar iodide, thioanisole, and guaiacol activities. While not surprising, the latter two results are interesting because guaiacol and iodide are probably oxidized near the heme 8-methyl group (Harris et al., 1993). Importantly, the heme modification does not impart to the enzyme the ability to oxidize

halides at an enhanced rate. Thus, it appears likely that the presence of a heteroatom at the heme periphery of lactoperoxidase does not, by itself, increase the enzyme's ability to oxidize halides and pseudohalides.

8HM-HRP and HRP also appear to react similarly with azide and ethylhydrazine (Figures 4.3.10-4.3.12) (Ator et al., 1987; Ortiz de Montellano et al., 1988). Both enzymes oxidize these molecules to reactive radicals that mediate enzyme inactivation. In the case of HRP, the azidyl radical adds to the heme edge, producing  $\delta$ -meso-azidoheme (Ortiz de Montellano et al., 1988). In the case of 8HM-HRP, the azidyl radical adds to the heme edge, producing  $\delta$ -meso-azido-8-hydroxymethylheme (Figures 4.3.13-4.3.14). Interestingly, 8HM-HRP is inactivated by azide at a greater rate and more efficiently than is HRP, yet is inactivated by ethylhydrazine at a slower rate than is HRP. Thus, the substituent on the 8-methyl group does have a subtle effect on the inactivation of the enzyme. Presumably, this is a steric rather than an electronic effect.

In contrast to 8HM-HRP, 8F-HRP is markedly different from HRP. The electron-withdrawing formyl group causes a significant red-shift of the native and Compound II Soret bands, and the Compound I species is significantly less stable than that of 8HM-HRP or native HRP (Figure 4.3.6). This low stability of 8F-HRP Compound I is consistent with the report that the Compound I species of MPO is very unstable and short lived (Harrison et al., 1980; Hurst, 1991).

The ability of 8F-HRP to oxidize guaiacol, thioanisole and iodide is also greatly reduced. The reduction in guaiacol activity is due primarily to a decrease in  $k_{cat}$  (Figure 4.3.7). There are at least three possible explanations for this reduction in  $k_{cat}$ . First, a fraction of the enzyme may have normal guaiacol activity, and the remaining enzyme may have no guaiacol activity. Second, the formyl group may create a steric barrier that disrupts (yet does not prevent) guaiacol binding to the enzyme and prevents the orbital overlap needed for full activity. Third, the electron-withdrawing formyl group may change the electronic characteristics of the enzyme in a manner that lowers enzymatic activity. The first possibility can be eliminated because the half-life of inactivation of 8F-HRP by azide or ethylhydrazine is greatly reduced compared to the half-life of HRP or 8HM-HRP inactivation (Figure 4.3.11). If a small amount of enzyme had normal activity, the half-life of inactivation by a suicide substrate should not have been decreased.

There is precedent for the second possibility. Previous studies have shown that guaiacol binds to, but is not oxidized by  $\delta$ -*meso*-ethylheme reconstituted HRP (Ator et al., 1987). The inactivity of  $\delta$ -*meso*-ethylheme reconstituted HRP is due to a steric effect because  $\delta$ -*meso*-methyl reconstituted HRP is active (Ator et al., 1987). However, the fact that HRP reconstituted with 8-hydroxymethylheme has normal guaiacol activity, makes it doubtful that the effect of the formyl group is due to steric interference because a formyl and a hydroxymethyl group are similar in size. It is possible that the formyl group is hydrated. A hydrated formyl group, which is relatively large,

may cause a steric effect that a hydroxyl group does not cause. However, the fact that the spectrum of 8F-HRP is significantly red-shifted suggests that the formylheme is not hydrated to a high degree. Therefore, the third possibility seems the most likely. The electron-withdrawing formyl group alters the electronic characteristics of the enzyme in a manner that not only changes the spectral characteristics but also decreases the ability of the enzyme to abstract electrons (a kinetic effect). Consistent with this possibility is the report that HRP reconstituted with a heme containing a formyl group at either the 2 or 4 positions has approximately 75% the activity of native HRP, whereas other, similarly sized groups at the 2 or 4 positions do not lower HRP activity (DiNello and Dolphin, 1981). Thus, the formyl group appears to have an electronic effect that lowers HRP activity by approximately one third. The additional inhibition observed when the formyl group is linked to the 8 position may be a steric effect.

The formyl group should increase the reduction potential of the heme and thus make the Compound I and II species of 8F-HRP more powerful oxidizing agents. It is therefore reasonable to hypothesize that it is this heme modification that endows MPO with the ability to oxidize chloride. However, the results from this study show that HRP reconstituted with a formylheme is no better able to oxidize chloride than is unmodified HRP. Thus, this heme modification alone is not likely to be responsible for the unique ability of MPO to oxidize chloride. It is possible that a chlorin is actually the prosthetic group of MPO. It has been suggested that a chlorin group could also affect the electronic properties of a peroxidase in a manner that would

increase the enzyme's ability to oxidize chloride (Hurst, 1991). A characterization of chlorin-reconstituted HRP would be quite interesting.

Because the formyl group should increase the oxidation potential of the heme, it is also conceivable that reconstitution with the formylheme would endow HRP with P-450-like activity. However, 8F-HRP could not oxidize styrene to styrene oxide and could not form an iron-phenyl complex. These findings support the hypothesis that the location of substrate binding relative to the heme group is the major determinant as to whether a hemoprotein behaves as a peroxidase or a P-450.

It is not clear why MPO and lactoperoxidase have evolved to have modified heme prosthetic groups. The benefits of the heme modifications must outweigh the extra energy required for their synthesis. In the future, it will be interesting to see the effect of reconstituting heme and modified hemes into myeloperoxidase and lactoperoxidase. The fact that myeloperoxidase was recently expressed in a baculovirus system (Taylor et al., 1992) makes some of these experiments imminent.

## **5.0 Enzyme Engineering Through the Reconstitution of HRP with Chemically Modified Hemes**

### **5.1 Introduction**

Enzyme engineering, the generation of novel enzyme catalysts, is a field that has grown immensely over the past 10 years. Novel enzymes can provide insights into the strategies that nature employs to catalyze chemical reactions, and can also provide a (potentially profitable) way of creating catalysts of synthetically useful reactions. Novel enzymes can be created in many ways. For example, they may be formed through the generation of catalytic antibodies that bind transition state or bisubstrate analogs (Lerner et al., 1991; Martin et al., 1991). This interesting technique is limited by the availability of the appropriate transition state analog and it has therefore been primarily used to create proteins that catalyze simple hydrolytic reactions. Novel enzymes can also be created through site directed mutagenesis (Gillett et al., 1992; Nickell et al., 1992). While tremendously useful, this technique is limited to proteins that have been expressed. Also, the nature of the alterations are usually limited to the 20 naturally occurring amino acids. [Recent methodologies have allowed incorporation of unnatural amino acids (Ellman et al., 1992), but these methods are still too difficult for general use.] Novel enzymes can also be generated through chemical modification of a naturally occurring enzyme (Butenas et al., 1992; Kaiser, 1988; Neet and Koshland, 1966). This technique is useful because the nature of the change is not confined to the side chains of the 20 naturally occurring amino acids. However, it is limited to enzymes that have appropriate



amino acids within their active sites. Also, it is often difficult to perform chemical modifications without damaging the enzyme.

This chapter describes a novel variation of the final technique: the reconstitution of chemically modified prosthetic groups into apoenzyme. More specifically, HRP was reconstituted with modified heme groups in an attempt to alter its catalytic activity in a predictable fashion. Although there have been previous studies in which HRP has been reconstituted with modified hemes (Chapter 4 section 1), the purpose of those studies was primarily to determine which heme substituents were required for normal peroxidase activity. In contrast, the purpose of these studies is to create novel enzymes that utilize hydrogen peroxide to catalyze oxidations that unmodified HRP cannot normally catalyze.

Horseradish peroxidase is a hemoprotein that normally mediates one electron oxidations of a variety of organic molecules (Chapter 1, section 3). Previous studies have shown that electron transfer from substrate to HRP occurs near the  $\delta$ -*meso*-carbon and the 8-methyl group of the heme edge, and that the rest of the heme is sheltered by protein (Chapter 1 section 13; Figure 5.1.1).

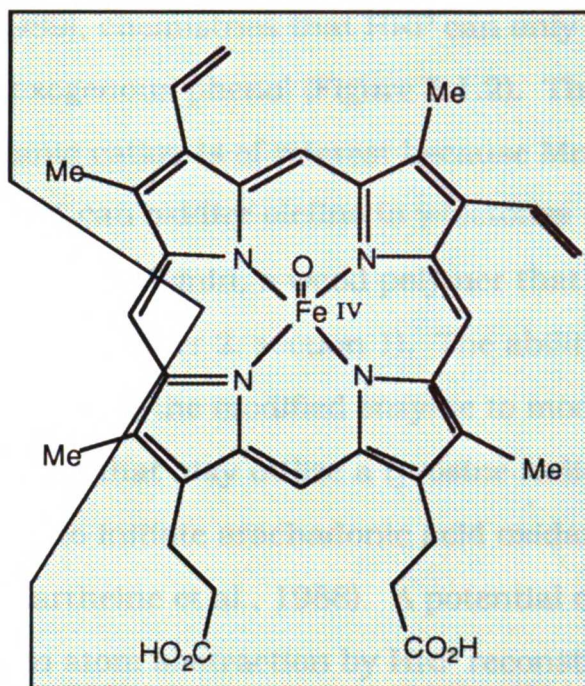


Figure 5.1.1. A model of the HRP active site.

Presumably there is a large substrate binding pocket near the heme edge since HRP is a promiscuous enzyme that can oxidize a variety of substrates of different shapes and sizes. Thus, there should be little difficulty in reconstituting a heme that is chemically modified at this edge position into apoenzyme, and the heme modification should come in contact with the substrate. Therefore, a redox active heme modification has the potential to dramatically influence the catalytic activity of the enzyme.

For example, it may be possible to link a phenol group to the heme edge. HRP can oxidize phenol to the phenolic radical (Chapter, section 3). The phenolic radical can catalyze manganese oxidation (Kenten and Mann, 1950; Kenten and Mann, 1952) and hydrogen atom abstraction

(Lehmann et al., 1989), chemistries that HRP can only efficiently catalyze in the presence of exogenous phenol (Figure 5.1.2). The ability to generate the manganic cation is of interest because Mn(III) is a useful synthetic reagent that can oxidize olefins to  $\gamma$ -lactones (Heiba et al., 1974). It can also degrade lignin, a wood polymer that is extremely degradation resistant (Chapter 2, section 1). The ability to abstract hydrogen atoms may allow the modified enzyme to model prostaglandin H synthase, an enzyme that may utilize a tyrosine radical, generated within its active site, to initiate arachadonic acid oxidation via hydrogen atom abstraction (Kartheine et al., 1988). A potential cycle for the catalysis of hydrogen atom abstraction by HRP reconstituted with a phenol-linked heme is shown in Figure 5.1.3.

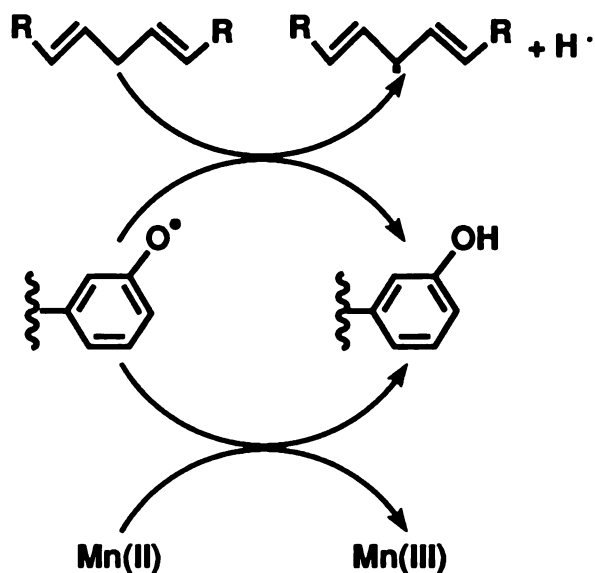


Figure 5.1.2 Hydrogen atom abstraction (top) and manganese oxidation (bottom) mediated by the phenolic radical.

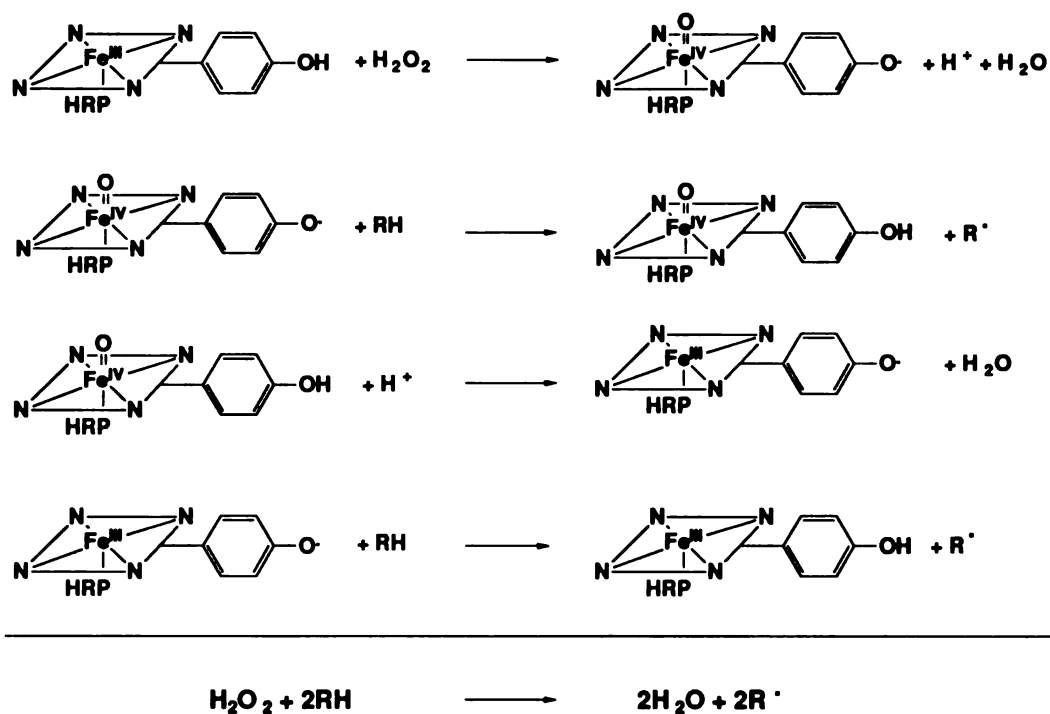


Figure 5.1.3. A potential cycle for the catalysis of hydrogen atom abstraction by HRP reconstituted with a phenol linked heme. The modified enzyme should also have the potential to catalyze manganese oxidation.

Another group that could potentially be linked to the heme edge is 2,2,6,6-tetramethylpiperidine-1-oxyl (TEMPO). The chemistry of TEMPO is shown in Figure 5.1.4. Previous studies have shown that TEMPO can be chemically oxidized to a nitrosonium ion by a variety of oxidants (Semmelhack et al., 1983; Semmelhack et al., 1984). The nitrosonium ion can then be reduced to the hydroxylamine via the oxidation of primary alcohols to aldehydes (Semmelhack et al., 1983). Thus, the TEMPO system provides a method for oxidizing alcohols to aldehydes, a reaction that HRP does not normally catalyze. It is not known whether HRP is able to function as the TEMPO oxidant in these systems, but the oxidation potential of HRP Compounds I and II is sufficiently high (1 V) to oxidize the hydroxyl amine (0.66 V) and the nitroxyl radical (0.33 V) to

the nitrosonium ion (Endo et al., 1984; Semmelhack et al., 1983). Furthermore, previous studies have shown that hemoglobin can promote hydrogen peroxide dependent oxidation of TEMPO (Yamaguchi et al., 1984). If HRP proves to be a feasible oxidant of TEMPO in solution, then HRP reconstituted with a heme to which a TEMPO molecule is linked may be able to generate a nitrosonium ion within its active site. The net effect would be the creation of a novel enzyme that harnesses the oxidative power of hydrogen peroxide to oxidize primary alcohols to aldehydes (Figure 5.1.5).

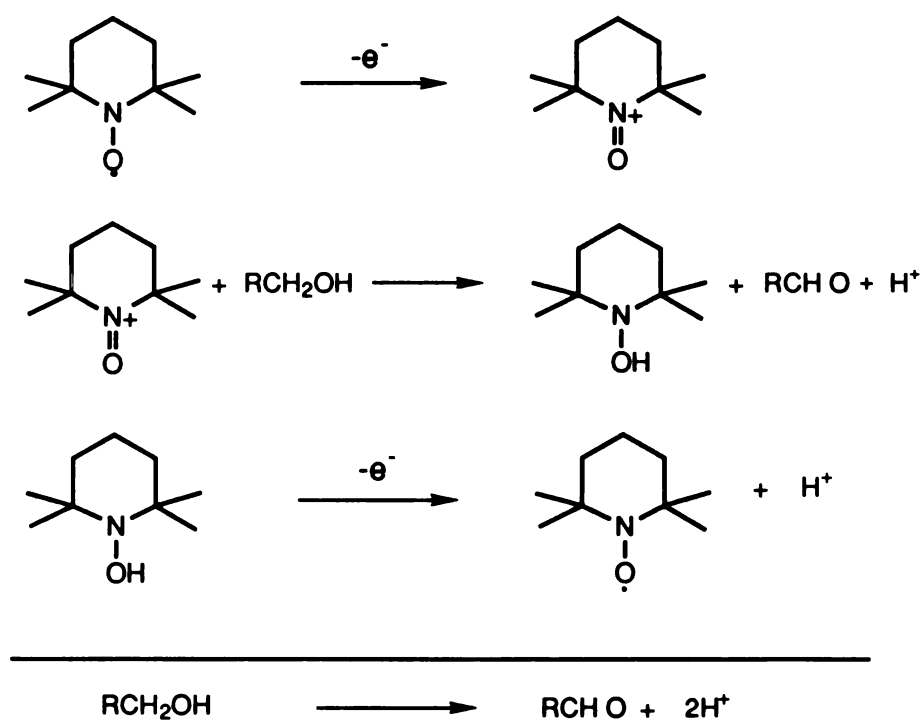


Figure 5.1.4. TEMPO chemistry.

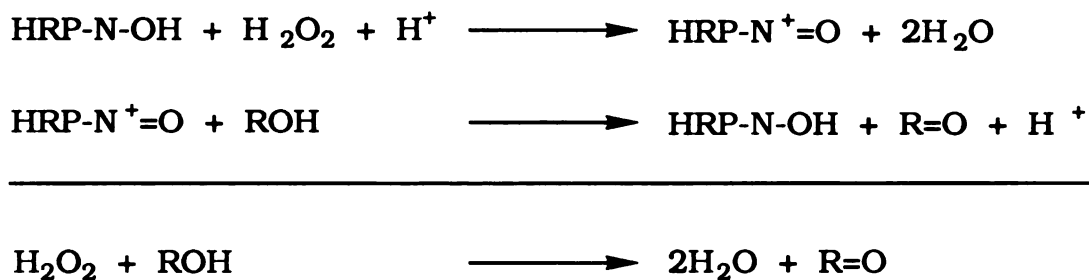


Figure 5.1.5. The potential catalytic cycle of HRP reconstituted with a TEMPO linked heme.

## 5.2 Experimental

### 5.2.1 Materials

Benzyl alcohol, benzaldehyde, phenethyl alcohol, TEMPO, 3-carboxy-PROXYL, tyramine, 2-aminophenol, 4-methylmorpholine N-oxide, tetrapropylammonium perruthenate, sodium cyanoborohydride, copper(II) chloride, diisopropylethylamine, trimethyloxonium tetrafluoroborate, hydrogen peroxide, and cumene hydroperoxide were purchased from Aldrich. Horseradish peroxidase (type VI), and 4-hydroxy-TEMPO, were purchased from Sigma. Ethyl hydroperoxide was from Polysciences Inc., and manganese sulfate was purchased from Mallinckrodt.

### 5.2.2 Analytical Methods

HPLC was performed on a Hewlet Packard model 1040A system equipped with a diode array detector and a Varian 9010 solvent pump. Kinetic assays were performed on a Hewlet Packard model 8450A diode

array spectrophotometer. Absorption spectra were recorded on an Aminco DW-2000 spectrophotometer. EPR spectra were recorded on a Varian E-104 instrument interfaced to an IBM XT computer. NMR spectra were obtained on a General Electric GN-500 MHz spectrometer. Chemical shifts are reported in parts per million relative to tetramethylsilane.

### **5.2.3 HRP - TEMPO Solution Studies**

#### **Benzaldehyde Production**

In a typical incubation, HRP (25  $\mu$ M), 4-hydroxy TEMPO (250  $\mu$ M), and benzyl alcohol (10 mM, added neat) in a volume of 5 mL were stirred at room temperature for 10 minutes to assure maximal dissolution of the benzyl alcohol. Hydrogen peroxide (50  $\mu$ L of a 0.5 M solution) was then added over two hours to give a final peroxide concentration of 5 mM. The solution was then extracted with 10 mL of diethyl ether that contained 5  $\mu$ L of phenethyl alcohol (a standard), and the ether was removed under a stream of nitrogen. The product was analyzed by normal phase HPLC on a Partisil 5 $\mu$  silica column eluted isocratically with 85% hexane, 15 % dry THF, at a flow rate of 1.5 mL/min. The absorbance was monitored at 235 nm with a bandwidth of 40 nm. The large bandwidth allows detection of both the benzaldehyde and the alcohols. Incubations were carried out in pH 6, 7, and 8 phosphate buffer, pH 4 and 5 acetate buffer and pH 9 borate buffer. Control incubations that lacked either TEMPO or hydrogen peroxide were also performed.

In order to determine the effect of slow addition of hydrogen peroxide, incubations in which the hydrogen peroxide was delivered slowly over 12 hours by a Sage Instruments syringe pump model 355 were also performed.

### **Time-Dependence of Benzaldehyde Production**

In 30 mL of pH 4.5 acetate buffer, HRP (20  $\mu\text{M}$ ), 4-hydroxy-TEMPO (80  $\mu\text{M}$ ), and ethyl hydroperoxide (200  $\mu\text{M}$ ) were mixed at room temperature. All of the ethyl hydroperoxide was added via a single aliquot. At various times, a 5 mL portion was removed from the incubation and analyzed for benzaldehyde production. A control incubation that lacked TEMPO was also performed.

### **Electronic Absorption Spectra of HRP in the Presence of TEMPO**

A 5  $\mu\text{L}$  aliquot of hydrogen peroxide (50  $\mu\text{M}$  final concentration) was added to a quartz cuvette containing a solution of HRP (10  $\mu\text{M}$ ), and 4-hydroxy TEMPO (200  $\mu\text{M}$ ) in 1 mL of pH 7 phosphate buffer. The electronic absorption spectrum was recorded and additional aliquots of hydrogen peroxide were added.

### **Decay of the Nitroxyl Radical Signal**

To a solution containing 4-hydroxy TEMPO (1 mM), and HRP (100  $\mu\text{M}$ ) in 1 mL of pH 4.5 acetate buffer was added 12  $\mu\text{L}$  of a 0.05 M



solution of hydrogen peroxide (0.63 mM final peroxide concentration). A 50  $\mu$ L aliquot was then transferred to a capillary tube and placed into a quartz tube aligned in the sample cavity of the EPR. The sample was scanned, and additional aliquots of peroxide were added. Signal amplitude was measured as the peak to trough distance of the radical signal. The EPR instrument settings were: scan range, 10 x 10 Gauss; time constant, 0.25 sec; field set 3400 Gauss; scan time, 4 minutes; modulation amplitude, 1 x 1 Gauss; gain,  $5 \times 10^3$ ; power, 10 db = 20 mW; microwave frequency, 9.51 GHz; second harmonic, 100 KHz.

### **Oxygen Evolution**

A Yellow Springs oxygen electrode hooked to a Simpson power source/ amp meter was used to measure oxygen evolution. In a Gilson sample chamber at room temperature, hydrogen peroxide (25  $\mu$ L of a 250  $\mu$ M solution) was added to a rapidly stirring of HRP (100  $\mu$ M), and TEMPO (25 mM) in 1 mL of chelexed sodium phosphate buffer, pH 7.0. A control incubation in which the HRP and TEMPO were replaced with catalase (450  $\mu$ g/mL) was also performed.

### **Cupric Mediated TEMPO Oxidation**

A method for utilizing TEMPO to oxidize benzyl alcohol to benzaldehyde in DMF (Simmelhack et al., 1984) was attempted in aqueous medium. Benzyl alcohol (200 mM), 4-hydroxy TEMPO (20 mM) and cupric chloride (20 mM) were dissolved in 4 mL of either DMF or chelexed 50 mM sodium phosphate buffer, pH 7. The incubations were

bubbled with oxygen for 4 hours and then mixed with 5 mL of 10% HCl. The products were extracted into 10 mL of diethyl ether and analyzed by HPLC.

### **Formation of the Hydroxylamine of TEMPO**

Sodium hydrosulfite was added to a 1 mL solution of 0.1 M 4-hydroxy-TEMPO in pH 7 phosphate buffer. The elimination of the nitroxyl radical EPR signal was taken as an indication of complete nitroxide reduction. Incubations containing the hydroxylamine of TEMPO were then performed as described above.

### **5.2.4 Modified Heme Studies**

#### **Synthesis of O-(3-oxomethyl-PROXYL)-8-hydroxymethylheme (1)**

In an ice bath, 225  $\mu\text{L}$  (450  $\mu\text{mol}$ ) of a solution of oxaylyl chloride (2 M) was added to 85 mg (470  $\mu\text{mol}$ ) of 3-carboxy-PROXYL in 3 mL of dichloromethane. One drop of DMF was added and the solution was removed from the ice bath and stirred at room temperature for 15 minutes. A 300  $\mu\text{L}$  (45  $\mu\text{mol}$ ) aliquot of the resulting acid chloride solution was then added to 3 mg (4.5  $\mu\text{mol}$ ) of 8-hydroxymethylheme dissolved in 400  $\mu\text{L}$  of 50% (vol./vol.) pyridine in dichloromethane. The solution was stirred for 30 minutes at room temperature and a few drops of  $\text{H}_2\text{O}$  were then added to hydrolyze excess acid chloride. The solution was diluted with 5 mL of ethyl acetate and then washed once with 5 mL of brine. The organic layer was collected and the ethyl acetate was

removed *in vacuo*. The modified heme was purified on a semiprep HPLC column packed with Whatman Partisil ODS-3 and eluted with 70:30:10 ACN:H<sub>2</sub>O:CH<sub>3</sub>COOH, at a flow rate of 1 mL/min.

**Synthesis of N-(2-hydroxyphenylethyl)-8-aminomethylheme (2), N-(phenylethyl)-8-aminomethylheme (3), and N-(2-hydroxyphenyl)-8-aminomethylheme (4)**

8-Formylheme was synthesized from 8-hydroxymethylheme as already described (Chapter 4, section 2). Tyramine (30 mM) was dissolved in 100 mM chelexed sodium phosphate buffer and the pH was adjusted to 7.0 by addition of HCl. 8-Formylheme (0.5 mg, 0.8 μmol) was then dissolved in a few drops of pyridine and diluted with 10 mL of the tyramine solution. The mixture was bubbled with argon for 10 minutes and sodium cyanoborohydride (0.5 mg) was then added. The reaction stood at room temperature for 30 minutes and the heme **2** was purified by direct injection into a semi-prep HPLC system (column packed with Whatman Partisil ODS-3, eluted with 60:40:10 ACN:H<sub>2</sub>O:CH<sub>3</sub>COOH at a flow rate of 1 mL/min). An identical procedure was used to link 2-phenylethylamine (to produce heme **3**) and 2-aminophenol (to produce heme **4**) to 8-formylheme except that 10% acetonitrile was added to the former reaction in order to increase the solubility of 2-phenylethylamine.

**Heme Esterification and Demetallation**

Heme samples were esterified in preparation for NMR. In a 10 mL round bottom flask, the modified heme was dissolved in 4.5 mL of ethanol, 250 μL of H<sub>2</sub>O, and 125 μL of diisopropylethylamine. A few

crystals of trimethyloxonium tetrafluoroborate were then added over 15 minutes. The solution was then diluted with 20 mL of H<sub>2</sub>O and the esterified heme was extracted into dichloromethane. All of the color went into the organic phase indicating that the esterification was complete. The dichloromethane was washed with brine and evaporated to dryness.

The sample was then demetallated. Under argon the heme was dissolved in 300  $\mu$ L of pyridine. Acetic acid (10 mL) that had been bubbled with argon for 10 minutes was added, followed by 100  $\mu$ L of concentrated HCl that was saturated with iron(II) sulfate. The mixture was stirred for 5 minutes and then poured into a separatory funnel containing 50 mL of diethyl ether and 50 mL of a saturated solution of sodium acetate in H<sub>2</sub>O. The ether layer was washed with brine and the sample was evaporated to dryness.

### **Heme Reconstitution**

The modified hemes were reconstituted into HRP by a procedure that is similar to that which has already been described (Ortiz de Montellano et al., 1988), except that it was carried out at room temperature for 3 hours to insure maximal reconstitution.

### **Detection of Enzyme Intermediates**

Hydrogen peroxide was added to the modified enzyme (20  $\mu$ M) in pH 7.0 sodium phosphate buffer and the electronic absorption spectrum

was acquired. The concentration of peroxide was varied as described in the Results section.

### **Catalytic Activities**

The rates of guaiacol and thioanisole oxidation were measured as described in Chapter 3 section 2. Manganese oxidation was measured directly by monitoring the formation of the manganic cation at 240 nm in the presence of pyrophosphate (Glenn and Gold, 1985). The ability to oxidize linoleic acid was measured using an assay developed by Dr. Satish Rao. Incubations (1 mL) were prepared containing enzyme (60  $\mu\text{M}$ ), and linoleic acid (400  $\mu\text{M}$ , delivered from a stock solution in ethanol) in 0.2 M phosphate buffer (pH 7.4). The final concentration of ethanol was 2 %. The solutions were pre-incubated for 10 minutes, and the reaction initiated by the addition of cold  $\text{H}_2\text{O}_2$  (final concentration of 900  $\mu\text{M}$ ). The reaction was allowed to proceed for 30 min at 4 °C. The reaction mixture was then extracted with 2 x 4 mL of diethyl ether. The combined ethereal extracts were taken to dryness, and the residue was dissolved in 0.25 mL of ethanol. A 50  $\mu\text{l}$  aliquot was injected onto HPLC. Separations were performed using a 5  $\mu\text{m}$ , 250 x 4.6 mm Partisil ODS-3 column (Alltech), and eluted with acetonitrile : water : phosphoric acid (65 : 35 : 0.1) at a flow rate of 1 mL/min. The eluant was monitored at 217 nm and 234 nm using a diode array detector. Linoleic acid is detected at 217 nm but not at 234 nm, whereas the linoleic acid hydroperoxide is detected both at 217 nm and 234 nm (with a higher extinction coefficient at 234 nm). Under these conditions, linoleic acid hydroperoxide elutes at 8.7 minutes, and linoleic acid at 26 minutes.

## **Protein EPR**

In a quartz EPR tube, hydrogen peroxide (48  $\mu\text{M}$ ) was added to enzyme (20  $\mu\text{M}$ ) and the mixture was immediately frozen in a liquid nitrogen bath. The sample was then inserted into a liquid nitrogen containing Dewar flask that was aligned in the EPR cavity, and immediately scanned. EPR parameters were: field, 3269 Gauss; scan range, 5 x 100 Gauss; microwave frequency, 9.07 GHz; power, 2 mW; 2nd harmonic, 100 KHz; modulation amplitude, 0.8 x 10; scan time, 2 minutes; and time constant 0.5.

## **5.3 Results**

### **5.3.1. HRP-TEMPO Studies**

#### **Oxidation of TEMPO by HRP**

HRP is able to oxidize TEMPO. When  $\text{H}_2\text{O}_2$  was added to an incubation that contained TEMPO and HRP, the nitroxyl radical signal was immediately reduced (Figure 5.3.1). A 64 % decrease in the EPR signal was observed when 0.63 M hydrogen peroxide was added to 1 mM TEMPO. If additional peroxide was added, only a very small decrease in the nitroxyl radical signal was observed (Figure 5.3.2). The disappearance of the radical signal was long lived, and the addition of benzyl alcohol did not cause an increase in its regeneration rate.

However, heating the solution to 80°C for 10 minutes led to a partial restoration of the radical signal (Figure 5.3.2).

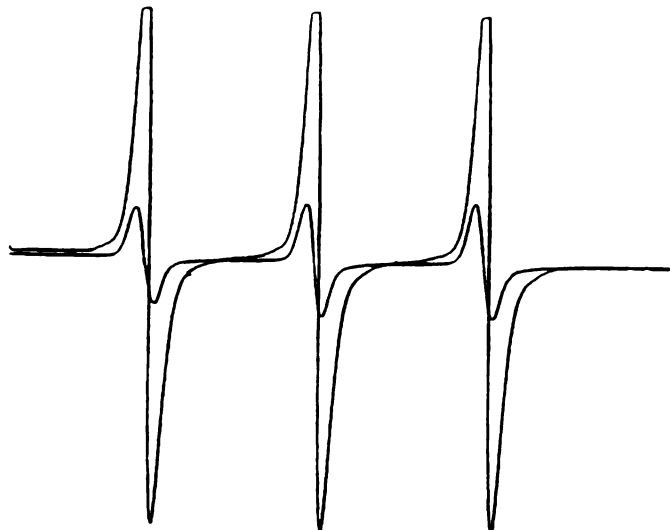


**Figure 5.3.1. EPR signal of TEMPO before (large signal) and after (small signal) the addition of hydrogen peroxide in the presence of HRP. Identical results were obtained if the TEMPO was replaced with 4-hydroxy-TEMPO, or 3-carboxy PROXYL. No reduction in the radical signal was observed in the absence of HRP.**

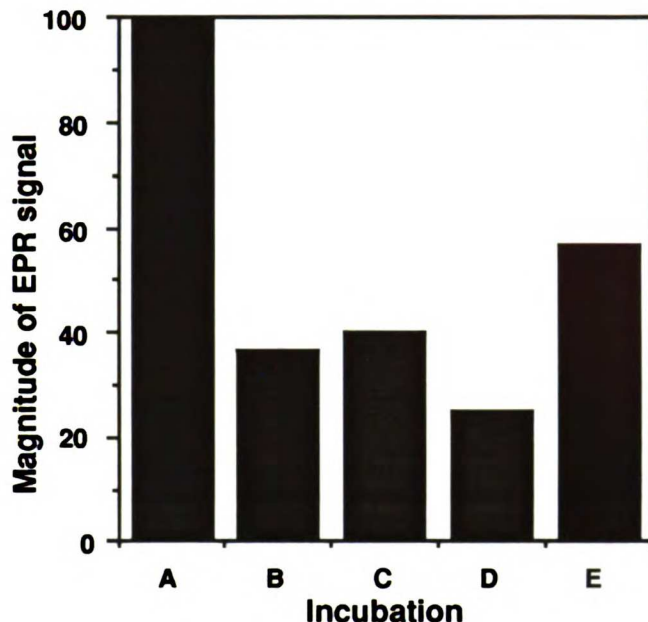


Figure 5.3.2. Magnitude of the EPR signal in an incubation that contained 1 mM TEMPO and 20  $\mu$ M HRP: A) Before the addition of hydrogen peroxide. B) After addition of an aliquot of hydrogen peroxide (0.63 mM final concentration). C) 10 Minutes after the addition of hydrogen peroxide. D) After the addition of a second aliquot of hydrogen peroxide. E) After heating the sample in described in B.

### **Benzaldehyde Formation**

A significant amount of benzaldehyde was produced in incubations that contained HRP, TEMPO, benzyl alcohol, and H<sub>2</sub>O<sub>2</sub> (Figure 5.3.3). Benzaldehyde production was dependent on the presence of peroxide, TEMPO, and enzyme. The benzaldehyde production was also dependent on the slow delivery of H<sub>2</sub>O<sub>2</sub> (Figure 5.3.3). When a syringe pump was used to deliver the peroxide over 12 hours, a relatively high amount of benzaldehyde production was observed, whereas if the peroxide was delivered in a single aliquot, no product was observed. Similar results



were obtained when TEMPO was replaced with 4-hydroxy-TEMPO or 3-carboxy-PROXYL.

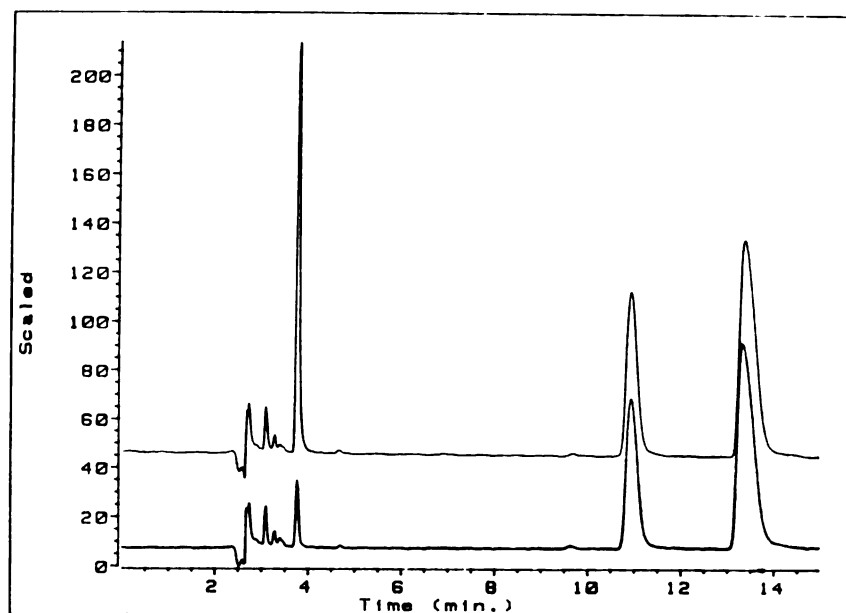


Figure 5.3.3. HPLC chromatogram of the products from an incubation that contained HRP, benzyl alcohol, TEMPO, and  $H_2O_2$ . Bottom: all of the  $H_2O_2$  added via a single aliquot. Top:  $H_2O_2$  added slowly over 12 hours. The peak at 13.5 minutes is the standard phenylethyl alcohol, the peak at 11 minutes is benzyl alcohol, and the peak at 4 minutes is benzaldehyde.

### Oxygen Evolution

It is possible that the lack of benzaldehyde production, when hydrogen peroxide was not added slowly, was due to catalytic activity of HRP in the presence of TEMPO. In the presence of TEMPO, HRP may be able to promote the dismutation of hydrogen peroxide via the mechanism shown in Figure 5.3.4.

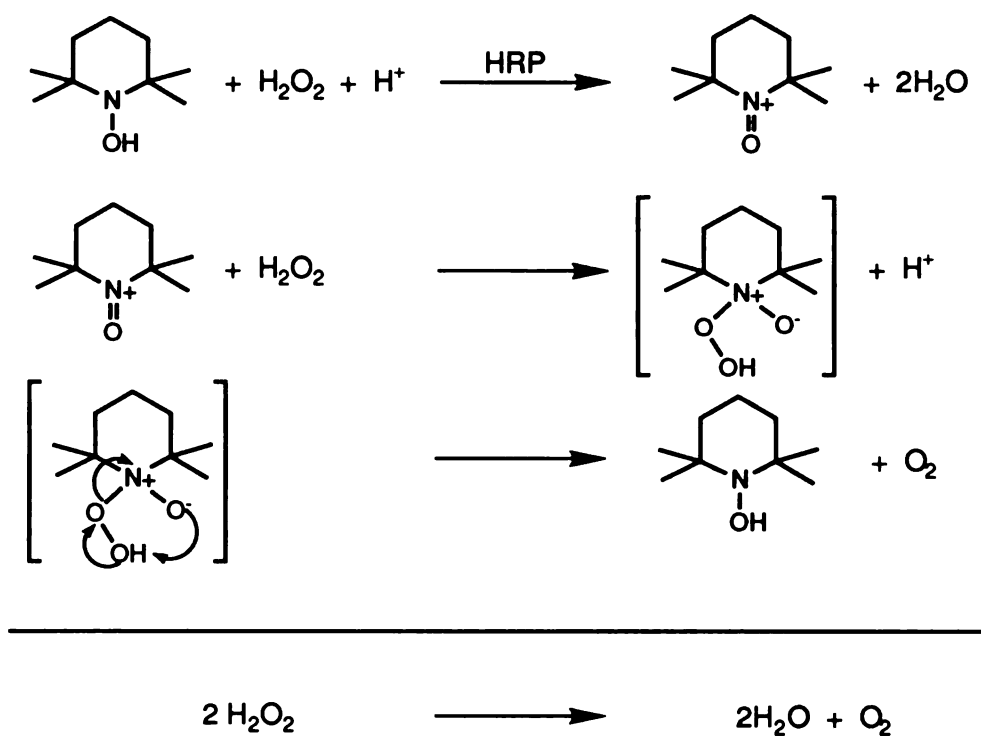


Figure 5.3.4. A possible mechanism for the catalytic activity of HRP in the presence of TEMPO.

Consistent with this hypothesis, oxygen evolution was observed when  $\text{H}_2\text{O}_2$  was added to a solution containing TEMPO and HRP (Table 5.3.1). Approximately half of the peroxide was destroyed via this catalytic activity. Surprisingly, HRP alone also had a large amount of catalytic activity (Table 5.3.1). It has previously been reported that pure HRP, in the absence of iodide (Dunford, 1991) or certain other electron donors (Barr and Aust, 1993) exhibits virtually no catalytic activity. However, contamination of the enzyme was probably not responsible for the observed catalytic activity in these studies because it was not eliminated by purification of the HRP on Sephadex G-25. There is a possibility that the phosphate used in the buffers contained a trace contaminant, yet this seems unlikely. A high amount of catalytic activity by HRP in the

presence of TEMPO has been previously observed (Mehlhorn and Swanson, 1992). Also, it has been reported that in the absence of TEMPO, HRP has a moderate amount of catalatic activity which is presumably due to oxygen release by HRP Compound III (Moore et al., 1992).

When hydrogen peroxide was replaced by ethyl hydroperoxide, oxygen evolution was eliminated (Table 5.3.1), and an increase in benzaldehyde production was observed (Table 5.3.2), both in the presence and absence of TEMPO. Slow, versus rapid, addition of ethyl hydroperoxide only slightly increased the amount of benzaldehyde produced. The catalatic activity of HRP thus appears to be eliminated when the hydrogen peroxide is replaced with ethyl hydroperoxide.

<u>System</u>	<u>Oxygen Evolution</u>
Catalase	100
HRP	51
HRP + TEMPO	54
TEMPO	0
HRP ± TEMPO + ethyl hydroperoxide	0

Table 5.3.1. Oxygen evolution in various incubations. In all incubations oxygen evolution was complete within 40 seconds.

<u>Method of addition</u>	<u>Benzaldehyde production</u>
hydrogen peroxide- single aliquot	0
ethyl hydroperoxide- single aliquot	95
hydrogen peroxide- slow addition	30
ethyl hydroperoxide- slow addition	100

Table 5.3.2. The effect of the substitution of ethyl hydroperoxide for hydrogen peroxide on benzaldehyde production.

### **HRP Intermediates**

When 50  $\mu\text{M}$   $\text{H}_2\text{O}_2$  was added to a solution containing 10  $\mu\text{M}$  HRP and 200  $\mu\text{M}$  4-hydroxy TEMPO, Compound II formed very fast and then decayed back to native enzyme in approximately 10 minutes. Compound I was not detected. Upon addition of peroxide to a control incubation that lacked TEMPO, Compound I formed and then decayed to Compound II in approximately one minute. In the absence of TEMPO, Compound II did not decay back to native enzyme in over 20 minutes. When an additional aliquot of hydrogen peroxide was added to the TEMPO containing incubations, Compound II again formed and decayed to native enzyme in approximately five minutes. Even when the total amount of peroxide added was in four-fold molar excess over TEMPO, the same behavior was observed. After a total of eight aliquots of hydrogen peroxide were added, the activity of the HRP was assayed by monitoring its ability to oxidize guaiacol. The HRP in the TEMPO incubation retained full activity.

## Dependencies of Benzaldehyde Production

The time-dependence of benzaldehyde production is shown in Figure 5.3.5. Benzaldehyde production is nearly completed in 90 minutes.

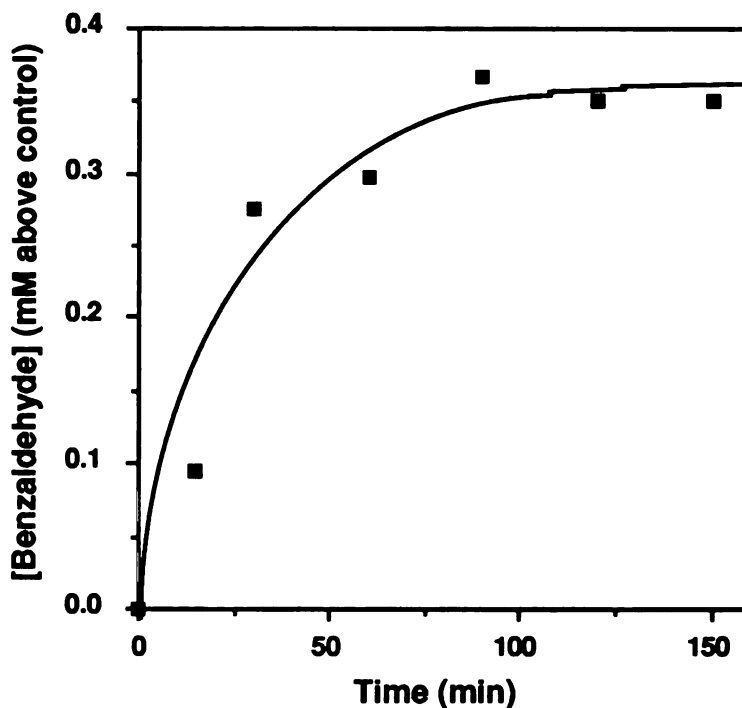


Figure 5.3.5. Time-dependence of benzaldehyde production. The control incubations produced benzaldehyde ranging from 20  $\mu\text{M}$  (time = 0 minutes) to 90  $\mu\text{M}$  (time = 150 minutes).

The pH-dependence of benzaldehyde production is shown in Figure 5.3.6. An increase in benzaldehyde production is observed at low pH.

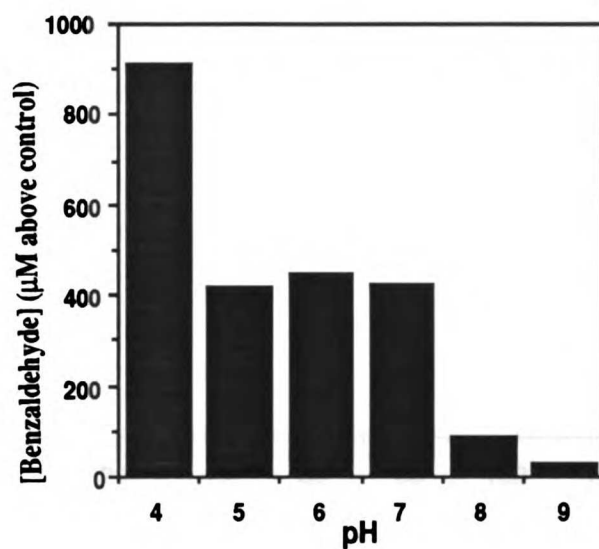


Figure 5.3.6. pH-dependence of benzaldehyde production. The concentration of benzaldehyde produced in the control incubations was approximately 84  $\mu\text{M}$ .

The dependence of benzaldehyde production on HRP concentration is shown in Figure 5.3.7. The fact that the graph is linear over a large range of HRP concentrations illustrates that the reaction is catalytic with respect to HRP.

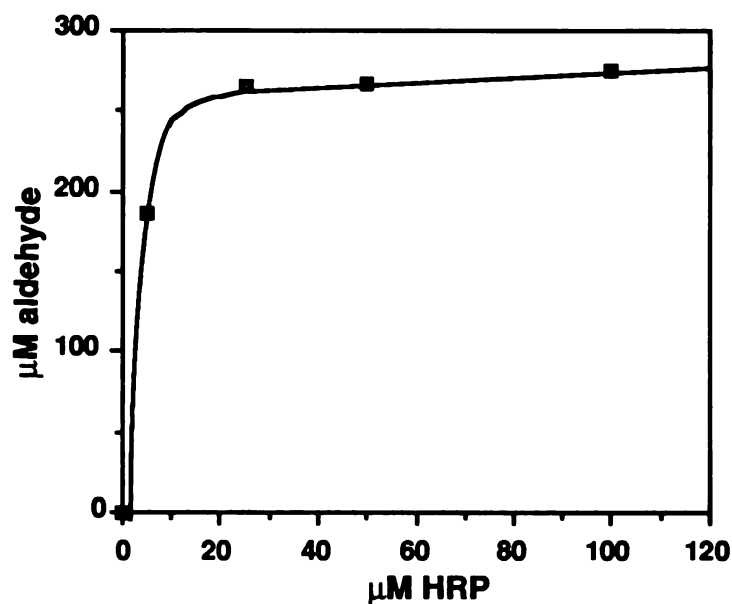


Figure 5.3.7. The dependence of benzaldehyde production on HRP concentration.

The dependence of benzaldehyde production on TEMPO concentration is shown in Figure 5.3.8. In short incubations (6 minutes) the production of benzaldehyde varies linearly with the TEMPO concentration (Figure 5.3.8A). This result is expected because the reaction was not allowed to run to completion. Figure 5.3.8B shows the result of a 2 hour incubation. Ideally, if TEMPO was a catalyst, the amount of product would be independent of the TEMPO concentration. Instead, the amount of benzaldehyde produced varies linearly with the TEMPO concentration. Also, the concentration of benzaldehyde produced is never significantly higher than the TEMPO concentration.

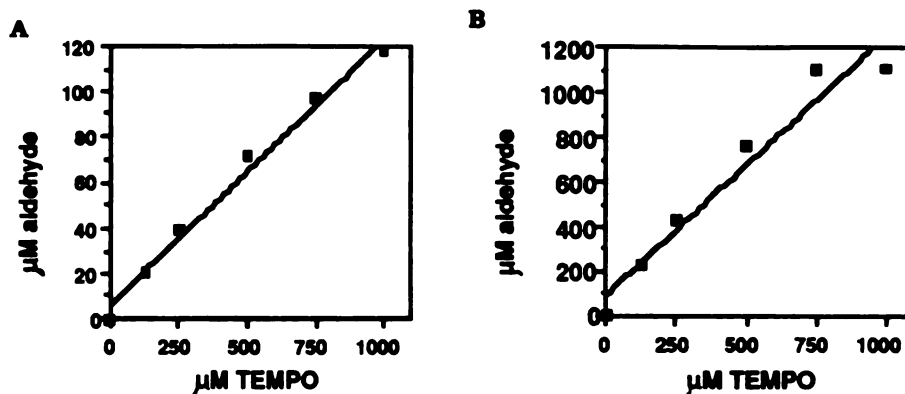


Figure 5.3.8. Dependence of benzaldehyde production on TEMPO concentration in a 6 minute (A) and 2 hour (B) incubation.

The dependence of benzaldehyde production on ethyl hydroperoxide concentration is shown in Figure 5.3.9. If the system was catalytic, there would be a linear dependence of aldehyde production on peroxide concentration. Instead, there was a linear dependence only when the peroxide concentration was lower than the TEMPO concentration.

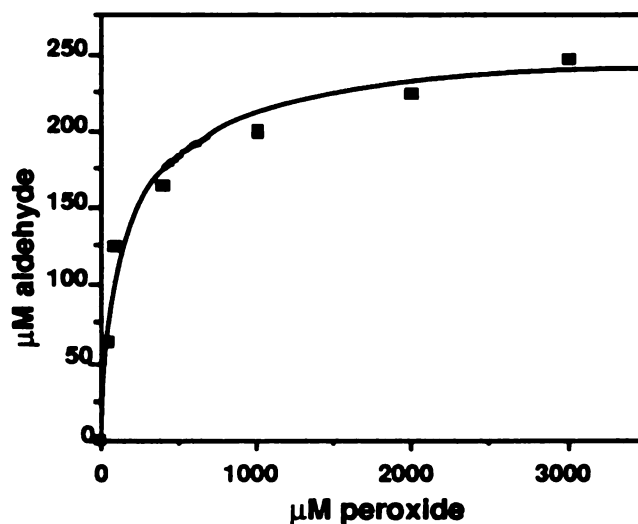


Figure 5.3.9. The dependence of benzaldehyde production on ethyl hydroperoxide concentration.



## Cupric Mediated Benzaldehyde Production

As previously reported (Semmelhack et al., 1984), cuprous ions, in the presence of oxygen, are able to promote TEMPO mediated oxidation of benzyl alcohol in DMF (Table 5.3.2). The cuprous ions are oxidized by oxygen to cupric ions, which in turn, oxidize TEMPO. When the reaction was carried out in pH 7.0 phosphate buffer, no benzaldehyde was produced (Table 5.3.2). However, when the reaction was carried out in H<sub>2</sub>O, the amount of benzaldehyde produced was equal to the amount produced in DMF. Thus, the TEMPO system appears to function in the aqueous phase. Phosphate likely inhibited the reaction by chelating the copper ions.

Reaction medium	Benzaldehyde Yield
DMF	100
pH 7.0 phosphate buffer	2
H <sub>2</sub> O	105

Table 5.3.3. Benzaldehyde production in various reaction media.

### 5.3.2 Synthesis of Modified Hemes

Attempts were made to synthesize the modified hemes shown in Figure 5.3.10.

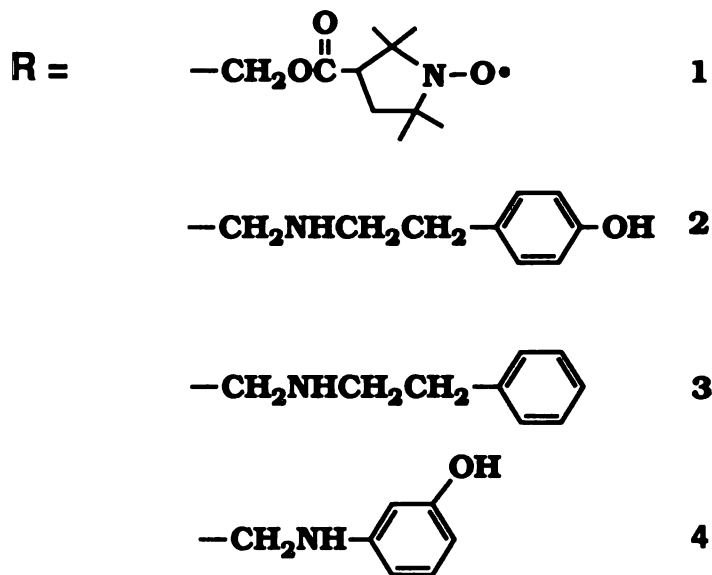
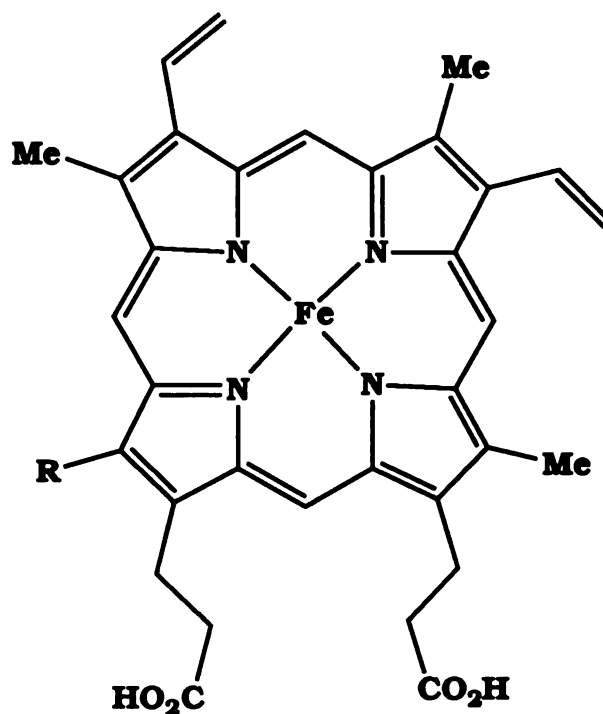


Figure 5.3.10. Modified hemes.

Concomitant with the HRP-TEMPO solution studies, an attempt was made to synthesize heme **1** through the reaction of an acid chloride with

the hydroxyl group of 8-hydroxymethylheme. As expected, the product had a Soret band at 397 nm, identical to that of 8-hydroxymethylheme. The heme also had an strong nitroxyl radical signal, confirming that a PROXYL group was linked to the heme (Figure 5.3.12). Further structural characterization of heme **1** was not pursued due to lack of sample and due to the apparent inefficiency of HRP-TEMPO system (see Discussion section).



Figure 5.3.12. EPR spectrum of heme **1**.

Heme **2** was synthesized via condensation of tyramine with 8-formylheme in the presence of sodium cyanoborohydride. The modified heme had an HPLC retention time that differed from that of 8-formylheme and 8-hydroxymethylheme (Figure 5.3.13). The product also had a Soret absorbance at 398 nm, 10 nm blue-shifted from the Soret absorbance of 8-formylheme (5.3.14). Mass spectroscopy revealed the expected molecular ion  $m/z = 752$  (Figure 5.3.15). The small amount of sample available prevented unambiguous structural determination by NMR. It should be noted that in the absence of amine, sodium

cyanoborohydride very slowly reduces 8-formylheme to 8-hydroxymethylheme.

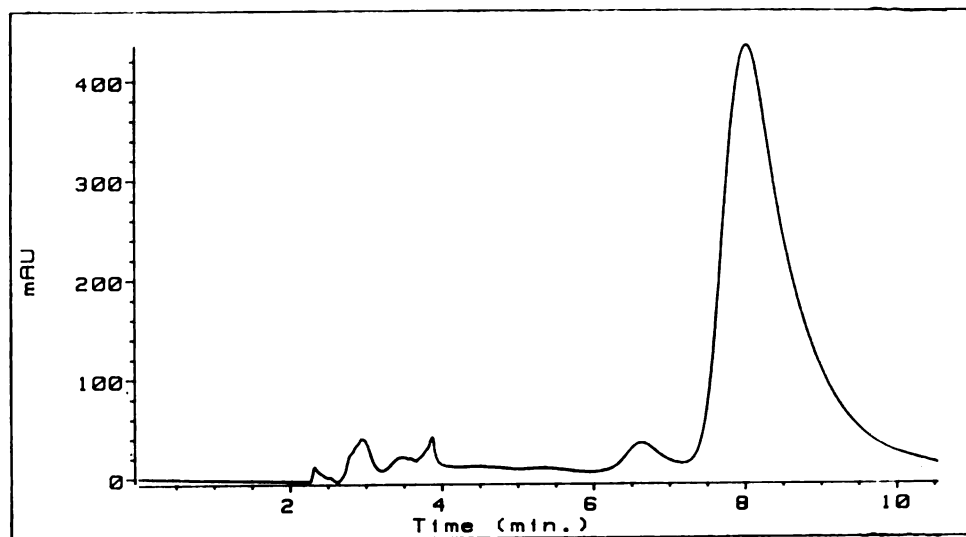


Figure 5.3.13. HPLC chromatogram of heme **2** produced synthetically from 8-formylheme. The peak at 6.5 minutes is 8-formylheme, the peak at 8 minutes is **2**.

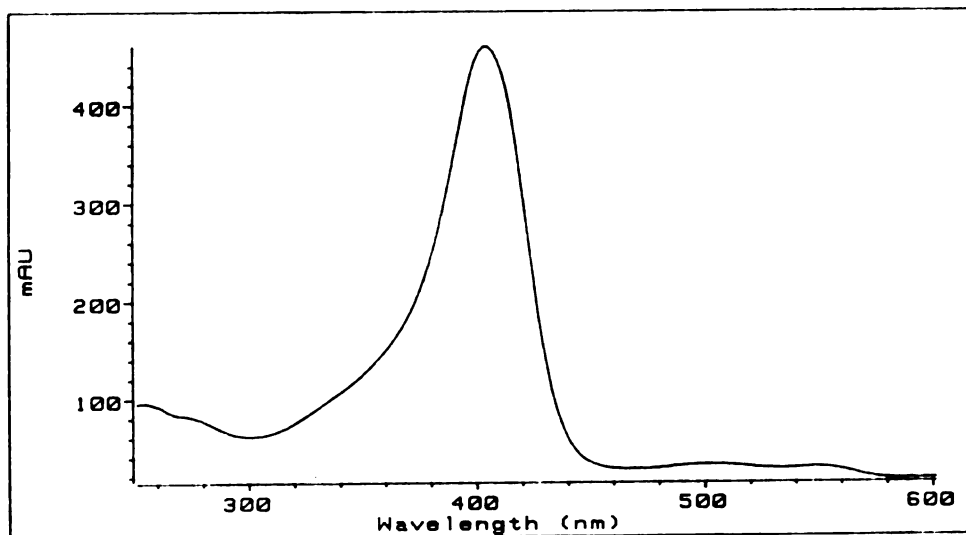


Figure 5.3.14. Electronic absorption spectrum of heme **2**.

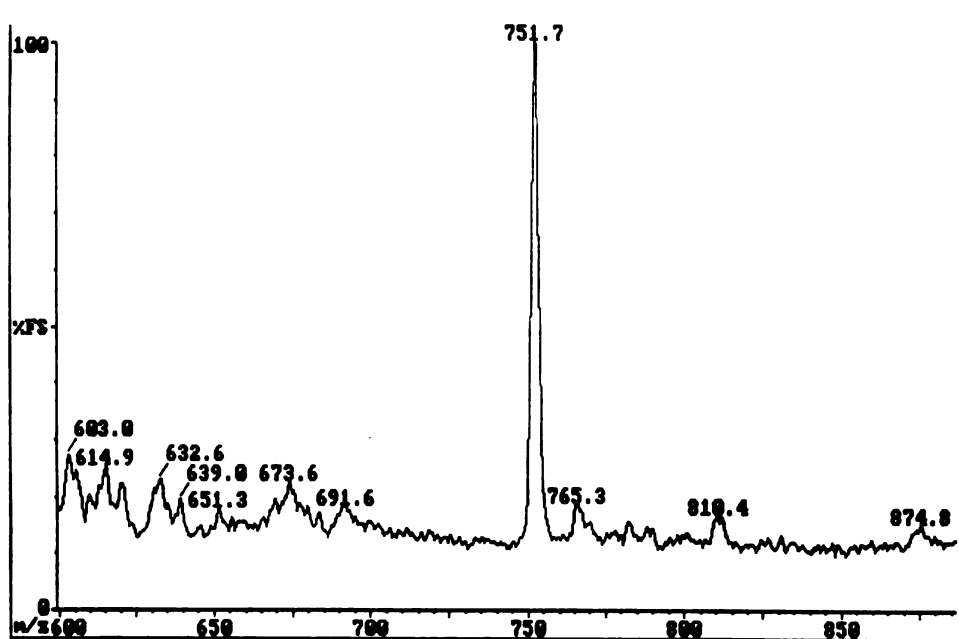


Figure 5.3.15. Mass spectrum of heme **2** ( $m/z = 752$ ).

Hemes **3** and **4** were formed via a method similar to that used to form **2**. Both modified hemes had a Soret absorption of 399 nm and HPLC retention time distinct from those of 8-hydroxymethylheme, 8-formylheme, and **2**.

### 5.3.3 Characterization of HRP Reconstituted with Heme **1** (HRP-1)

Although the definite structure of heme **1** was not proven, HRP was nevertheless reconstituted with this PROXYL containing heme. The electronic absorption spectrum of HRP reconstituted with **1** is shown in Figure 5.3.16. The modified enzyme had a weak nitroxyl radical signal (Figure 5.3.17) that disappeared upon addition of hydrogen peroxide.

Importantly, the modified enzyme did not have the ability to oxidize benzyl alcohol to benzaldehyde. Due to the inefficiency of the HRP-TEMPO system as revealed by the solution studies (see Discussion), the modified enzyme was not further characterized and these studies were not continued.

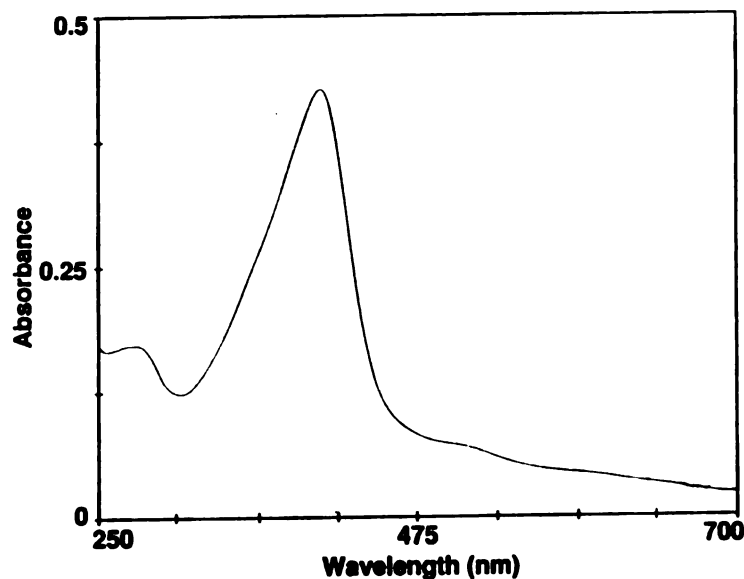


Figure 5.3.16. Electronic absorption spectrum of HRP-1.

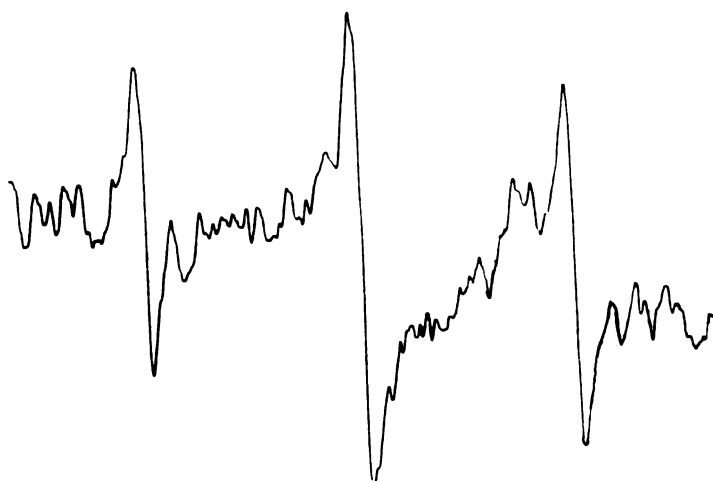


Figure 5.3.17. EPR spectrum of HRP-1.

### **5.3.4 Characterization of HRP Reconstituted with Heme 4**

#### **Electronic Absorption Spectra**

Initially, the Soret band of HRP reconstituted with **4** (HRP-**4**) was at 402 nm, identical to that of native HRP. The next day the Soret band appeared to have red-shifted 3 nm to 405 nm. When a 2-fold excess of hydrogen peroxide was added to the enzyme, only a small decrease in the Soret absorbance was observed (Figure 5.3.18). When a 50-fold excess of hydrogen peroxide was added, a larger decrease along with a slight red-shifting of the Soret band (to 409 nm) was observed. The classical Compound I and Compound II species normally formed when hydrogen peroxide is added to HRP were not observed. Therefore, the modified enzyme did not react normally with peroxide. Subsequent studies showed that HRP reconstituted with  $\delta$ -*meso*-phenylethylheme or  $\delta$ -*meso*-ethylheme also reacts abnormally with peroxide.

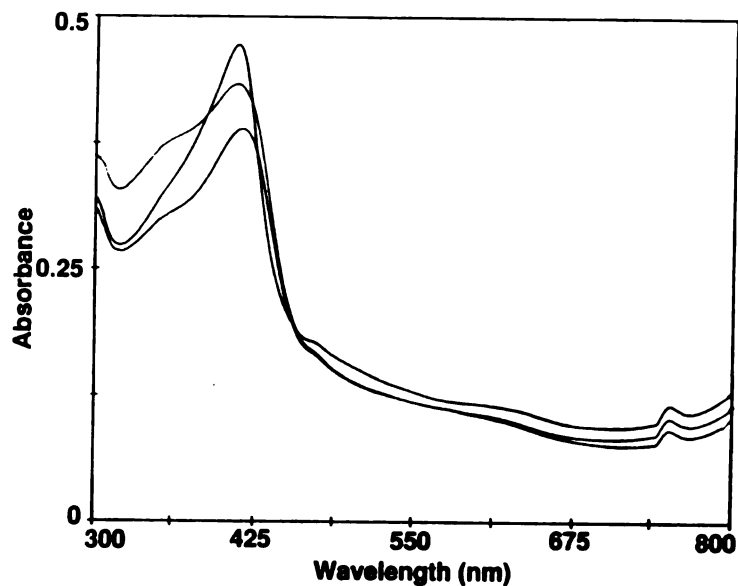


Figure 5.3.18. Spectrum of HRP-4, A) in the absence of  $\text{H}_2\text{O}_2$  (Soret absorbance = 406 nm), B) reacted with 2 x  $\text{H}_2\text{O}_2$  (Soret absorbance = 406 nm), and C) reacted with 50 x  $\text{H}_2\text{O}_2$  (Soret absorbance = 409 nm).

### **Enzymatic Activity of HRP-4**

The guaiacol activity of HRP-4 was measured over a large pH range (Table 5.3.3). The activity of the modified enzyme was significantly lower than that of native HRP at every pH tested. The pH profile of the modified enzyme roughly paralleled that of native HRP. The observed activity may, at least in part, be due to a small amount of 8-hydroxymethylheme-reconstituted HRP. In any case, it is clear that the modified enzyme has little or no ability to oxidize guaiacol.



% GUAIACOL ACTIVITY		
pH	HRP	HRP-4
3.0	27	1.9 (21)
5.0	81	6.9 (77)
7.0	100	9.0 (100)
8.0	36	2.1 (23)
9.0	5.3	0.7 (7.8)

Table 5.3.4. Guaiacol activity of HRP and HRP-4 at various pH values. The activity of HRP at pH 7.0 is defined as 100 %, (in parentheses the activity of HRP-4 at pH 7.0 is defined as 100 %). The buffers were: 50 mM borate, pH 9.0; 50 mM Tris, pH 8.0; 50 mM, phosphate pH 7.0; and 50 mM acetate, pH 5.0 and pH 3.0.

HRP-4 had less than 25 % of the sulfoxxygenase activity of native HRP. The enantiomeric excess of the product sulfoxide was 36 compared to 72 for that formed by native HRP. Thus, in contrast to that of  $\delta$ -*meso*-ethylheme-reconstituted HRP (Chapter 3), the sulfoxxygenase activity of HRP-4 is significantly lower than that of unmodified enzyme.

#### **EPR spectroscopy of HRP-4**

A phenolic radical was not detected by EPR when H<sub>2</sub>O<sub>2</sub> was added to HRP-4. Thus, there is no evidence for the formation of a phenolic radical in this modified enzyme.

## Ligand Binding Studies

In order to determine whether hydrogen peroxide has access to the heme iron of HRP-4, ligand binding studies were performed (Figures 5.3.19-20). HRP-4 appears to form normal cyanide and reduced CO complexes. Thus, it is likely that hydrogen peroxide has access to the iron. The peroxidase machinery appears to be perturbed in a way that prevents the enzyme from efficiently promoting heterolysis of the peroxide bond. HRP-4 also did not react normally with ethyl hydroperoxide, cumene hydroperoxide, or *m*-chloroperbenzoic acid.

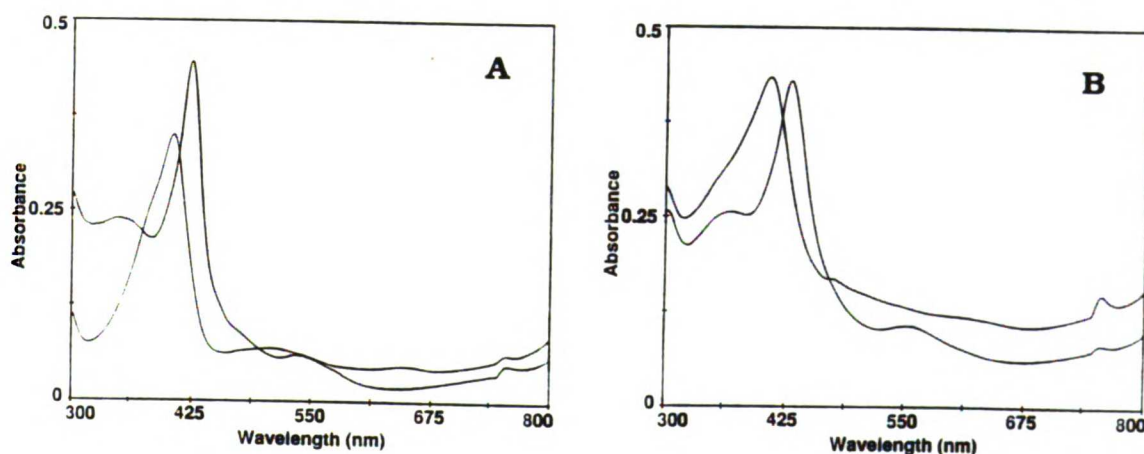


Figure 5.3.19. Spectra of native enzyme and cyanide complex of A) HRP, B) HRP-4. The cyanide complex was formed by addition of a crystal of potassium cyanide to a cuvette containing enzyme. The cyanide complex of HRP had a Soret peak at 422 nm, that of HRP-4 had a Soret peak at 425 nm.

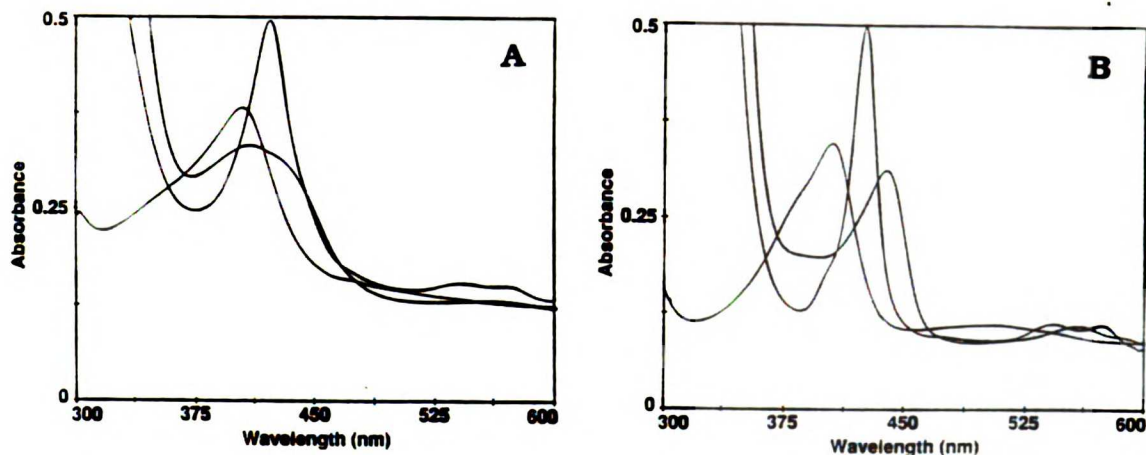


Figure 5.3.20. Spectra of native enzyme, reduced enzyme, and the reduced CO complex of A) HRP, and B) HRP-4. Reduced enzyme was formed by the addition of a pinch of sodium dithionite to a cuvette containing enzyme. The CO complex was formed by bubbling the reduced enzyme with CO for 1 minute. The CO complex of both HRP and HRP-4 had a Soret peak at 423 nm.

### 5.3.5 Characterization of HRP-2 and HRP-3

#### Electronic Absorption Spectra

The electronic absorption spectrum of HRP reconstituted with heme **2** (HRP-2) is shown in Figure 5.3.20. The enzyme appears to react relatively normally with hydrogen peroxide to form a Compound II species. HRP-3 behaved identically.

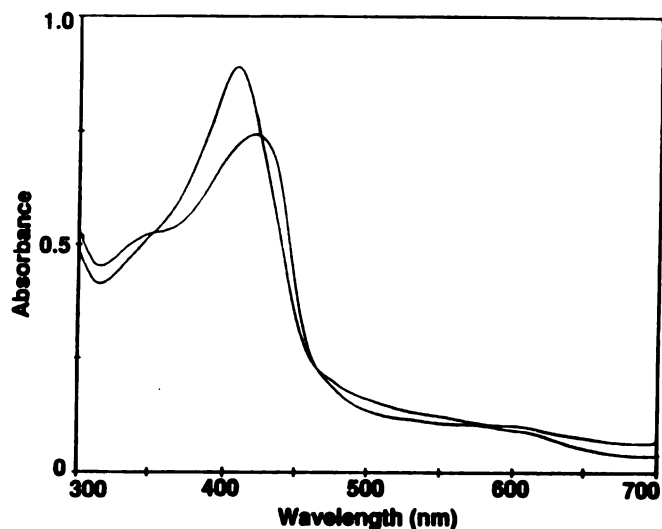


Figure 5.3.21. Electronic absorption spectra of HRP-**2** (Soret absorbance at 405 nm) and its Compound II species (Soret absorbance at 419 nm).

### Enzymatic Activities

Various activities of HRP reconstituted with **2** and **3** are shown in Figure 5.3.22. Importantly, HRP reconstituted with **2** did not have an enhanced ability to oxidize manganese or linoleic acid. HRP reconstituted with **2** did have a moderate ability to oxidize guaiacol, but HRP reconstituted with **3** had a nearly identical guaiacol activity. Thus the ability of HRP-**2** to oxidize guaiacol cannot be attributed to the formation of a phenolic radical within the HRP active site.

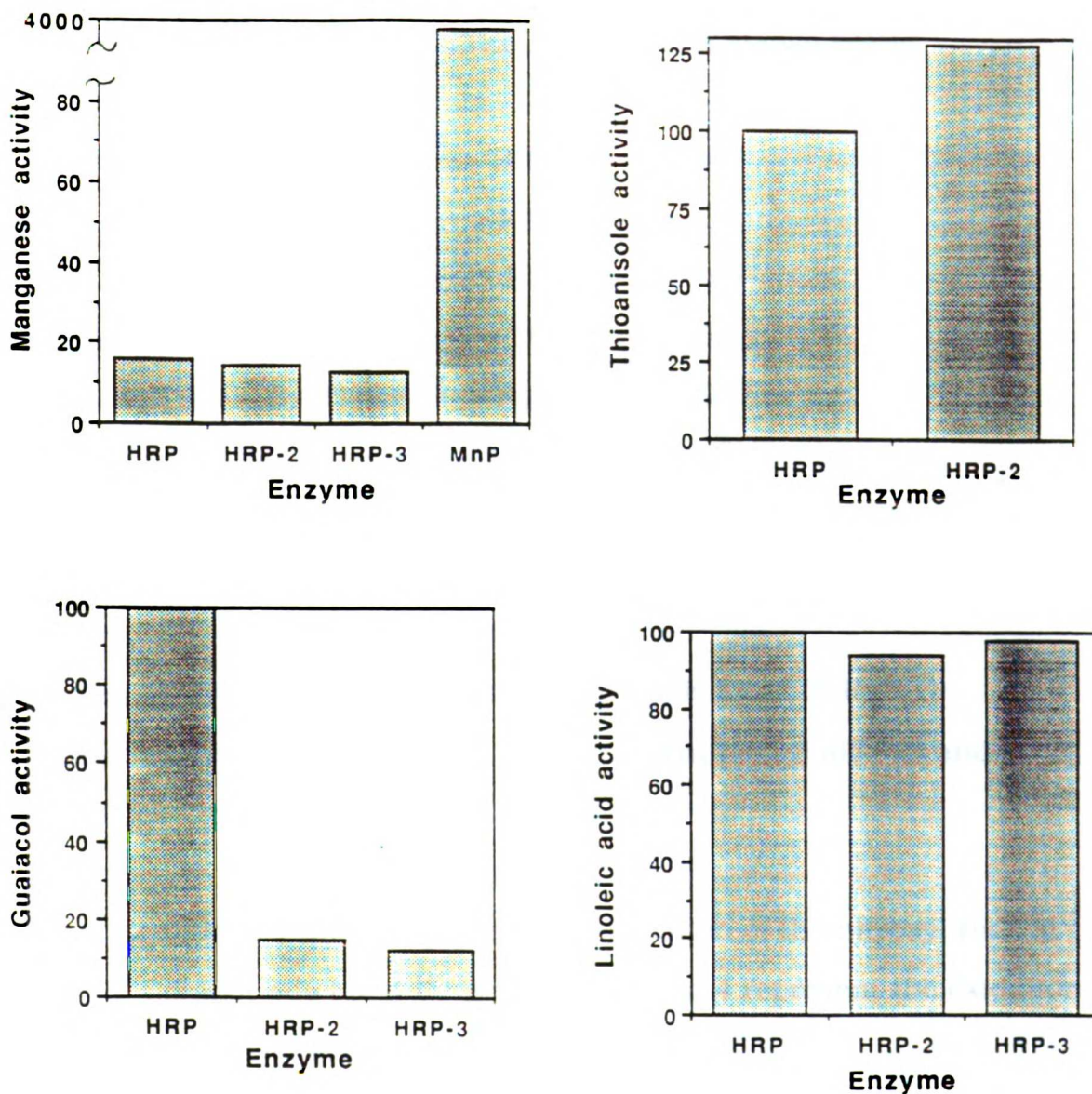


Figure 5.3.22. Enzymatic activities of HRP-2 and HRP-3.

### Formation of a Protein Radical

A phenolic radical was not detected by EPR when hydrogen peroxide was added to HRP-2 or HRP-3.

#### 5.4. Discussion

A scheme for the HRP - TEMPO system is shown below:

1.  $\text{HRP I} + \text{R}_2\text{N-O}\cdot \longrightarrow \text{HRP II} + \text{R}_2\text{N}^+=\text{O}$
2.  $\text{HRP II} + \text{R}_2\text{N-O}\cdot \longrightarrow \text{HRP} + \text{R}_2\text{N}^+=\text{O}$
3.  $\text{HRP I} + \text{R}_2\text{N-OH} \longrightarrow \text{HRP II} + \text{R}_2\text{N-O}\cdot$
4.  $\text{HRP II} + \text{R}_2\text{N-OH} \longrightarrow \text{HRP} + \text{R}_2\text{N-O}\cdot$
5.  $\text{R}_2\text{N}^+=\text{O} + \text{B-OH} \longrightarrow \text{R}_2\text{N-OH} + \text{B=O}$
6.  $\text{HRP} + 2 \text{H}_2\text{O}_2 \longrightarrow \text{HRP} + 2 \text{H}_2\text{O} + \text{O}_2$
7.  $\text{HRP} + \text{R}_2\text{N-O}\cdot + 2 \text{H}_2\text{O}_2 \longrightarrow \text{HRP} + \text{R}_2\text{N-O}\cdot + 2 \text{H}_2\text{O} + \text{O}_2$
8.  $\text{R}_2\text{N-OH} + \text{R}_2\text{N}^+=\text{O} \rightleftharpoons 2 \text{R}_2\text{N-O}\cdot$

where HRP I and HRP II represent Compounds I and II,  $\text{R}_2\text{N-O}\cdot$  represents TEMPO and B-OH & B=O represent benzyl alcohol and benzaldehyde.

Equations 1 and 2 represent the oxidation of the nitroxyl radical by HRP Compounds I and II. Equations 3 and 4 represent the oxidation of the hydroxylamine by HRP Compounds I and II. Equation 5 describes the oxidation of benzyl alcohol to benzaldehyde by the nitrosonium cation. Equation 5 represents a second order reaction, whereas equations 1 through 4 represent enzymatic processes that are second order at low substrate concentrations and show saturation at higher substrate concentrations. Equations 6 and 7 describe TEMPO independent and TEMPO dependent catalytic reactions. Equation 8 represents the equilibrium for the disproportionation of TEMPO.

In the presence of TEMPO, HRP is able to oxidize benzyl alcohol to benzaldehyde. However, the amount of benzaldehyde produced is quite low, barely in excess over the amount of TEMPO. There are at least three explanations for the inefficiency of the system. First, one of the steps may be very slow. Second, a competing side reaction may consume most of the hydrogen peroxide. Third, one of the reaction components may degrade during the incubations.

Steps 1-2, the oxidation of the TEMPO by HRP, appear to be fast. When hydrogen peroxide is added to a solution of HRP and TEMPO, an immediate decay in the radical signal is observed. The decay is complete within one minute. (Note that the amount of decay is not always 100%, but the rate of decay is always fast). If steps 1 or 2 were rate-limiting there would be a slower decay of the radical signal. The facile oxidation of TEMPO by HRP is also consistent with the relatively low (0.33 V) oxidation potential of TEMPO (Endo et al., 1984; Semmelhack et al., 1983).

Step 8 provides a mechanism for the regeneration of the nitroxyl radical from the hydroxylamine (Semmelhack et al., 1983). However, steps 3 and 4, the direct oxidation of the hydroxylamine by HRP also appear to be fast. When the nitroxyl radical is replaced by the hydroxylamine of TEMPO, no change in benzaldehyde production is observed. Also, the fact that benzaldehyde production is insensitive to the concentration of HRP supports the conclusion that steps 1-4 are quite facile. The fact that HRP does not lose the ability to oxidize



guaiacol during a TEMPO incubation indicates that the enzyme is not degraded by the nitrosonium ion.

The time-dependence of aldehyde production seems most consistent with step 5 being rate-limiting. Benzaldehyde production is complete in approximately 90 minutes, yet the peroxide is used up in approximately 20 minutes (as indicated by return of soret to 404 nm). Thus, the nitrosonium ion may form relatively quickly and then slowly oxidize the benzyl alcohol to benzaldehyde. The fact that step 5 is rate-limiting does not explain the inefficiency of benzaldehyde production during the long incubations. If the reaction was allowed to go to completion, the concentration of benzaldehyde formed should have been equal to the concentration of peroxide, assuming that the catalytic activity of HRP had been eliminated (see below).

The inefficiency of benzaldehyde production in incubations containing hydrogen peroxide may partially be due to a competing catalytic side reaction. HRP displayed catalytic activity in the presence (equation 7) or absence of TEMPO (equation 6). This activity likely accounts for the fact that very little product is formed when hydrogen peroxide is added to incubations via one aliquot, whereas a relatively large amount of benzaldehyde is formed when the peroxide is added slowly. When the hydrogen peroxide is added all at once, the catalase reaction probably becomes significant, and most of the peroxide is quickly destroyed. Similarly, when the concentration of TEMPO is low, the TEMPO independent catalytic reaction may become significant. The fact that TEMPO cannot efficiently eliminate hydrogen peroxide



oxidation by HRP indicates that TEMPO is not efficiently regenerated (i.e. step 5 is slow, or TEMPO is degraded). The fact that the benzaldehyde concentration was not in excess over the TEMPO concentration, when the hydrogen peroxide was delivered slowly or replaced with ethyl hydroperoxide, indicates that the catalytic activity of HRP is not solely responsible for the inefficiency of the TEMPO system, because these two methodologies appear to eliminate the catalytic activity of HRP.

The inefficiency of catalysis could also be explained by the reduction of the nitrosonium ion by a species other than benzyl alcohol. The spectral data which show that hydrogen peroxide is consumed when TEMPO is added to a solution containing HRP and hydrogen peroxide is consistent with this hypothesis. However, the finding that benzaldehyde production does not increase when the amount of ethyl hydroperoxide is increased contradicts this hypothesis. The spectral data are likely due to the catalytic activity of HRP in the presence of TEMPO. The experiment could be repeated with ethyl hydroperoxide replacing hydrogen peroxide.

Benzaldehyde production increases when the amount of TEMPO is increased. If the system were truly catalytic with respect to TEMPO, the amount of benzaldehyde produced would solely be dependent on peroxide concentration over a large range of TEMPO concentrations. The fact that benzaldehyde production is roughly proportional to TEMPO concentration indicates that each TEMPO is capable of only one turnover on average. This is not solely a kinetic effect (i.e., the reactions were stopped before all of the peroxide was consumed) because the incubations were run 2 to 12 hours and the peroxide was used up well

before this time. A possible explanation for these results is that TEMPO forms an inactive complex with the product benzaldehyde. This explanation does not seem likely, however, because addition of exogenous benzaldehyde to control incubations does not inhibit benzaldehyde production. It therefore appears that TEMPO may degrade during the incubations. This conclusion is supported by the fact that the majority of the nitroxide radical signal permanently disappears in the HRP incubations. It has also been previously reported that the nitrosonium ion is unstable in aqueous medium, presumably due to its rapid reduction by water (Inokuchi et al., 1990).

The results from the copper-oxygen system indicate that the nitrosonium ion should be able to oxidize alcohols in H<sub>2</sub>O at a comparable rate to their oxidation in organic solvent. Nonetheless, all of the other data support the conclusion that step 5 is slow, and that the TEMPO is destroyed in the aqueous phase. It should be noted that the utilization of detergent, a two phase system, or 10% organic solvent did not increase benzaldehyde production. Perhaps the system would be more efficient if the incubations were run in an organic solvent. Recent studies indicate that under appropriate conditions, unmodified (Ryu and Dordick, 1992) and modified (Wirth et al., 1991) HRP has activity in organic media.

HRP reconstituted with a PROXYL containing heme may have formed a nitrosonium ion within the enzyme. When hydrogen peroxide was added to the modified enzyme, an immediate disappearance of the radical signal was observed. Not surprisingly, HRP-1 was not able to

oxidize benzyl alcohol at a rate above background. The inability of the enzyme to catalyze the reaction may be due to the inefficiency of the TEMPO system in the aqueous phase.

HRP reconstituted with heme **4** did not react normally with hydrogen peroxide. Subsequent studies revealed that HRP reconstituted with  $\delta$ -*meso*-ethyl- or  $\delta$ -*meso*-phenethylheme also reacts abnormally with hydrogen peroxide. It appears that steric bulk near the  $\delta$ -*meso* position perturbs the active site in a manner that hinders normal heterolysis of the peroxide oxygen-oxygen bond. HRP-**4** also lacked the ability to oxidize thioanisole, guaiacol, and manganese at significant rates. A phenolic radical was not detected by low temperature EPR upon addition of hydrogen peroxide to HRP-**4**.

HRP reconstituted with hemes **2** and **3** reacted relatively normally with hydrogen peroxide. Thus, the addition of an ethylene group allowed the phenyl moiety to adopt a position that does not prevent the enzyme from reacting normally with hydrogen peroxide. Disappointingly, HRP-**2** did not have an enhanced ability to oxidize manganese or linoleic acid. Also, although HRP-**2** did have a modest ability to oxidize guaiacol, the ability cannot be attributed to the existence of a phenolic radical because HRP-**3** had a nearly identical guaiacol activity. HRP-**2** thus does not appear to form a phenolic radical within its active site. The inability to detect a radical phenolic radical signal in HRP-**2** by EPR is consistent with this conclusion.

A possible explanation as to why no radical is detected in HRP-2 is that the phenol group could not achieve an orientation within the HRP active site necessary for oxidation. The results of these studies have shown that the phenol must be linked to the heme by at least an ethylene group for normal peroxidase reactivity towards hydrogen peroxide. Perhaps a longer linker, such as a trimethylene or a tetramethylene, would give the heme modification the additional conformational flexibility necessary to achieve the proper positioning within the enzyme active site. Similarly, an alkoxy substitution on the phenol ring may properly position the phenol by hydrogen bonding to a residue within the enzyme active site. An alkoxy substitution may also promote radical formation by lowering the oxidation potential of the phenol.

In conclusion, enzyme engineering through the reconstitution of HRP with modified hemes has promise that is not yet fulfilled. Perhaps the changes suggested in the above paragraph may improve the system, or perhaps other redox active molecules could be linked to the heme edge in order to generate different types of novel catalysts. For example, HRP that contains a flavin may be able to catalyze the 2 electron oxidation of NADH, or HRP that contains ferrocene may be able to function as a cyanide biosensor (Smith and Cass, 1990).

## 6.0 References

- Adachi, S., Nagano, S., Watanabe, Y., Ishimori, K. and Morishima, I. (1991). *Biochem. Biophys. Res. Comm.* **180**, 138-144.
- Adediran, S. A. and Dunford, H. B. (1983). *Eur. J. Biochem.* **132**, 147-150.
- Aitken, M. D. and Irvine, R. L. (1990). *Arch Biochem Biophys* **276**, 405-14.
- Alic, M., Letzring, C. and Gold, M. H. (1987). *Appl. Environ. Microbiol.* **53**, 1464-1469.
- Araiso, T. and Dunford, H. B. (1981). *Archiv. Biochem. Biophys.* **211**, 346-351.
- Araiso, T., Dunford, H. B. and Chang, C. K. (1979). *Biochem. Biophys. Res. Comm.* **90**, 520-524.
- Ator, M. A., David, S. K. and Ortiz de Montellano, P. R. (1987). *J. Biol. Chem.* **262**, 14954-14960.
- Ator, M. A., David, S. K. and Ortiz de Montellano, P. R. (1989). *J. Biol. Chem.* **264**, 9250-9257.
- Ator, M. A. and Ortiz de Montellano, P. R. (1987). *J. Biol. Chem.* **262**, 1542-1551.
- Augusto, O., Kunze, K. L. and Ortiz de Montellano, P. R. (1982). *J. Biol. Chem.* **257**, 6231-6241.
- Babcock, G. T., Ingle, R. T., Oertling, W. A., Davis, J. C., Averill, B. A., Hulse, C. L., Stufkens, D. J., Bolscher, B. G. M. and Wever, R. (1985). *Biochim. Biophys. Acta* **828**, 58-66.
- Banci, L., Bertini, I., Pease, E. A., Tien, M. and Turano, P. (1992). *Biochem.* **31**, 10009-10017.
- Barr, D. P. and Aust, S. D. (1993). submitted for publication.
- Battersby, A. R., McDonald, E., Thompson, M., Chaudhry, I. A., Clezy, P. S., Fookes, C. J. and Hai, T. T. (1985). *J. Chem. Soc. Perkin Trans. I*, 135-143.
- Bosshard, H. R., Anni, H. and Yonetani, T. (1991). Yeast Cytochrome c Peroxidase, in *Peroxidases in Chemistry and Biology*. CRC Press (Boca Raton), 51-84.

Bosshard, H. R., Bänziger, J., Hasler, T. and Poulos, T. L. (1984). *J. Biol. Chem.* **259**, 5683-5690.

Brathwaite, K. G. (1976). *J. Mol. Biol.* **106**, 229-230.

Bumpus, J. A., Tien, M., Wright, D. and Aust, S. D. (1985). **228**, 1434-1436.

Butenas, S., Orreo, T., Lawson, J. H. and Mann, K. G. (1992). *Biochem.* **31**, 5399-5411.

Chance, B. (1952). *Arch. Biochem. Biophys.* **41**, 404-415.

Choe, Y. A. and Ortiz de Montellano, P. R. (1991). *J. Biol. Chem.* **266**, 8523-8530.

Cochran, A. G. and Schultz, P. G. (1990). *J. Am. Chem. Soc.* **112**, 9414-9415.

Colonna, S., Gaggero, N. and Manfredi, A. (1990). *Biochemistry* **28**, 10465-10468.

Crawford, R. L. (1981). *Lignin Biotransformation and Degradation*. New York, Wiley-Interscience.

Dawson (1988). *Science* **240**, 433-439.

Dawson, J. H., Trudell, J. R., Barth, G., Linder, R. E., Bunnenberg, E., Djerassi, C., Chiang, R. and Hager, L. P. (1976). *J. Am. Chem. Soc.* **98**, 3709-3710.

Deits, T., Farrance, M., Kay, E. S., Medill, L., Turner, E. E., Weidman, P. J. and Shapiro, B. M. (1984). *J. Biol. Chem.* **259**, 13525-.

DePillis, G. D. and Ortiz De Montellano, P. R. (1989). *Biochemistry* **262**, 7947-7952.

DiCosimo, R. and Szabo, H. C. (1987). *J. Org. Chem.* **53**, 1673-1679.

DiNello, R. K. and Dolphin, D. H. (1981). *J. Biol. Chem.* **266**, 6903-6912.

Doerge, D. R. (1988). **27**, 3697-3700.

Doerge, D. R., Cooray, N. M. and Brewster, M. E. (1991). *Biochemistry* **30**, 8960-4.

Dolphin, D. and Felton, R. H. (1974). *Accts. Chem. Res.* **7**, 26-32.

- Dolphin, D., Felton, R. H., Borg, D. C. and Fajer, J. (1970). *J. Am. Chem. Soc.* **92**, 743-745.
- Dolphin, D., Forman, A., Borg, D. C., Fajer, J. and Felton, R. H. (1971). *Proc. Natl. Acad. Sci. USA* **68**, 614-618.
- Dugad, L. B., La Mar, G. N., Lee, H. C., Ikeda-Saito, M., Booth, K. S. and Caughey, W. S. (1990). *J. Biol. Chem.* **265**, 7173-7179.
- Dunford, H. B. (1991). Horseradish Peroxidase: Structure and Kinetic Properties, in *Peroxidases in Chemistry and Biology*. CRC Press (Boca Raton), 1-24.
- Ellman, J. A., Mendel, D. and Schultz, P. G. (1992). *Science* **255**, 197-200.
- Endo, T., Miyazawa, T., Shiihashi, S. and Okawara, M. (1984). *J. Am. Chem. Soc.* **84**, 3877-3878.
- Fidy, J., Paul, K.-G. and Vanderkooi, J. M. (1989). *Biochem.* **28**, 7531-7541.
- Finzel, B. C., Poulos, T. L. and Kraut, J. (1984). *J. Biol. Chem.* **259**, 13027-13036.
- Fishel, L. A., Farnum, M. F., Mauro, J. M., Miller, M. A. and kraut, J. (1991). *Biochemistry* **30**, 1986-1996.
- Geigert, J., Neidleman, S. L. and Dalietos, D. J. (1983). *J. Biol. Chem.* **258**, 2273-2277.
- Gilbert, G. C., Hodgeman, K. C. and R.O.C., N. (1973). *J. Chem. Soc. Perkin Trans.* **2**, 1748-1751.
- Gillett, D., Ducanel, F., Pradel, E., Leonetti, M., Menza, A. and Boulain, J. C. (1992). *Protein Engin.* **5**, 273-278.
- Glenn, J. K., Akileswaran, L. and Gold, M. H. (1986). *Arch. Biochem. biophys.* **251**, 688-696.
- Glenn, J. K. and Gold, M. H. (1985). *Arch. Biochem. Biophys.* **242**, 329-341.
- Glenn, J. K., Morgan, M. A., Mayfield, M. B., Kuwahara, M. and Gold, M. H. (1983). *Biochem. Biophys. Res. Commun.* **114**, 1077-1083.

Gold, M. H., Wariishi, H. and Valli, K. (1989). *Extracellular Peroxidases Involved in Lignin Degradation by the White Rot Basidiomycete Phanerochaete chrysosporium*. ACS Symposium on Biocatalysis in Agricultural Biotechnology, Washington D.C., American Chemical Society.

Griffith, W. P., Ley, S. V., Whitcombe, G. P. and White, A. D. (1987). *J. Chem. Soc. Chem. commun.* 1625-1627.

Groves, J. T., Taushalter, R. C., Nakamura, M., Nemo, T. E. and Evance, B. J. (1981). *J. Am. Chem. Soc.* **103**, 2884-2886.

Guengerich, F. P. (1987). *Mamalian Cytochromes P-450*. Boca Raton, CRC Press.

Hager, L. P., Morris, D. R., Brown, F. S. and Eberwein, H. (1967). *J. Biol. Chem.* **242**, 1769-1777.

Hammel, K. E., Kalyanaraman, B. and Kirk, T. K. (1986). *J. Biol. Chem.* **261**, 16948-16952.

Hammel, K. E., Tardone, P. J., Meon, M. A. and Price, L. A. (1989). *Archiv. Biochem. Biophys.* **270**, 404-409.

Harris, R. Z., Newmyer, S. and Ortiz de Montellano, P. R. (1993). *J. Biol. Chem.* in press.

Harris, R. Z., Wariishi, H., Gold, M. H. and Ortiz de Montellano, P. R. (1991). *J. Biol. Chem.* **266**, 8751-8.

Harrison, J. E., Araiso, T., Palcic, M. M. and Dunford, H. B. (1980). *Biochem. Biophys. Res. Comm.* **94**, 34-40.

Harrison, J. E. and Schultz, J. (1976). *J. Biol. Chem.* **251**, 1371-1374.

Hashimoto, S., Tatsuno, Y. and Kitagawa, T. (1986). *Proc. Natl. Acad. Sci. USA* **83**, 2417-2421.

Hayashi, Y. and Yamazaki, I. (1979). *J. Biol. Chem.* **254**, 9101-9106.

Heiba, E. I., Dessau, R. M. and Rodewald, P. G. (1974). *J. Am. Chem. Soc.* **96**, 1917-1921.

Henderson, W. R., Jr. (1991). Eosinophil Peroxidase: Occurrence and Biological Function, in *Peroxidases in Chemistry and Biology*. CRC Press (Boca Raton), 105-122.

Hosoya, T., Sakurada, J., Kurokawa, C., Toyoda, R. and Nakamura, S. (1989). **28**, 2639-2644.



- Hurst, J. K. (1991). Myeloperoxidase: Active Site Structure and Catalytic Mechanisms, in *Peroxidases in Chemistry and Biology*. CRC Press (Boca Raton), 37-62.
- Inokuchi, T., Matsumoto, S., Nishiyama, T. and Torii, S. (1990). *J. Org. Chem.* **55**, 462-466.
- Job, D. and Dunford, H. B. (1975). *Eur. J. Biochem.* **66**, 607-614.
- Job, D. and Dunford, H. B. (1977). *Can. J. Biol. Chem.* **55**,
- Kaiser, E. T. (1988). *Angew. Chem. Ont. Ed. Eng.* **27**, 913-922.
- Kartheine, R., Dietz, R., Nastainczyk, W. and Ruf, H. H. (1988). *Eur. J. Biochem.* **171**, 313-320.
- Kassner, R. J. (1972). *Proc. Nat. Acad. Sci. USA* **69**, 2263-2267.
- Kedderis, G. L., Rickert, D. E., Pandey, R. N. and Hollenberg, P. F. (1986). *J. Biol. Chem.* **261**, 15910-15914.
- Kenten, R. H. and Mann, P. J. G. (1950). *Biochem. J.* **46**, 67-73.
- Kenten, R. H. and Mann, P. J. G. (1952). *Biochem. J.* **52**, 125-130.
- Kimura, S. and Yamazaki, I. (1979). *Arch. Biochem. Biophys.* **198**, 580-588.
- Kirk, T. K. and Farrell, R. L. (1987). *Ann. Rev. Microbiol.* **41**, 465-505.
- Klebanoff, S. J. (1991). Myeloperoxidase: Occurrence and Biological Function, in *Peroxidases in Chemistry and Biology*. CRC Press (Boca Raton), 1-36.
- Kobayashi, S., Nakano, M., Goto, T., Kimura, T. and Schaap, A. P. (1986). *Biochem. Biophys. Res. Commun.* **135**, 166-171.
- Kobayashi, S., Nakano, M., Kimura, T. and Schaap, A. P. (1987). *Biochemistry* **26**, 5019-5022.
- La Mar, G. N., de Ropp, J. S., Smith, K. M. and Langry, K. C. (1981). *J. Biol. Chem.* **256**, 237-243.
- La Mar, G. N., Pande, U., Hauksson, J. B., Pandley, R. K. and Smith, K. M. (1989). *J. Am. Chem. Soc.* **111**, 485-491.
- Lehmann, F.-M., Brentz, N., Bruchhausen, F. V. and Wurm, G. (1989). *Biochem. Pharmacol.* **38**, 1209-1216.

- Leisola, M. S., Kozulic, B., Meussdoerffer, F. and Flechter, A. (1987). *J. Biol. Chem.* **262**, 419-424.
- Lerner, R. A., Benkovic, S. T. and Schultz, P. G. (1991). *Science* **252**, 659-667.
- Levy, M. J., La Mar, G. N., Jue, T., Smith, K. M., Pandley, R. K., Smith, W. S., Livingston, d. J. and Brown, W. D. (1985). *J. Biol. Chem.* **260**, 13694-13698.
- Loprasert, S., Neguros, S. and Okara, H. (1989). *J. Bacterology* **171**, 4871-4875.
- Lukat, G., Jabro, M. N., Rodgers, K. R. and Goff, H. M. (1988). *Biochim. Biophys. Acta* **954**, 265-270.
- Magnussen, R. P. (1991). Thyroid Peroxidase, in *Peroxidases in Chemistry and Biology*. CRC Press (Boca Raton), 199-220.
- Marnett, L. J., Weller, P. and Battista, J. R. (1986). Comparison of the Peroxidase Activity of Heme proteins and Cytochrome P-450, in *Cytochrome P-450 Structure, Mechanism, and Biochemistry*. Plenum Press (New York), 29-65.
- Martin, M. T., Nopper, A. D., Schultz, P. G. and Rees, A. R. (1991). *Biochem.* **30**, 9757-9761.
- Mazza, G., Charles, C., Bouchet, M., Ricard, J. and Reynaud, J. (1968). *Biochim. Biophys. Acta* **167**, 89-98.
- McCarthy, M. B. and White, R. E. (1883). *J. Biol. Chem.* **19**, 11610-11616.
- McMurry, T. J. and Groves, J. T. (1986). Metalloporphyrin models for cytochrome P-450, in *Cytochrome P-450 Structure, Function and Mechanism*. Plenum Press (New York), 1-28.
- Mehlhorn, R. J. and Swanson, C. E. (1992). *Arch. Free Radical Res. Commun.* **17**, 157-175.
- Meunier, B. (1991). N- and O-Demethylations Catalyzed by Peroxidases, in *Peroxidases in Chemistry and Biology*. CRC Press (Boca Raton), 201-218.
- Miller, V. P., DePillis, G. D., Ferrer, J. C., Mauk, A. G. and Ortiz de Montellano, P. R. (1992). *J. Biol. Chem.* **267**, 9836-9842.

- Millis, C. D., Cai, D., Stankovich, M. T. and Tien, M. (1989). **28**, 8484-8489.
- Mino, Y., Wariishi, H., Blackburn, N. J., Loehr, T. M. and Gold, M. H. (1988). *J Biol Chem* **263**, 7029-36.
- Miwa, G. T., Walsh, J. S. and Lu, A. Y. H. (1983). *J. Biol. Chem.* **259**, 3000-3004.
- Modi, S., Behere, D. V. and Mitra, S. (1989). *Biochem.* **28**, 4689-4694.
- Moore, K. L., Moronne, M. M. and Mehlhorn, R. J. (1992). **299**, 47-58.
- Morishima, I. and Ogawa, S. (1979). *J. Biol. Chem.* **254**, 2814-2820.
- Morita, Y., Mikami, B., Yamashita, H., Lee, J. Y., Aibara, S., Sato, M., Katsube, Y. and Tanaka, N. (1991). in *Biochemical, Molecular and Physiological Aspects of Plant Peroxidases*. University of Geneva (Switzerland), 81-88.
- Nadler, V., Goldberg, I. and Hochman, A. (1986). *Biochim. Biophys. Acta.* **882**, 234-241.
- Naruta, Y., Tani, F. and Maruyama, K. (1990). *J. Chem. Soc., Chem. Commun.* 1378-1380.
- Neet, K. E. and Koshland, D. E. (1966). *Proc. Natl. Acad. Sci. USA* **56**, 1606-1616.
- Nichol, A. W., Angel, L. A., Moon, T. and Clezy, P. S. (1987). *Biochem. J.* **247**, 147-150.
- Nickell, C., Prince, M. A. and Lloyd, R. S. (1992). *Biochem.* **31**, 4189-4198.
- Odajima, T. (1980). *J. Biochem.* **87**, 397-404.
- Ogura, T. and Kitagawa, T. (1987). *J. Am. Chem. Soc.* **109**, 2177-2179.
- Ortiz de Montellano, P. R. (1986). Oxygen Activation and Transfer, in *Cytochrome P-450: Structure, Mechanism, and Biochemistry*. Plenum Press (New York), 217-272.
- Ortiz de Montellano, P. R. (1987). *Acc. Chem. Res.* **20**, 289-294.
- Ortiz de Montellano, P. R. (1992). *Annu. Rev. Pharmacol. Toxicol.* **32**, 89-107.



Ortiz de Montellano, P. R. and Catalano, C. E. (1985). *J. Biol. Chem.* **260**, 9265-9271.

Ortiz de Montellano, P. R., Choe, Y. S., DePillis, G. and Catalano, C. E. (1987). *J. Biol. Chem.* **262**, 11641-11646.

Ortiz de Montellano, P. R., David, S. K., Ator, M. A. and Tew, D. (1988). *J. Biol. Chem.* **263**, 5470-5476.

Ortiz de Montellano, P. R. and Grab, L. A. (1987). *J. Biol. Chem.* **262**, 5310-5314.

Ortiz de Montellano, P. R. and Kerr, D. E. (1983). *J. Biol. Chem.* **258**, 10558-10563.

Pascynski, A., Huynh, V. D. and Crawford, R. (1986). *Arch. Biochem. Biophys.* **244**, 750-756.

Paul, K.-G. and Ohlsson, P.-I. (1978). *Acta Chem. Scand. B* **32**, 395-404.

Paul, K. G. (1959). *Acta. Scand.* **13**, 1239-1251.

Pease, E. A., Andrawis, A. and Tien, M. (1989). *J Biol Chem* **264**, 13531-5.

Pease, E. A., Aust, S. D. and Tien, M. (1991). *Biochem Biophys Res Commun* **179**, 897-903.

Penner-Hahn, J. E., Eble, K. S., McMurry, T. J., Renner, M., Balch, A. L., Groves, J. T., Dawson, J. H. and Hodgson, K. O. (1986). *J. Am. Chem. Soc.* **108**, 7819-7825.

Perez, U. and Dunford, H. B. (1990a). *Biochim Biophys Acta* **1038**, 98-104.

Perez, U. and Dunford, H. B. (1990b). *Biochemistry* **29**, 2757-63.

Pérez, U. and Dunford, H. B. (1990c). *Biochemistry* **29**, 2757-2763.

Poulos, T. L. (1986). The crystal structure of Cytochrome P-450cam, in *Cytochrome-P450 Structure, Mechanism, and Biochemistry*. Plenum Press (New York), 505-523.

Poulos, T. L., Finzel, B. C. and Howard, A. J. (1986). *J. Biol. Chem.* **261**, 5314-5322.

Poulos, T. L., Freer, S. T., Alden, R. A., Edwards, S. L., Skogland, U., Takio, K., Eriksson, B., Xuong, N.-h., Yonetani, T. and Kraut, J. (1980). *J. Biol. Chem.* **255**, 575-580.

Poulos, T. L., Freer, S. T., Alden, R. A., Xuong, N. H., Edwards, S. L., Hamlin, R. C. and Kraut, J. (1978). *J. Biol. Chem.* **253**, 3730-3735.

Poulos, T. L. and Kraut, J. (1980). *J. Biol. Chem.* **255**, 8199.

Pribnow, D., Mayfield, M. B., Nipper, V. J., Brown, J. A. and Gold, M. H. (1989). *J Biol Chem* **264**, 5036-40.

Raag, R., Swanson, B. A., Poulos, T. L. and Ortiz de Montellano, P. R. (1990). *Biochem.* **29**, 8119-8126.

Reiter, B. and Perraudin, J.-P., Ed. (1991). *Lactoperoxidase: Biological Function*. Peroxidases in Chemistry and Biology. Boca Raton, CRC Press.

Ringe, D., Petsko, G. A., Kerr, D. E. and Ortiz de Montellano, P. R. (1984). *Biochem.* **23**, 2-4.

Roberts, J. E., Hoffman, B. M., Rutter, R. and Hager, L. P. (1981). *J. Biol. Chem.* **256**, 2118-2121.

Roman, R. and Dunford, H. B. (1972). **11**, 2076-2082.

Roman, R., Dunford, H. B. and Evett, M. (1971). *Can. J. Chem.* **49**, 3059-3062.

Ryu, K. and Dordick, J. S. (1992). *Biochem.* **31**, 2588-2598.

Sakurada, J., Takahashi, S. and Hosoya, T. (1987a). *J. Biol. Chem.* **262**, 4007-4010.

Sakurada, J., Takahashi, S., Shimizu, T., Hatano, M., Nakamura, S. and Hosoya, T. (1987b). *Biochem.* **26**, 6478-6483.

Saxena, A., Modi, S., Behere, D. V. and Mitra, S. (1990a). *Biochim. Biophys. Acta* **1041**, 83-93.

Saxena, A., Modi, S., Behere, D. V. and Mitra, S. (1990b). *Biochim Biophys Acta* **1041**, 83-93.

Schejter, A., Lanir, A. and Epstein, N. (1975). *Archives Biochem. Biophys.* **174**, 36-44.

Schultz, C. E., Devaney, P. W., Winkler, H., Devrunner, P. G., Doan, N., Chiang, R., Rutter, R. and Hager, L. P. (1979). *FEBS Lett.* **103**, 102-105.

Schultz, C. E., Rutter, R., Sage, J. T., DeBrunner, P. G. and Hager, L. P. (1984). *Biochemistry* **23**, 4743-4754.

- Segel, I. H. (1986). *Biochemical Calculations*. N.Y., John Wiley & Sons.
- Semmelhack, M. F., Chou, C. S. and Cortes, D. A. (1983). *J. Am. Chem. Soc.* **105**, 4492-4494.
- Semmelhack, M. F., Schmid, C. R., Cortes, D. A. and Chou, C. S. (1984). *J. Am. Chem. Soc.* **106**, 3374-3376.
- Sibbett, S. S. and Hurst, J. K. (1984). *Biochem.* **23**, 3007-3013.
- Smith, A. T., Sanders, S. A., Thorneley, R. N. F., Burke, J. F. and Bray, R. C. (1992). *Eur. J. Biochem.* **207**, 507-519.
- Smith, M. H. and Cass, A. E. (1990). *Anal. Chem.* **62**, 2429-2436.
- Snow, K. M. and Smith, K. M. (1989). *J. Org. Chem.* **54**, 3270-3281.
- Sono, M., Bracete, A. M., Huff, A. M., Ikeda-Saito, M. and Dawson, J. H. (1991). *Proc. Natl. Acad. Sci. U.S.A.* **88**, 11148-11152.
- Stellwagen, E. (1978). *Nature* **275**, 73-74.
- Strickland, E. H., Kay, E., Shannon, L. M. and Horwitz, J. (1968). *J. Biol. Chem.* **243**, 3560-3565.
- Swanson, B. A., Dutton, D. R., Lunetta, J. M., Yang, C. M. and Ortiz de Montellano, P. R. (1991). *J. Biol. Chem.* **266**, 19258-19264.
- Takata, T., Yamazaki, M., Fujimori, K., Kim, Y. H., Oae, S. and Iyanagi, T. (1980). *Chem. Lett.* 1441-1444.
- Takio, K., Titani, K., Ericsson, L. H. and Yonetani, T. (1980). *Arch. Biochem. Biophys.* **203**, 615.
- Tamura, M., Asakura, T. and Yonetani, T. (1972). *Biochim. Biophys. Acta* **268**, 294-304.
- Taylor, K. L., David, J. U. and Kinkade, J. M. (1992). *Biochem. Biophys. Res. Commun.* **187**, 1572-1578.
- Thanabal, V., de Ropp, J. S. and La Mar, G. N. (1987). *J. Am. Chem. Soc.* **109**, 7516-7525.
- Thanabal, V. and La Mar, G. N. (1989). *Biochem.* **28**, 7038-7044.
- Thanabal, V., LaMar, G. N. and de Ropp, J. S. (1988). *Biochem.* **27**, 5400-5407.

- Theorell, H. (1940). *Ark. Kemi Mineral. Geol.* **14B**, 1-3.
- Thomas, E. L., Bozeman, P. M. and Learn, D. B. (1991). Lactoperoxidase: Structure and Catalytic Properties, in *Peroxidases in Chemistry and Biology*. CRC Press (Boca Raton), 123-142.
- Thomas, E. L. and Learn, D. B. (1991). in *Peroxidases in Chemistry and Biology*. CRC Press (Boca Raton), 83-103.
- Tien, M. and Kirk, T. K. (1983). *Science* **221**, 661-663.
- Ugarova, N. N., Kutuzova, G. D., Rogozhin, V. V. and Berezin, I. V. (1984). *Biochim. Biophys. Acta* **790**, 22-30.
- Uneyama, K. and Tori, S. (1971). *Tetrahedron Lett.* 329-332.
- van Huystee, R. B. (1991). Molecular Aspects and Biological Functions of Peanut Peroxidase, in *Peroxidases in Chemistry and Biology*. CRC Press (Boca Raton), 155-170.
- Van Wart, H. E. and Zimmer, J. (1985). *J. Am. Chem. Soc.* **107**, 3379-3382.
- Vietch, N. C., Williams, R. P. J., Bray, R. C., Burke, J. F., Sanders, S. A., Thorneley, R. N. F. and Smith, A. T. (1992). *Eur. J. Biochem.* **207**, 521-531.
- Wariishi, H., Akileswaran, L. and Gold, M. H. (1988). *Biochemistry* **27**, 5365-70.
- Wariishi, H. and Gold, M. H. (1989). *FEBS Lett.* **243**, 165-168.
- Watanabe, Y., Iyanagi, T. and Oae, S. (1980). *Tet. Let.* **21**, 3685-3688.
- Weiss, S. J. (1989). *New Eng. J. Med.* **320**, 365-376.
- Welinder, K. G. (1985). *Eur. J. Biochem.* **151**, 497-504.
- Welinder, K. G. (1991). *Biochimica et Biophysica Acta.* **1080**, 215-220.
- Wever, R., Oetrling, W. A., Hoogland, H., Bloscher, B. G. J. M., Kim, Y. and Babcock, G. T. (1991). *J. Biol. Chem.* **266**, 24308-24313.
- Wever, R. and Plat, H. (1981). *Biochim. Biophys. Acta* **661**, 235-239.
- Wirth, P., Soupe, J., Tritsch, D. and Biellman, J. P. (1991). *Biorg. Chem.* **19**, 133-142.



Wiseman, J. S., Nichols, J. S. and Kolpak, M. X. (1982). *J. Biol. Chem.* **257**, 6328-6332.

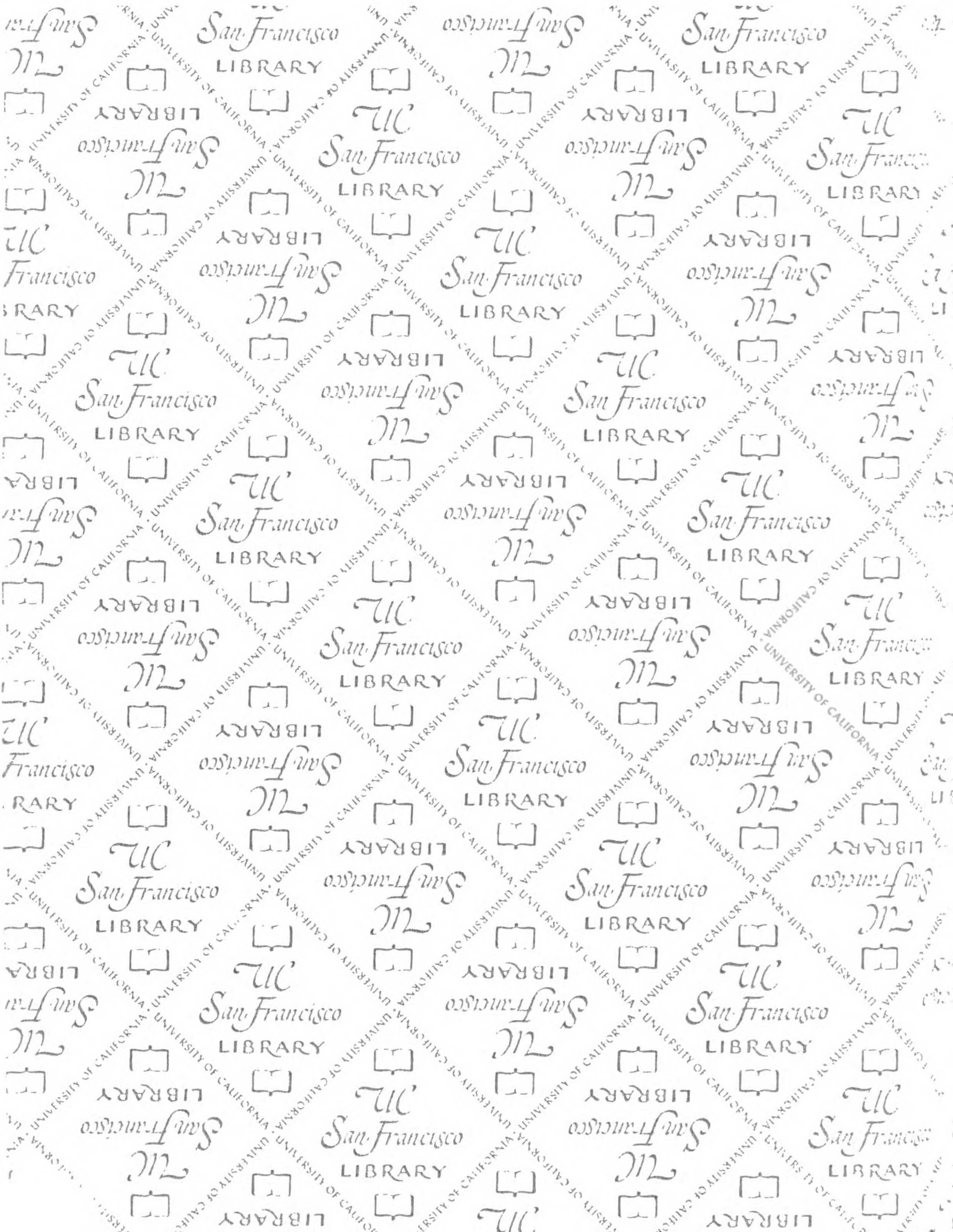
Yamaguchi, T., Nakano, T. and Kimoto, E. (1984). *Biochem. Biophys. Res. Commun.* **120**, 534-539.

Yonetani, T. (1965). *J. Biol. Chem.* **240**, 4509-4514.

Yonetani, T. and Ray, G. S. (1965). *J. Biol. Chem.* **240**, 4503-4508.

Yonetani, T., Schleyer, H. and Ehrenberg, A. (1966). *J. Biol. Chem.* **241**, 3240-3243.

Zeng, J. and Fenna, R. E. (1992). *J. Mol. Biol.* **226**, 185-207.



San Francisco

LIBRARY

608865



3 1378 00608 8655

FOR REFERENCE

NOT TO BE TAKEN FROM THE ROOM



CAT. NO. 23 012

